

**Biosynthesis and Analysis of
3-Isobutyl-2-methoxypyrazine
in *Capsicum annuum* (Bell Pepper) Plants**

Dissertation

zur

Erlangung des Doktorgrades (Dr. rer. nat.)

der Mathematisch-Naturwissenschaftlichen Fakultät
der Rheinischen Friedrich-Wilhelms-Universität Bonn

vorgelegt von

Francesca Zamolo

aus

Münster

Bonn

2023

Angefertigt mit Genehmigung der Mathematisch-Naturwissenschaftlichen Fakultät
der Rheinischen Friedrich-Wilhelms-Universität Bonn.

1. Gutachter:	Prof. Dr. Matthias Wüst
2. Gutachter:	Prof. Dr. Andreas Schieber
Tag der Promotion:	24.05.2023
Erscheinungsjahr:	2023

The work and research towards this dissertation were carried out between July 2020 and February 2023 at the Institute of Nutritional and Food Sciences (IEL) of the *Rheinische Friedrich-Wilhelms-Universität Bonn* under supervision of *Prof. Dr. M. Wüst*.

Abstract

3-Alkyl-2-methoxypyrazines (MPs) are highly odorous compounds occurring in a wide range of raw vegetables. Due to their high odor activity, they have been of great research interest. The most prominent MPs are 3-isopropyl-2-methoxypyrazine (IPMP), 3-sec-butyl-2-methoxypyrazine (sBMP) and 3-isobutyl-2-methoxypyrazine (IBMP). While their occurrence has been widely studied, less is known about their biosynthesis. The identification of *Vitis vinifera* O-methyltransferases (VvOMTs) catalyzing the O-methylation of 3-alkyl-2-hydroxy-pyrazines (HPs) gave an important insight into the last step of MP-biosynthesis. However, precursors and earlier biosynthetic steps are still unknown. Different pathways of MP-biosynthesis have been proposed, but none of them has been confirmed yet.

The main objective of this study was thus to identify precursors of MPs. For this purpose, *in vivo* feeding experiments were conducted using stable isotope labeled compounds. Feeding experiments were conducted focusing on the IBMP-biosynthesis in bell pepper fruits (*Capsicum annuum* L.). Volatiles were extracted by headspace solid-phase microextraction (HS-SPME) and analyzed by comprehensive two-dimensional gas chromatography (GC×GC) coupled to time-of-flight mass spectrometry (ToF-MS). Feeding studies revealed an incorporation of L-leucine and α -ketoisocaproic acid (α -KIC) into IBMP. It could be shown that L-serine plays a key role in the biosynthesis of IBMP not only as a C₂-building block, but also as nitrogen source. Indeed, the incorporation of L-serine as well as a C₁-unit of glycine and glyoxylic acid into IBMP gave evidence for a metabolic interface of the IBMP-biosynthesis and photorespiration.

Besides, the distribution of IBMP within the bell pepper plant was examined. Therefore, a method combining a stable isotope dilution assay (SIDA) with HS-SPME, GC and ToF-MS was developed and validated. IBMP was found in all plant organs. However, unripe bell pepper pericarp turned out to be the main site of IBMP-accumulation. *In vivo* feeding experiments revealed that IBMP is biosynthesized in all plant parts apart from roots and ripe bell pepper fruits. A long-distance transport of IBMP via the phloem was not detected.

Table of Content

Chapter 1 Introduction	1
1. <i>Pyrazines</i>	1
2. <i>HS-SPME-GC×GC-ToF-MS-Analysis</i>	15
3. <i>Objective of the Study</i>	20
4. <i>List of Publications</i>	21
Chapter 2	22
1. <i>General Introduction</i>	22
<i>Investigation of Biosynthetic Precursors of 3-Isobutyl-2-methoxypyrazine Using Stable Isotope Labeling Studies in Bell Pepper Fruits (Capsicum annuum L.)</i>	24
Chapter 3	29
1. <i>General Introduction</i>	29
<i>L-Serine is the Direct Precursor for the Pyrazine Ring Construction in the Biosynthesis of 3-Isobutyl-2-methoxypyrazine in Bell Pepper Fruits (Capsicum annuum L.)</i>	32
Chapter 4	37
1. <i>General Introduction</i>	37
<i>Sites of Biosynthesis, Distribution and Phloem Transport of 3-Isobutyl-2-methoxypyrazine in Capsicum annuum (Bell Pepper) Plants</i>	39
Chapter 5 Summary and Outlook	42
Chapter 6 References	46
Chapter 7 Abbreviations	56
Chapter 8 Appendix	61

Chapter 1 Introduction

1. Pyrazines

Pyrazine (1,4-diazine) is a six-membered, monocyclic aromatic ring molecule with two nitrogen atoms in the *para*-1,4-position. As almost all *N*-heterocycles, pyrazine is a basic compound.^[1,2]

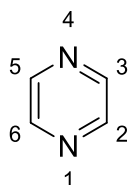


Figure 1: Chemical structure and numbering of pyrazine.

Its chemical structure as well as the numbering according to the nomenclature of the *International Union of Pure and Applied Chemistry* (IUPAC) are displayed in **Figure 1**. Given that, pyrazine is a symmetrical molecule, all carbon positions are chemically identical, so numbering is usually omitted for monosubstituted pyrazines like (2-)methylpyrazine.^[2] The first pyrazine derivate was chemically synthesized in 1844. It was initially called 'Amarone' until it was confirmed to be 2,3,5,6-tetraphenylpyrazine in 1897 (**Figure 2**).^[3]

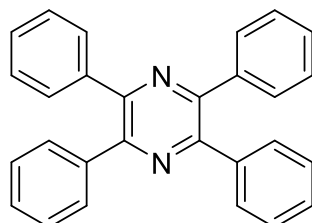
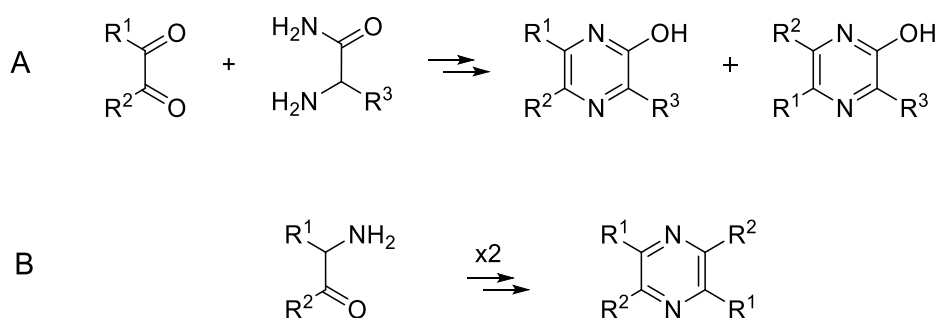


Figure 2: Chemical structure of 2,3,5,6-tetraphenylpyrazine.

Over the years many synthetic routes to pyrazines have been developed. Amongst others, pyrazines are obtained by direct ring closure e.g. a cyclodimerization of α -aminoketones or α -aminoaldehydes or a condensation of a 1,2-diketone with a 1,2-diamine (**Scheme 1**).^[4,5,6]



Scheme 1: Synthetic routes to pyrazines. **(A)** Condensation of a 1,2-diketone with a 1,2-diamine generating hydroxypyrazines.^[4] **(B)** Self-cyclization of two α -aminoketones.^[6]

As pyrazines exhibit a wide range of biological functions like antibacterial, antiviral and anticancer properties, they are often used as pharmaceuticals.^[7] Some examples are displayed in **Figure 3**. Pyrazinamide (**1**) as well as morinamide (**2**) for example are used for the treatment of tuberculosis, whereas oltipraz (**3**) serves as an anti-tumor agent.^[8] Moreover, pyrazines are used as pesticides. Thionazin (**4**) for example serves as a nematicide.^[9]

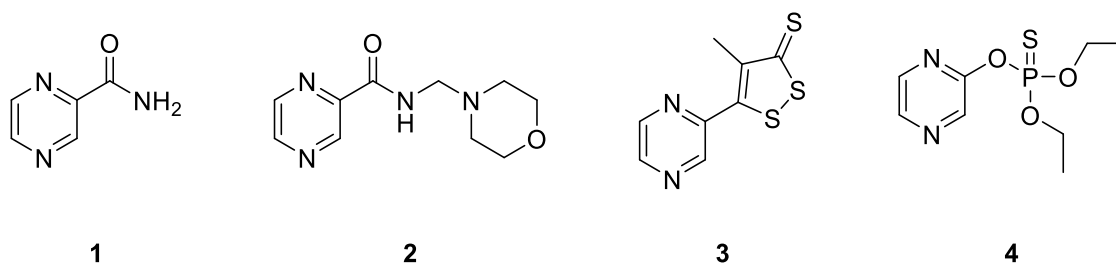


Figure 3: Chemical structures of pyrazines used as pharmaceuticals or pesticides. Pyrazinamide (**1**), morinamide (**2**), oltipraz (**3**) and thionazin (**4**).

However, pyrazines are not only synthesized chemically, but can also be obtained from nature, where they are widespread. Pyrazines are biosynthesized as primary and secondary metabolites by bacteria, fungi, yeast, insects, invertebrates and plants.^[10,11,12–14] Aspergillilic acid, which has antibiotic and antimycotic properties is for example a commonly known pyrazine biosynthesized by *Aspergillus flavus* (**Figure 4**).^[15]

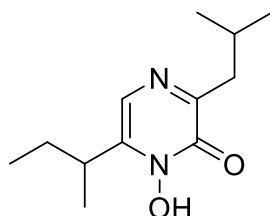


Figure 4: Chemical structure of aspergillilic acid.

In nature, pyrazines are often used as semiochemicals. Pyrazines serve as pheromones for intraspecific communication or as allelomones for interspecific communication. Allelomones are subdivided into allomones, which benefit the emitter, kairomones, which favor the receiver and synomones, which are beneficial for both, emitter and receiver.^[13,16,17] Four semiochemically active pyrazines are displayed in **Figure 5**. 3-Ethyl-2,5-dimethylpyrazine (**5**) is biosynthesized by an ant-associated bacterium (*Serratia marcescens*) and serves as an important trail and alarm pheromone of ants (*Atta sexdens rubropilosa*).^[18,19] 2,5-Dimethyl-3-(2-methylbutyl)-pyrazine (**6**) is used for the chemical defense by the phasmid insect *Phyllium westwoodii* (Phylliidae).^[20] Several trisubstituted alkylpyrazines like 2-propyl-3,5-dimethylpyrazine (**7**) are used for the pollinator attraction of *Drakaea glyptodon* flowers.^[21] 3-Isopropyl-2-methoxypyrazine (IPMP) (**8**) turned out to be biosynthesized as attractant by

ladybird beetles, but is also known to be emitted by the roots of spinach (*Spinacea oleracea*) to attract the root knot nematode *Meloidogyne incognita*.^[22]

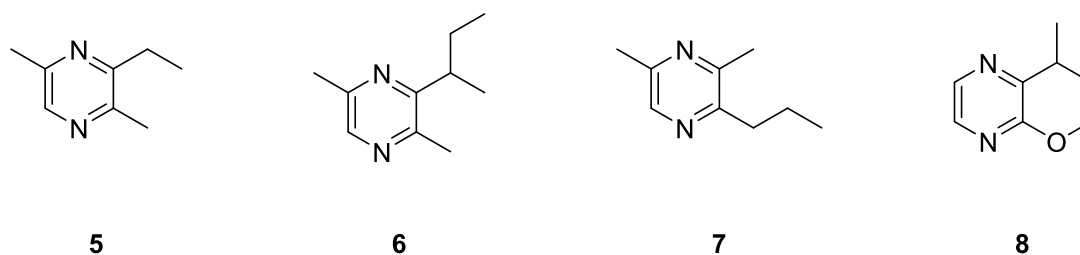


Figure 5: Chemical structures of semiochemically active pyrazines. 3-Ethyl-2,5-dimethylpyrazine (**5**), 2,5-dimethyl-3-(2-methylbutyl)pyrazine (**6**), 2-propyl-3,5-dimethylpyrazine (**7**) and 3-isopropyl-2-methoxypyrazine (IPMP, **8**).

In addition, pyrazines serve as key odorants in food. Due to their flavor and aroma properties, they are frequently used for improving the organoleptic quality of food products.^[23] Their sensory impact is based on their odor detection thresholds (OTs), which is defined as the compound's lowest concentration that can still be perceived by the human sense of smell.^[24] Human perception of odorants occurs via specific olfactory receptors (ORs) on olfactory neurons found in a specialized epithelium in the nose. In 2021, it was shown that the pyrazine-selective OR called OR5K1 is responsible for humans perceiving the odor of pyrazines. Notably, OR5K1 is especially activated by pyrazines, which serve as semiochemicals and key aroma compounds. Their perception is assumed to depend on the receiver: 2,3,5-trimethylpyrazine (**Figure 6, 8**) for example is perceived as aversive by mice, for which it serves as an alarm semiochemical. In contrast, it is attractive to humans due to its roasted nut- or cocoa-like smell. The unnatural process of roasting is thought to be responsible for this ambiguous perception of several alkylpyrazines.^[25]

Alkyl- and alkoxy-pyrazines are important aroma impact compounds. Possessing low OTs, makes them extremely odorous even when present in low amounts.^[23,26–28] A compound's impact on the overall aroma of food is defined as its odor activity value (OAV). The OAV is calculated as the ratio of a compound's concentration in the sample to its OT.^[24] IPMP for example reaches the highest OAV (90) in raw peanuts (*Arachis hypogaea* L.) and the third highest OAV (114) in raw mustard seeds (*Sinapis alba* L.).^[29,30] In contrast, 3-isobutyl-2-methoxy-pyrazine (IBMP) reaches the highest OAV (490) in raw coffee beans (*Coffea arabica* var. *tipica*).^[31]

1.1 Alkylpyrazines

Alkylpyrazines contribute to the aroma properties of a wide range of foods. They can have a roasted or nutty flavour.^[32] On the one hand, their aroma activity depends on their substituents: the more bulky the alkyl side chain the lower its OT.^[33] 2,3,5-Trimethylpyrazine (**Figure 6, 8**) for instance turned out to be the methyl-substituted pyrazine with the highest aroma activity. However, lower OTs were obtained by the substitution of the methyl-substituent in position C-2 by an ethyl-substituent (2-ethyl-3,5-dimethylpyrazine, **9**) or a vinyl-group (2-ethenyl-3,5-dimethyl-pyrazine, **10**).^[34]

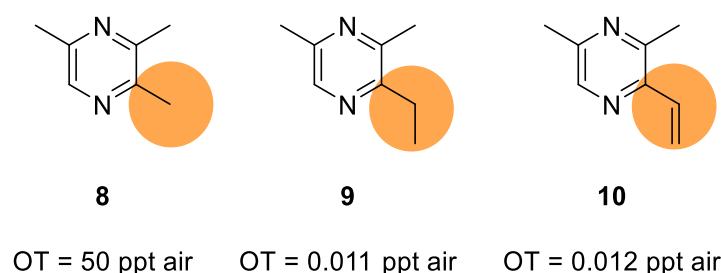


Figure 6: Structure-odor relationship of alkylpyrazines I. Chemical structures and OTs of aroma active 2,3,5-trimethylpyrazine (**8**), 2-ethyl-3,5-dimethylpyrazine (**9**) and 2-ethenyl-3,5-dimethylpyrazine (**10**).^[34]

On the other hand, the aroma activity of multi-alkylated pyrazines is influenced by their substitution pattern. As displayed in **Figure 7**, the OT of 2,5-dimethylpyrazine (**11**) is lower than the OTs of 2,6-dimethylpyrazine (**12**) and 2,3-dimethylpyrazine (**13**).^[35]

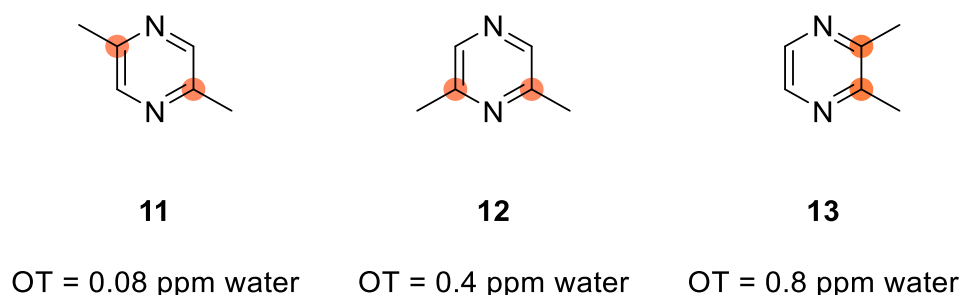


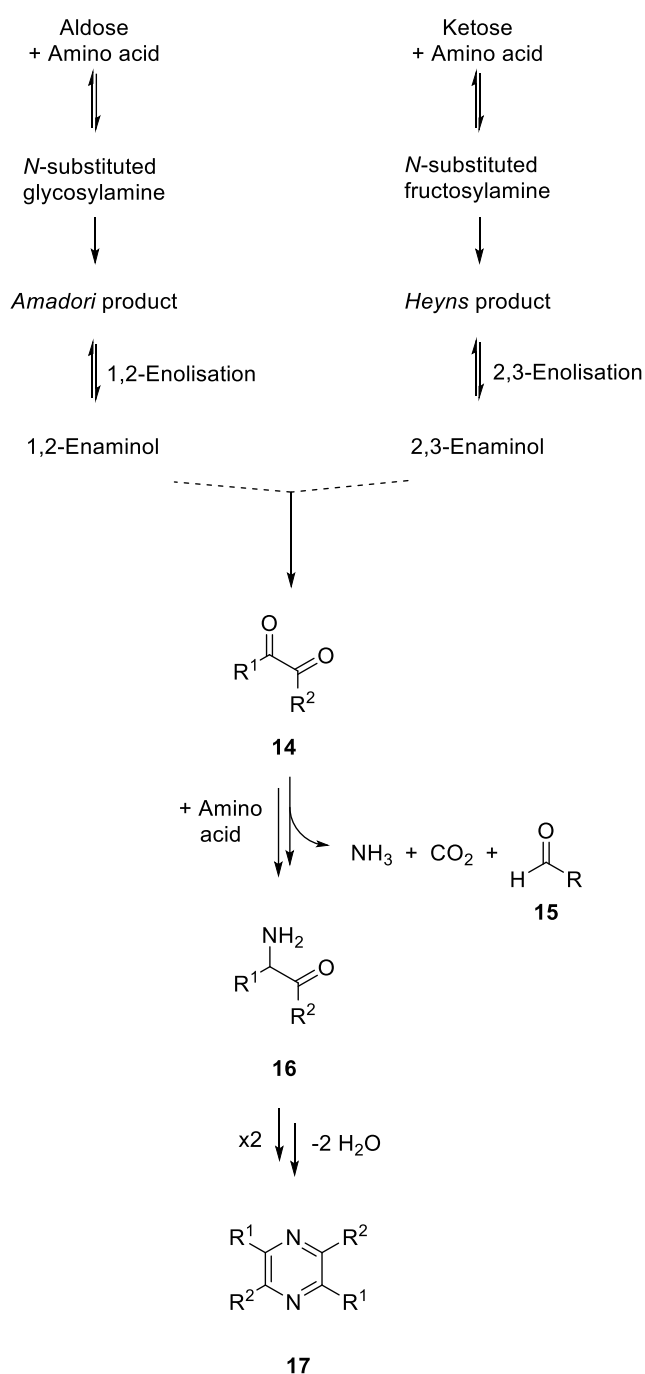
Figure 7: Structure-odor relationship of alkylpyrazines II. Chemical structures and OTs of aroma active 2,5-dimethylpyrazine (**11**), 2,6-dimethylpyrazine (**12**) and 2,3-dimethylpyrazine (**13**).^[35]

1.1.1 Occurrence of Alkylpyrazines

Alkylpyrazines are widely distributed in nature. They are biosynthesized by several insects, bacteria, and plants.^[12,17,36] Moreover, they can be found in a wide range of thermally processed food like baked bread and potatoes, beef and in roasted peanuts and coffee and cocoa powder.^[26,37] Additionally, they occur in various fermented soybean products like miso, natto, and soy sauce, biosynthesized by bacteria like *Bacillus natto* and *Lactococcus lactis*.^[38]

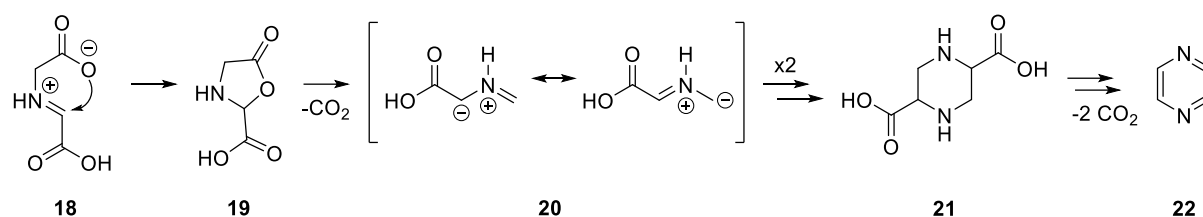
1.1.2 Biosynthesis of Alkylpyrazines

Alkylpyrazines can be formed as typical *Maillard* reaction products during thermal food processing.^[39] As displayed in **Scheme 2**, the *Maillard* reaction initiates with the condensation of a reducing carbohydrate with an amino group (amino acid, protein, peptide) forming an *N*-glycosyl-amine or *N*-fructosyl-amine, which in turn generates either an *Amadori* or a *Heyns* product. These products undergo an enolization and form an α -dicarbonyl compound (**14**), which again reacts with an amino acid releasing a *Strecker* aldehyde (**15**) and generating an α -aminoketone (**16**) that dimerizes to the respective pyrazines (**17**).^[40,41]



Scheme 2: Pyrazine generation from the *Maillard* reaction.^[41]

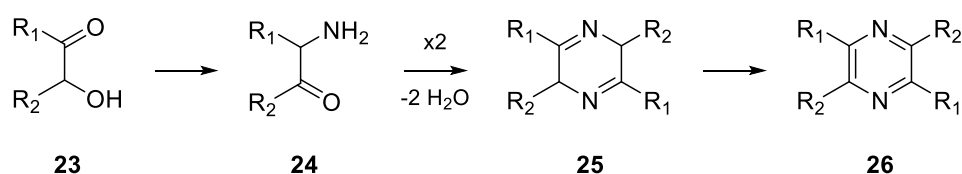
An alternative pathway via a dimerization of an azomethine ylide was proposed in 2010. Labeling studies showed that in the *Maillard* reaction α -keto acids and α -amino acids can generate a *Schiff* base (**18**) that – due to its instability – tends to undergo an intramolecular cyclization instead of an *Amadori* rearrangement. A decarboxylation of the resulting oxazolidine-5-one (**19**) leads to an azomethine ylide (**20**), which easily dimerizes to a piperazine (**21**). A decarboxylation and subsequent oxidation leads to the formation of pyrazine (**22**) (**Scheme 3**).^[42,43]



Scheme 3: Pyrazine generation via azomethine ylides (**20**) under *Maillard* reaction conditions.^[42]

Besides, alkylpyrazines are synthesized by different bacteria strains during fermentation processes. These biologically synthesized alkylpyrazines are subdivided into three classes: alkylated pyrazines with up to four alkyl side chains (usually methyl- or ethyl-substituted) belong to the first class, while pyrazines having two branched side chains are classified as the second class and the third class consists of alkylated methoxypyrazines.^[44] Due to the great structural diversity of alkylated pyrazines, different biosynthetic pathways have been proposed. However, by far not all biosynthetic pathways have been elucidated yet.

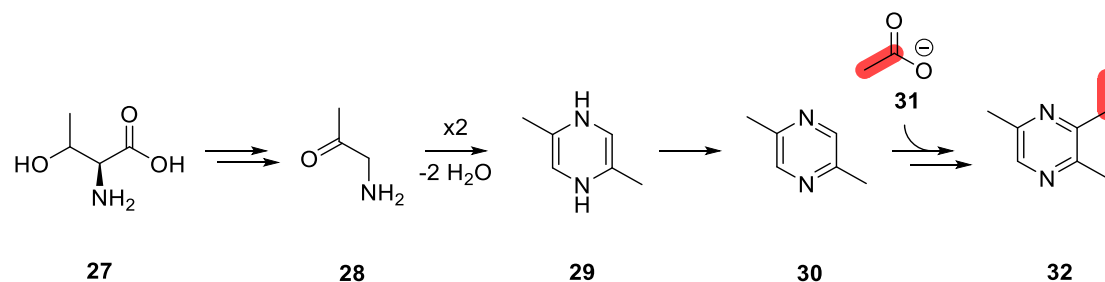
Feeding experiments with *Corynebacterium glutamicum* revealed the biosynthesis of mono- and multi-alkylated pyrazines. Their biosynthesis starts with a non-enzymatic amination of acyloin (**23**), which generates α -aminocarbonyls (**24**). A self-condensation of two α -aminocarbonyls yields a dihydropyrazine (**25**), which easily oxidizes to the respective pyrazine (**26**) (**Scheme 4**).^[10] Depending on the substitution pattern of the acyloin, a wide variety of alkylated pyrazines can be formed.^[44,45]



Scheme 4: Proposed pathway of alkylpyrazines via acyloin (**23**).^[10]

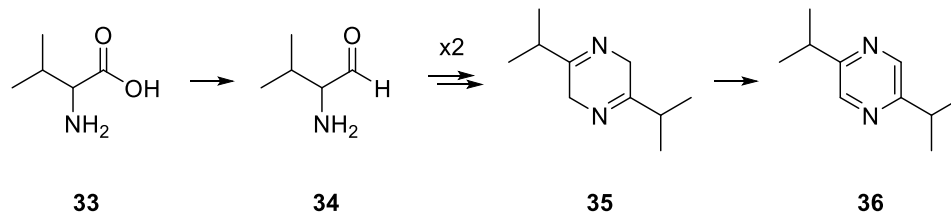
Furthermore, aminoacetone turned out to be a direct precursor for alkylpyrazines. As displayed in **Scheme 5**, it is formed as an instable intermediate during the catabolism of L-threonine (**27**). The condensation of two molecules of aminoacetone (**28**) results in 2,5-dimethyl-3,6-dihydropyrazine (**29**), which can be oxidized to 2,5-dimethylpyrazine (**30**). Feeding

experiments even demonstrated that acetate (**31**) serves as a precursor for the ethyl-substituent of 3-ethyl-2,5-dimethylpyrazine (**32**) in *Serratia marcescens*.^[18]



Scheme 5: Proposed pathway of 3-ethyl-2,5-dimethylpyrazine (**32**) via L-threonine (**27**) and aminoacetone (**28**).^[18]

In myxobacteria (*Nannocystis exedens* subsp. *cinnabarina* and *Chondromyces crocatus*) the biosynthesis of branched dialkylpyrazines is supposed to start with a reduction of a branched-chain amino acid to the corresponding α -aminoaldehyde. As α -aminoaldehydes are unstable and highly reactive, they tend to dimerize generating dihydropyrazines, which in turn can be oxidized to pyrazines. As displayed in **Scheme 6**, valine (**33**) for instance is first reduced to valinal (**34**), which dimerizes to 2,5-diisopropyl-3,6-dihydropyrazine (**35**) and generates 2,5-diisopropylpyrazine (**36**).^[36]



Scheme 6: Proposed pathway of 2,5-diisopropylpyrazine (**36**) via valine (**33**) and valinal (**34**).^[36]

1.2 3-Alkyl-2-methoxypyrazines

Pyrazines with a polar ethoxy- or methoxy- substituent tend to have even higher odor potencies than alkylated pyrazines.^[27,33,34] The odor of alkylated 2-ethoxypyrazines like 2-ethoxy-3-methyl-5-(2-methylpentyl)-pyrazine (**37**) for instance is described as nutty, coffee-like or fruity. In contrast, alkylated 2-methoxypyrazines like 2-methoxy-3-methyl-5-(2-methylpentyl)-pyrazine (**38**) are associated with woody and green attributes (**Figure 8**).^[27,46]

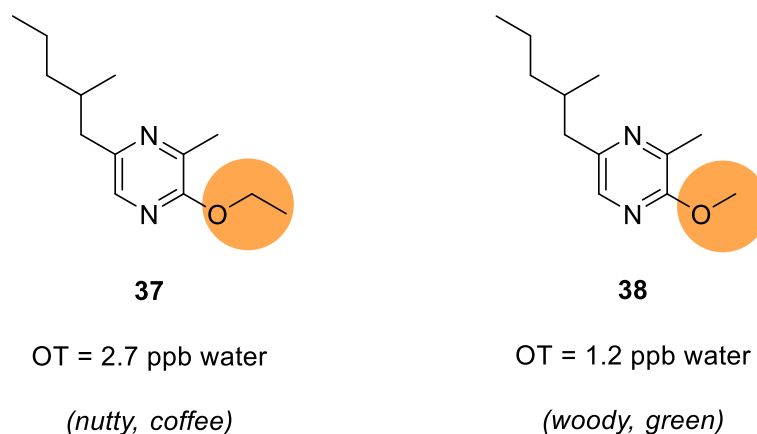


Figure 8: Structure-odor relationship of alkoxy pyrazines I. Chemical structures, OTs and odor descriptions of aroma active 2-ethoxy-3-methyl-5-(2-methylpentyl)-pyrazine (**37**) and 2-methoxy-3-methyl-5-(2-methylpentyl)-pyrazine (**38**).^[27]

The most prominent alkylated methoxypyrazines are 3-alkyl-2-methoxypyrazines (MPs). Sensory investigations showed that the OT of MPs is affected by the alkyl chain length: the longer the alkyl side chain the lower the OT. The OT of 3-ethyl-2-methoxypyrazine (**39**) for example is ten times higher than the OT of 3-propyl-2-methoxypyrazine (**40**) (**Figure 9**).^[32]

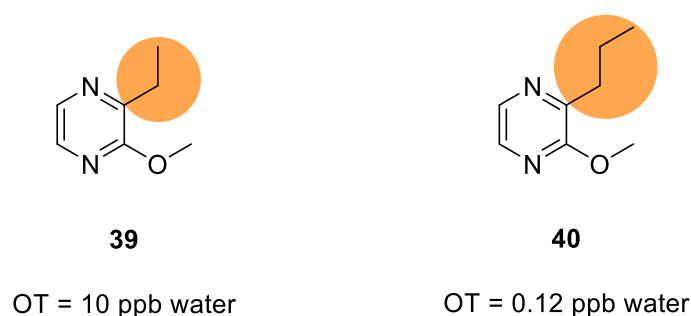


Figure 9: Structure-odor relationship of alkoxy pyrazines II. Chemical structures and OTs of aroma active 3-ethyl-2-methoxypyrazine (**39**) and 3-propyl-2-methoxypyrazine (**40**).^[32]

In addition, the substitution pattern of alkoxy-pyrazines plays a significant role in their aroma-activity. For instance, 3-methyl-2-methoxypyrazine (**41**) has a lower OT than its 2,6-isomer (**42**) and 2,5-isomer (**43**) (**Figure 10**).^[35]

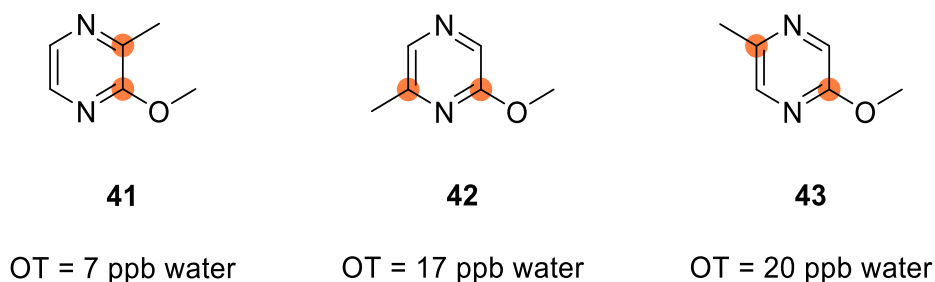


Figure 10: Structure-odor relationship of alkoxy pyrazines III. Chemical structures and OTs of aroma active 3-methyl-2-methoxy pyrazine (**41**), 6-methyl-2-methoxy pyrazine (**42**) and 5-methyl-2-methoxy pyrazine (**43**).^[35]

1.2.1 Occurrence of 3-Alkyl-2-methoxy pyrazines

MPs occur in trace quantities in several foods including raw vegetables as well as raw peanuts, coffee and fragrant vegetable oils.^[14,30,31,47–50] The most common MPs are 3-isopropyl-2-methoxy pyrazine (IPMP, **44**), 3-sec-butyl-2-methoxy pyrazine (sBMP, **45**) and 3-isobutyl-2-methoxy pyrazine (IBMP, **46**) (**Figure 11**). IBMP was first identified in bell pepper fruits (*Capsicum annuum* L.) in 1969, followed by the identification of sBMP in galbanum oil (*Ferula galbaniflua*) and IPMP in green peas (*Pisum sativum*).^[46,51,52] The highest IBMP-levels can be found in green bell pepper fruits (*Capsicum annuum* L. var. *grossum*), while beetroot (*Beta vulgaris*) and parsnip (*Pastinaca sativa*) contain the highest sBMP-concentrations and pea shells (*Pisum sativum*) are rich in IPMP.^[14]

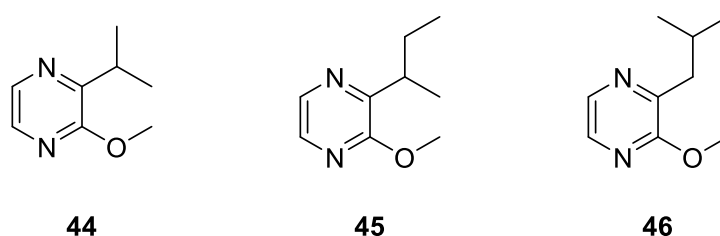


Figure 11: Chemical structures of 3-isopropyl-2-methoxy pyrazine (IPMP, **44**), 3-sec-butyl-2-methoxy pyrazine (sBMP, **45**), 3-isobutyl-2-methoxy pyrazine (IBMP, **46**).

In addition, MPs are found in several grapes of *Vitis vinifera* varieties and their respective wines like Cabernet Sauvignon, Sauvignon blanc, Cabernet franc, Pinot noir, Riesling, Chardonnay, Merlot and Carmenere, but also in *Vitis* species like *V. amurensis*, *V. cinerea*, *V. riparia* and *V. rupestris*.^[53,54–57] MPs have a strong influence on the aroma of wines. In fact, they are responsible for an herbaceous, earthy and bell pepper-like wine aroma, which contributes to the typical aroma of wine varieties such as Sauvignon Blanc in moderate concentrations. In contrast, MPs have detrimental effects on the wine quality when present in higher concentrations.^[57–59] Estimated OTs in wines are 10–16 ppt for IBMP and 1–2 ppt for

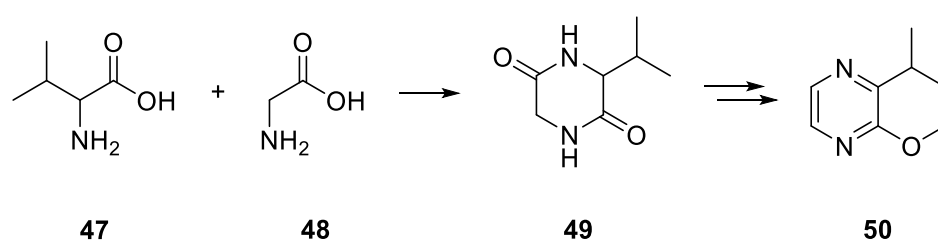
IPMP.^[46,51,56,57,60] While IBMP is mainly associated with a green bell pepper aroma, IPMP is primarily related to an earthy and herbaceous aroma.^[61] IBMP turned out to be the most abundant MP in grapes and wines. An aroma associated with unripe and green attributes is perceived by the consumers at IBMP-levels ≥ 8 ppt in white wine and ≥ 15 ppt in red wine.^[56,57]

MPs in wine are not only grape derived. IPMP for instance is considered to be the main cause for the off-flavor 'ladybug taint' (LBT), which is caused by the unintentional carry-over of the Coccinellidae ladybeetles *Harmonia axyridis* and *Coccinella septempunctata* into the wine during winemaking.^[62] Moreover, cork stoppers can lead to elevated MP-levels in wine.^[63] IBMP and IPMP, were identified as corky off-flavor compounds that can migrate from cork stoppers into the wine.^[64] MPs occur naturally in raw cork planks or can be microbially induced by for example *Pseudomonas* species as well as *Cedecea* and *Serratia* strains.^[65,66,67]

In addition, MPs have a significant impact on coffee quality. Elevated IPMP- and IBMP-levels are supposed to be responsible for the 'potato-taste defect' (PTD) found in roasted coffee made of *Coffea* species.^[68] The PDT is associated with potato peel aroma.^[69] It has been hypothesized that an insect-bacteria-interaction between the coffee bug (*Antestiopsis orbitales*) and bacteria species of the genus *Enterobacteriaceae* and *Pantoea* is causing an upregulation of genes and enzymes, which are involved in the biosynthesis of MPs.^[70]

1.2.2 Biosynthesis of 3-Alkyl-2-methoxypyrazines

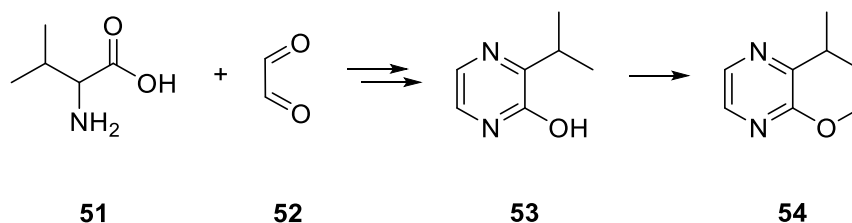
While the occurrence of MPs has been widely studied, less is known about their biosynthesis. In contrast to alkyipyrazines, MPs are not related to food processing. MPs are usually plant derived or biosynthesized by microorganisms. The bacterial IPMP-biosynthesis is assumed to start with a condensation of valine (**47**) and glycine (**48**) yielding 3-isopropylpiperazine-2,5-dione (**49**) followed by a dehydration and methylation forming IPMP (**50**) (**Scheme 7**).^[66,67]



Scheme 7: Postulated biosynthesis of 3-isopropyl-2-methoxypyrazine (IPMP, **50**) in *Pseudomonas* species.^[66]

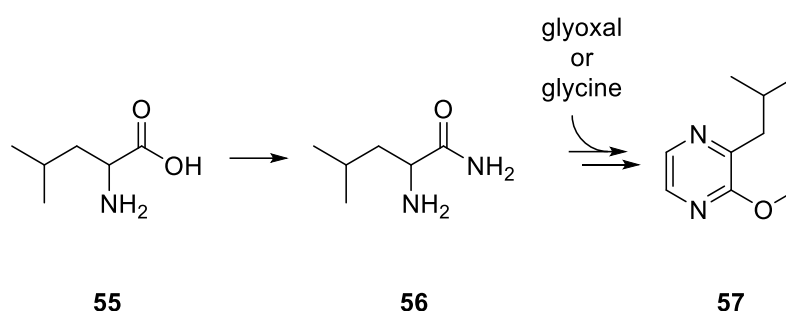
The knowledge about the biosynthesis of MPs in plants is limited. Biosynthetic precursors and intermediates are still unknown. Their biosynthesis is supposed to be linked to the metabolism of amino acids. In 1970, *Murray et al.* postulated a biosynthetic pathway starting with the amination of a branched-chain amino acid (BCAA) like valine (**51**) followed by a condensation

with glyoxal (**52**) forming 3-isopropyl-2-hydroxypyrazine (IPHP, **53**), which would in turn be enzymatically methylated to IPMP (**54**) (**Scheme 8**).^[51] However, this pathway has been discussed controversially, as neither α -amino acid amides nor free glyoxal had been detected in plants.^[14,71]



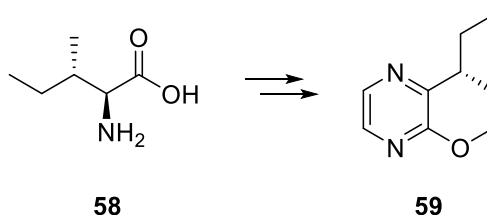
Scheme 8: Postulated biosynthesis of 3-isopropyl-2-methoxypyrazine (IPMP, **54**) in plants.^[51]

Another biosynthetic pathway was proposed in 2010. A significant increase in IBMP-content was detected when exogenous leucine and leucinamide (2-amino-4-methylpentanamide, AMPA) were added to Cabernet Sauvignon grapes. Hence, it has been hypothesized that leucine (**55**) serves as a precursor, while AMPA (**56**) acts as an intermediate in the biosynthesis of IBMP (**57**) (**Scheme 9**).^[72]



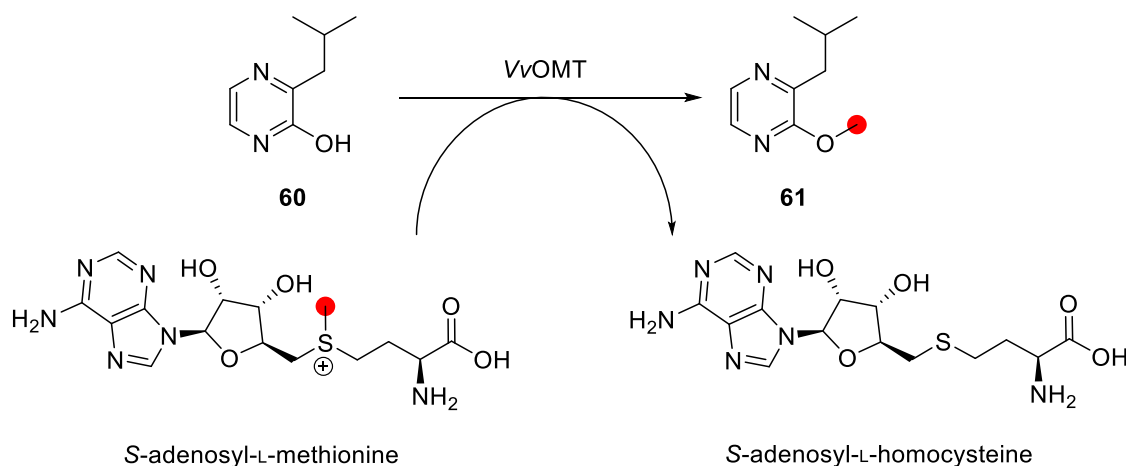
Scheme 9: Postulated biosynthesis of 3-isobutyl-2-methoxypyrazine (IBMP, **57**) via leucinamide (AMPA, **56**).^[72]

Enantioselective sBMP-analysis strengthened the hypothesis of natural amino acids being the precursors to MPs, as only (*S*)-sBMP was detected in raw vegetables. As displayed in **Scheme 10** the stereochemistry of L-isoleucine (**58**) is maintained during its incorporation into (*S*)-sBMP (**59**).^[47]



Scheme 10: Proposed incorporation of L-isoleucine (**58**) into (*S*)-sBMP (**59**). Retention of the stereochemistry of L-isoleucine during its incorporation.^[47]

While the first steps of the biosynthesis of MPs in plants are still discussed, the final enzymatically catalyzed step has already been confirmed. In 2001, an *S*-adenosyl-L-methionine (SAM) dependent enzyme has been identified to be responsible for the *O*-methylation (*O*-methyltransferase; OMT) of 3-alkyl-2-hydroxypyrazines (HPs) to MPs in *Vitis vinifera* grapes.^[73,74] Dunlevy *et al.* isolated the full-length sequences of two genes encoding *Vitis vinifera* *O*-methyltransferases (VvOMT1 and VvOMT2) in 2010.^[75] Two further VvOMTs (VvOMT3 and VvOMT4) were characterized in 2013.^[76,77]



Scheme 11: Final enzyme-catalyzed step in the biosynthesis of 3-alkyl-2-methoxypyrazines (MPs). Methylation of 3-isobutyl-2-hydroxypyrazine (IBHP, **60**) to 3-isobutyl-2-methoxypyrazine (IBMP, **61**) in *Vitis vinifera* grapes catalyzed by *S*-adenosyl-L-methionine dependent *Vitis vinifera* *O*-methyl-transferases (VvOMTs).^[73–75,77]

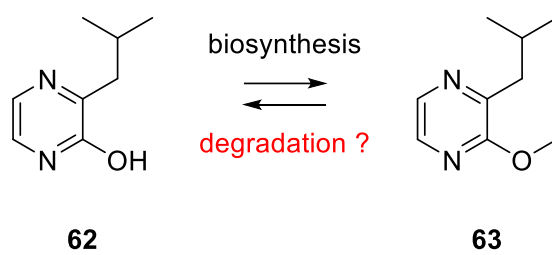
The VvOMTs differ in their affinities to catalyze the *O*-methylation of 3-isobutyl-2-hydroxypyrazine (IBHP) to 3-isobutyl-2-methoxypyrazine (IBMP) (**Scheme 11**).^[75] Differences in catalytic efficiencies are thought to be caused by steric hinderance and thus larger distances between the methyl-acceptor (HPs) and methyl-donor (SAM).^[78] The different catalytical efficiencies might be responsible for the varying distribution of IPMP, IBMP and sBMP within vegetables and grape tissues. Usually, all three MPs are present, but one is predominantly biosynthesized.^[14,75] In grapes for example IBMP is dominating. VvOMT3 is proposed to be mainly responsible for the *O*-methylation of IBHP in grapevines, as it is highly catalytically efficient and specific for the *O*-methylation of IBHP.^[76]

In 2016, three genes (*NbOMT1*, *NbOMT2*, and *NbOMT3*) encoding enzymes, which catalyze the *O*-methylation of IBHP in *Nicotiana benthamiana* (Solanaceae) were identified. *NbOMT1* showed the highest expression level. However, its expression decreased when plants were infected by bacterial phytopathogens (phytoplasmas).^[79]

Over the years it could be shown that IBMP-biosynthesis is affected by several abiotic and biotic stresses. As described above, in *Coffea* and *Nicotiana benthamiana* plants the IBMP-

biosynthesis seems to be up- or downregulated in response to biotic stress caused by insects or bacteria.^[70,79] In contrast, abiotic stresses including viticultural and environmental factors like temperature, sunlight exposure and soil as well as viticultural practices turned out to affect IBMP-levels in grapes.^[56,80] Especially cluster light exposure, and higher temperatures have shown to reduce MP-levels in grapes.^[81,82]

So far, it is unknown whether light suppresses IBMP-biosynthesis or if it causes IBMP-degradation. Light-induced photodegradation and a thermal-induced degradation are discussed in the literature.^[83] However, neither a degradation pathway nor degradation products have been identified yet. As decreasing IBMP-levels and increasing IBHP-levels have been observed during grape and bell pepper fruit ripening, it has been suggested that IBMP degrades back to IBHP (**Scheme 12**). However, not all of the IBMP was recovered as IBHP, so a subsequent IBHP-degradation, a coexisting degradation pathway or a volatilization of IBMP cannot be currently ruled out.^[75,84]



Scheme 12: Supposed degradation of IBMP (**63**) back to IBHP (**62**).^[84]

1.2.3 Analysis of 3-Alkyl-2-methoxypyrazines

Qualitative and quantitative analysis of MPs started with the first isolation of IBMP from bell peppers (*Capsicum annuum* L.) in 1969.^[46] Following that, isolation and extraction techniques as well as analytical methods were constantly optimized and adapted to different matrices. Over the years MP-analysis gained in importance, especially in complex matrices like vegetables, grapes and wine. Since MPs are ultra-trace components in grapes (ppt), wines (ppt) as well as in vegetables (ppb), sufficient extraction sensitivities must be ensured.^[48,84] Hence, powerful extraction techniques and extensive sample clean-up had to be developed.

IBMP was extracted for the first time from grapes using liquid-liquid extraction (LLE).^[54] Subsequently, many studies focused on improving the extraction of MPs. The extraction efficiencies of different LLE-solvents were examined.^[58,59,85] Moreover, various extraction techniques like (vacuum) distillation, stir bar sorptive extraction (SBSE), and headspace techniques like headspace solid-phase microextraction (HS-SPME) were implemented.^[55,56,81,86,87,88] Sample clean-up was mainly conducted by solid-phase extraction (SPE).^[55,87]

A few studies used liquid chromatography (LC) for the chromatographical separation of MPs.^[89] However, gas chromatography (GC) turned out to be the main separation technique. For MP-analysis, GC was hyphenated with different detection techniques like nitrogen phosphorus detection (NPD) as well as flame ionization detection (FID) and mass spectrometry (MS).^[54,90,91] Coelutions, which mainly occurred during the analysis of MPs in complex matrices affected the detection of MPs negatively. For this reason, multidimensional gas chromatography (MDGC), especially GC×GC-MS-hyphenation, became increasingly important.^[91–93]

2. HS-SPME-GC×GC-ToF-MS-Analysis

In the present thesis, MPs and their isotopologues were identified using HS-SPME-GC×GC-ToF-MS-analysis. HS-SPME-GC×GC-ToF-MS-analysis combines the headspace sampling technique and solid-phase microextraction with the comprehensive two-dimensional gas chromatography interfacing with time-of-flight-mass spectrometry. For MP-quantification, a stable isotope dilution assay was combined with a validated HS-SPME-GC-ToF-MS-method. SIDA-HS-SPME-GC-MS is widely used for the quantification of MPs in different matrices like coffee beans, wine and fragrant vegetable oils.^[49,58,94]

2.1 Solid-Phase Microextraction

SPME is a rapid, solvent-free sample preparation technique invented by *Arthur and Pawliszyn* in 1990.^[95] SPME is carried out using a sorbent-coated fused silica fiber, which is protected by a septum piercing needle. The SPME fiber can be inserted either directly into the sample (direct immersion solid-phase microextraction, DI-SPME) or into its headspace (headspace solid-phase microextraction, HS-SPME). DI-SPME is mainly used to extract non-volatile compounds, while HS-SPME usually extracts volatile and semi-volatile compounds.^[96]

2.1.1 Headspace Solid-Phase Microextraction

HS-SPME facilitates the extraction of analytes from a wide range of matrices. HS-SPME is a non-exhaustive extraction, as only parts of the analyte are removed from the sample. The SPME-process consists of three steps: incubation, extraction, and desorption.^[97]

First samples are incubated in a tightly sealed HS-vial for a predefined time. During incubation, analytes successively equilibrate among the HS and the sample. After incubation, extraction starts. The fiber is exposed to the sample's HS aiming the volatile's equilibria between the sample and the HS as well as the HS and the fiber coating (fiber) (**Figure 12**). Hence, for a complete extraction, the analyte needs to reach a distribution equilibrium between the sample, the headspace, and the fiber.^[98]

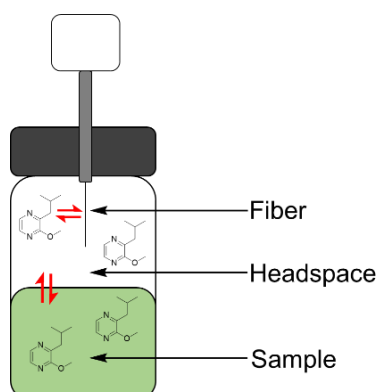


Figure 12: Principle of HS-SPME extraction.^[99]

As described in **Equation 1**, the amount of extracted analyte in equilibrium (n_{eq}) depends on the analyte's initial concentration (c_0), its distribution coefficients (K_x) between the three phases (fiber, HS, sample) and their volume ratios (V_x).^[99]

$$n_{eq} = \frac{K_{fs} V_f c_0 V_s}{K_{fs} V_f + K_{hs} V_h + V_s} \quad \text{Equation 1}$$

n_{eq} = mass analyte adsorbed by coating (fiber)

c_0 = initial concentration of the analyte

K_{fs} = distribution coefficient (fiber and sample)

K_{hs} = distribution coefficient (headspace and sample)

V_f = volume of coating (fiber)

V_s = volume of sample

V_h = volume of headspace

Reaching the equilibrium state may require a long extraction time, which, however, can be reduced by either higher temperatures or sample stirring. In fact, a combination of increasing temperature and sample agitation is often used to achieve a good extraction efficiency, while keeping the extraction time as short as possible.^[99,100] Besides, extraction efficiency depends on the physicochemical properties such as solubility, polarity, and volatility of the target analyte. Adding salt like sodium chloride (NaCl) to the sample improves the extraction of non-polar analytes (salting out effect). In contrast, pH-adjustment improves the recovery of acidic or basic analytes, as only undissociated compounds are adsorbed by SPME.^[101]

Extraction selectivity, in turn, is influenced by the fiber coating materials. SPME coatings differ in for example thickness, length, polarities as well as extraction mechanism (absorbent or adsorbent). Widely used coatings are PDMS (polydimethylsiloxane), PA (polyacrylate), DVB (divinylbenzene). PA- and DVB-fiber coatings are used for polar compounds, while a PDMS-coating is more convenient for the extraction of non-polar compounds. As samples generally consist of compounds having different polarities, mixed polymer coatings such as the Divinylbenzol/Carboxen/Polydimethylsiloxane (DVB/CAR/PDMS) coating were developed for the simultaneous extraction of analytes having different polarities.^[100,102]

SPME is compatible with GC and LC. After extraction, analytes are desorbed thermally from the SPME fiber into a GC- or LC-injector. The latter requires the use of suitable solvents as well as a special interface, which desorbs the analytes from the fiber into the mobile phase of the LC. In case of GC-analysis, splitless injection is usually used, as no solvent is present in the sample. The desorption efficiency is affected by parameters like desorption time and temperature as well as carrier gas flow.^[96]

SPME can be used for quantitative analysis. The equilibrium extraction method for instance uses the linear relationship between the mass of analyte extracted by SPME at equilibrium and its initial concentration ($n_{\text{eq}} \propto c_0$) (**Equation 1**).^[99] Once an equilibrium is reached the amount of the extracted compound does not increase even during further fiber exposure. Thus, the highest sensitivity is achieved at the extraction equilibrium.^[97] However, the time required to reach an equilibrium can take up to a few days. That is why the pre-equilibrium extraction method is often used instead. Using constant and reproduceable extraction conditions (extraction temperature, extraction time, agitation), quantification is possible even before equilibrium extraction is achieved. Moreover, appropriate calibration methods like standard addition, external standard calibration or internal standard calibration are required.^[103,104]

2.1.1.1 Stable Isotope Dilution Assay

Internal standard calibration is widely used for quantification, as it compensates potential matrix effects and significant losses of the target analyte during sample preparation and analysis. However, the choice of the internal standard is a crucial factor. The internal standard is added to the sample prior sample preparation and should, on the one hand, be a structural analog to the target analyte. It should have highly similar physicochemical properties such as solubility, polarity, and volatility like the analyte, as otherwise it would result in over- or underestimations of the analyte. On the other hand, the analyte and internal standard need to differ in their retention to provide a chromatographical separation.^[103] Thus, choosing a proper internal standard might be challenging.

A highly precise quantification method is the stable isotope dilution assay (SIDA), which was developed by *Schieberle and Grosch* in 1987.^[105] The use of a stable isotope labeled compound leads to accurate results. As the analyte and its stable isotope labeled counterpart are almost chemically identical, their concentration-ratio should remain stable during sample preparation and analysis. After adding the stable isotope labeled compound to the sample, it needs to equilibrate in the sample's matrix. Otherwise, the recovery of the added, isotope-labeled standard might be higher than for the matrix-bound analyte, resulting in an underestimation of the analyte.^[106] For calibration, solutions containing different analyte-concentrations and a fixed concentration of the stable isotope labeled standard are prepared. A calibration curve is developed by plotting the concentration ratios against the ratios of the respective peak areas.^[106,107]

The analyte and its stable isotope labeled analogue can be separated by gas chromatography (GC), due to the *inverse isotope effect*.^[108] In case of coelutions, they are distinguishable using mass spectral detection techniques. By introducing at least one stable isotope, the internal standard has a higher molecular weight compared to its unlabeled counterpart. The mass-to-charge-ratios (m/z) of the molecular ion (M^{+*}) is thus shifted to higher

m/z -values. A loss of the stable isotope labeled motif during fragmentation should be avoided, to enable the detection of mass shifts of fragment ions.^[106]

2.2 Multidimensional Gas Chromatography

GC is a method for separating analytes based on their volatility. The separation of compounds with similar boiling points is achieved using stationary phases with different polarities. The separation power is limited by the separation space i.e. the peak capacity of a conventional one-dimensional gas chromatography (1D GC).^[109]

To expand the separation space and thus increase the peak capacity, multidimensional gas chromatography (MDGC) was invented. MDGC requires at least two columns (two dimensions) with different chemical properties.^[110] However, coupling two columns directly has the same effect as mixing different stationary phases – it improves the separation, but does not increase the peak capacity. To enhance the peak capacity a modulator needs to be applied as an interface between the two columns. The modulator accumulates, refocuses, and reinjects the eluate from the first column (first dimension, ¹D) onto the second column (second dimension, ²D). There are several types of modulators commercially available such as valve-based, thermal- or cryo-modulators. A thermal loop modulator for instance traps and refocuses the analytes by a cold nitrogen gas jet at the end of the first column. It generates two cold spots on a twice looped segment of the ²D. While the cold nitrogen gas flows continuously, the hot jet is activated periodically and remobilizes the analytes releasing them onto the ²D. During the modulation process, the signal of an analyte eluting from the ¹D is cut into several fractions, which can then be transferred to the ²D. The time needed for one modulation cycle is called modulation period (P_M).^[111] Two-dimensional GC (2D GC) is classified into *heart-cutting* (H/C) 2D GC or *comprehensive* 2D GC (GC×GC). H/C 2D GC turned out to be an effective separation method for target analysis, as only preselected fractions of the sample are transferred to the ²D, whereas GC×GC enables a continuous two-column separation of the sample.^[112]

Moreover, to expand the separation space a so-called ‘orthogonality’ should be achieved. A 2D GC-system is described as ‘orthogonal’ when there is no correlation between the retention mechanism in the two dimensions. Thus, for orthogonality the separation mechanisms of the two dimensions need to be independent from another. Usually, the ¹D consists of an apolar column, while a (semi-) polar column is used as the ²D (apolar × (semi-)polar). In an apolar ¹D, analytes are separated according to their volatility. Coeluting analytes having the same volatility can then be separated based on their polarity using a (semi-)polar ²D. However, in practice ideal orthogonality is never achieved, due to dispersion interactions, which occur in

any stationary phase. Coeluting substances can be distinguished using different detection methods like mass spectrometry (MS).^[109,113]

2.2.1 Comprehensive Two-Dimensional Gas Chromatography – Time of Flight Mass Spectrometry

GC×GC was first developed in 1991.^[114] It provides a high peak capacity and thus enables the separation of a wide range of analytes in a highly complex matrix. As a continuous process, GC×GC requires a fast modulation process. A ¹D-signal should be modulated at least three times, so a P_M usually takes 2–10 s.^[115] ²D-separation should ideally be completed within one P_M to avoid the coelution of two subsequent fractions called 'wrap around'. To ensure a fast ²D-separation, a short column (1–2 m) having a thin film thickness (d_f 0.1 μm) and a narrow inner diameter (I.D. 0.1 mm) is usually used for the ²D.^[112]

The focusing effect during modulation reduces the signal widths of analytes leading to sharp signals and improved detection limits.^[116] Due to narrow peaks eluting from the ²D, detectors with high sampling rates are required for GC×GC-analysis. At least 10 data points per peak are required to ensure an accurate peak reconstruction and quantification. Thus, the acquisition rate of a mass spectrometer needs to be sufficiently high. That is why scanning detectors like quadrupole and ion traps are less suitable for GC×GC-analysis than time-of-flight mass spectrometer (ToF MS).^[117]

In fact, ToF-analyzers are known for their high acquisition rate. They separate ions of a pulsed ion beam according to the time they need to fly through a field-free flight path called 'drift tube'. The ion's velocity in the drift tube depends mainly on its mass. Therefore, high-mass ions reach a lower velocity than low-mass ions. To enhance the mass resolution of a ToF-analyzer, the drift path is usually elongated by an electric counter field (reflector), which reflects the entering ions. A reflector consists of ring-shaped electrodes with increasing potential. Thus, the higher the ion's kinetic energy the deeper it enters the reflector. After reaching a kinetic energy of zero the ions are expelled towards the detector. Ions having the same mass, but different kinetic energies are re-focused after passing the reflector, which leads to sharp signals.^[118]

The main advantage of a GC×GC-MS-hyphenation is additional structural information allowing the identification of many analytes within a single GC×GC-analysis.

3. Objective of the Study

The aim of this thesis was the identification of precursors in the biosynthesis of IBMP. For this purpose, *in vivo* feeding experiments were performed using stable isotope labeled compounds. To detect the incorporation of stable isotopes into IBMP a method combining HS-SPME with GC×GC and ToF-MS was developed.

Due to their high IBMP-contents, *Capsicum annuum* L. (bell pepper) fruits were used for feeding studies. First, experiments focused on the pericarp tissue, which is the edible part of the fruit. The incorporation of deuterium atoms leads to a decrease in the retention time of an analyte. This *inverse isotope effect* facilitates the detection of deuterium-incorporation, as the deuterated and the unlabeled, genuine analytes are separable by GC. However, the *inverse isotope effect* becomes weaker for stable isotope labeled carbon (^{13}C) and nitrogen (^{15}N).^[108] To identify ^{13}C -/ ^{15}N -incorporations, isotopic enrichments in distinct isotopic mass peaks, which can be detected by mass spectrometry are used instead. If ^{13}C -/ ^{15}N -incorporation rates are low the coeluting genuine compound can mask them, which makes the detection of ^{13}C -/ ^{15}N -incorporation more difficult or even impossible. Consequently, to identify even low incorporation rates of ^{13}C -/ ^{15}N -atoms into IBMP a new experimental design for feeding experiments needed to be developed (**Chapter 2** and **Chapter 3**).

Later, distinct parts of the fruit such as calyx, pedicel, placenta, and seed as well as different plant organs like flowers, leaves, shoots, and roots were analyzed regarding their ability to biosynthesize IBMP *de novo*. Moreover, the IBMP-distribution within the whole plant was examined. For IBMP-quantification a method combining HS-SPME-GC-ToF-MS-analysis and SIDA was developed and validated. Furthermore, a long-distance transport of IBMP through the plant via the phloem was examined. For this purpose, petiole phloem exudates were collected using the EDTA-(ethylenediaminetetraacetic acid)-facilitated method and analyzed by HS-SPME-GC-ToF-MS (**Chapter 4**).

4. List of Publications

Parts of this thesis have been published or are accepted for publication in peer-reviewed journals:

1. Zamolo, F.; Wüst, M. Investigation of Biosynthetic Precursors of 3-Isobutyl-2-Methoxypyrazine Using Stable Isotope Labeling Studies in Bell Pepper Fruits (*Capsicum annuum* L.), *J. Agric. Food Chem.* **2022**, *70*, 6719–6725.

DOI: 10.1021/acs.jafc.2c01747

This published article is summarized in **Chapter 2** of the thesis.

2. Zamolo, F.; Wüst, M. L-Serine is the Direct Precursor for the Pyrazine Ring Construction in the Biosynthesis of 3-Isobutyl-2-Methoxypyrazine in Bell Pepper Fruits (*Capsicum annuum* L.), *Chem. Eur. J.* **2023**, e202203674.

DOI: 10.1002/chem.202203674

This accepted article is summarized in **Chapter 3** of the thesis.

3. Zamolo, F.; Heinrichs, J. P.; Wüst, M. Sites of biosynthesis, distribution and phloem transport of 3-isobutyl-2-Methoxypyrazine in *Capsicum annuum* (bell pepper) plants, *Phytochemistry* **2023**, *205*, 113488.

DOI: 10.1016/j.phytochem.2022.113488

This published article is summarized in **Chapter 4** of the thesis.

Reprints of all mentioned publications are given in the appendix (**Chapter 8 Appendix E – G**) of this thesis.

Abstracts for poster flash talks:

1. Zamolo, F.; Wüst, M. Biosynthese von 3-Isobutyl-2-methoxypyrazin in Paprikafrüchten (*Capsicum annuum* L.). 50. Deutscher Lebensmittelchemikertag in Hamburg, September 19-21, **2022**, *Lebensmittelchemie*, *76*, S2-072-S2-072.

DOI: 10.1002/lemi.202259045

2. Zamolo, F.; Wüst, M. Biosynthesis of 3-Isobutyl-2-Methoxypyrazine in Bell Pepper Fruits (*Capsicum annuum* L.). BIOFLAVOUR 2022 - Biotechnology of Flavours, Fragrances and Functional Ingredients, Frankfurt, September 27-30, **2022**.

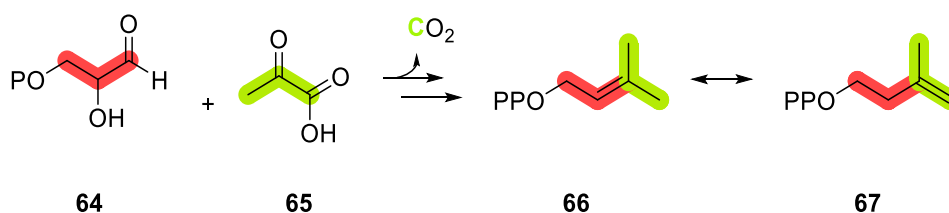
Chapter 2

1. General Introduction

The biochemistry of plants is complex. Due to the vast variety of plants, plant's metabolism cannot be generalized. Moreover, it is highly flexible since plants are sessile organisms. Plant's metabolism changes under certain circumstances. For instance, plants respond to abiotic and biotic stress by up- and downregulating enzymes and hence (in-)activating different metabolic pathways. This in turn leads to the biosynthesis and accumulation of certain secondary metabolites, which for instance serve for the plant's defense.^[119,120]

By far not all metabolic pathways involved in the metabolism of plants have been investigated yet. For pathway delineation different research areas need to be combined. Apart from genetic and enzymatic approaches, stable isotope labeling experiments play a key role in dissecting metabolic pathways. Following the fate of stable isotope labeled compounds through biosynthetic processes facilitates the elucidation of novel biosynthetic pathways. In fact, stable isotope labeling experiments turned out to be a crucial tool to decipher complex metabolic mechanisms. Via isotope tracer experiments, precursors, and intermediates and thus the origin of metabolites can be determined on a molecular level.^[121]

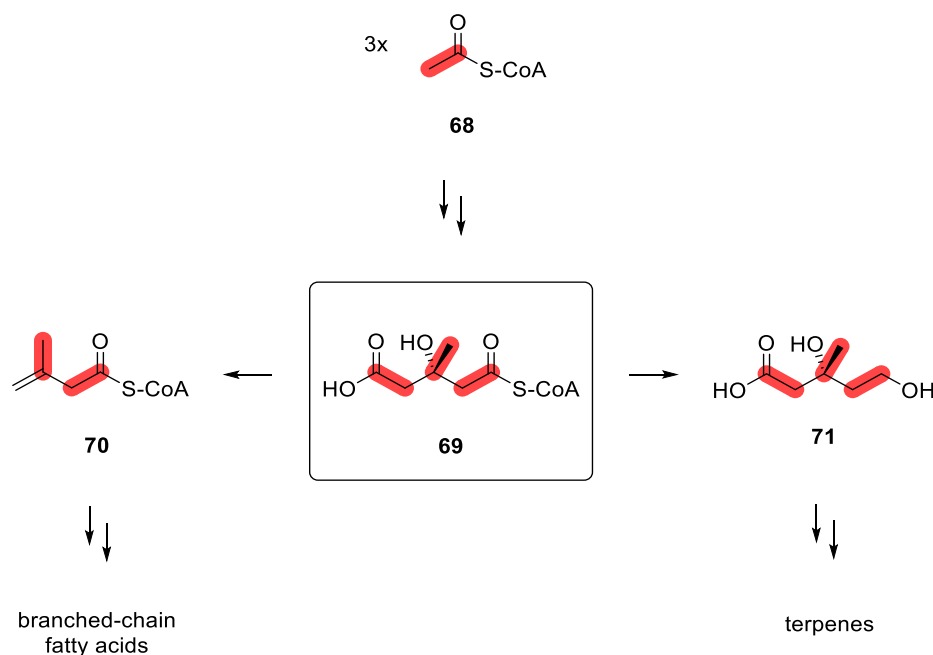
Over the years, many biosynthetic pathways have been elucidated using stable isotope techniques. The use of ¹³C-labeled compounds for example allowed the discovery of glyceraldehyde-3-phosphate (**64**) and pyruvate (**65**) as precursors to the isoprenoid building blocks dimethylallyl-diphosphate (DMAPP, **66**) and isopentenyl-diphosphate (IPP, **67**) (**Scheme 13**).^[122]



Scheme 13: Glyceraldehyde-3-phosphate (**64**) and pyruvate (**65**) as precursors of dimethylallyl-diphosphate (DMAPP, **66**) and isopentenyl-diphosphate (IPP, **67**). The MEP-(2-C-methyl-D-erythritol-4-phosphate)-pathway, as a non-mevalonate pathway to the isoprenoid building blocks IPP and DMAPP.^[122]

Moreover, stable isotope labeling studies proved a metabolic link between the mevalonate pathway and the biosynthesis of branched-chain fatty acid biosynthesis in myxobacteria. It could be shown that three molecules of acetyl-CoA (**68**) condensate to 3-hydroxy-3-methylglutaryl-CoA (3-HMG-CoA, **69**), which in turn can be converted into either

3-methylbut-3-enoyl-CoA (**70**), which is a precursor for branched-chain fatty acids or mevalonate (**71**), which serves as a precursor to terpenes (**Scheme 14**).^[123]



Scheme 14: Shunt pathway that connects the mevalonate pathway and branched-chain fatty acids via 3-hydroxy-3-methylglutaryl-CoA (3-HMG-CoA, **69**).^[121]

For stable isotope labeling experiments, samples like intact plant tissues (*in vivo*) or cell cultures (*in vitro*) are incubated with isotopically labeled compounds. As the labeled compound has almost the same chemical properties like its unlabeled counterpart, they are identically distributed within the plant and equally metabolized by the plant.^[124] The incorporation of a stable isotope labeled compound can be verified based on the labeling pattern of the metabolic product formed during incubation. Commonly used isotopes are deuterium, ¹³C, ¹⁵N and ³⁴S.^[124,125]

The identification and quantification of the incorporation of isotopically labeled precursors into the metabolites requires powerful analytical instruments like MS. The incorporation of stable isotopes leads to higher intensities in distinct isotopic mass peaks, which are detectable by MS. On the one hand, MS allows to figure out whether the compound is incorporated or not. On the other hand, it shows how often it has been incorporated and which building blocks have been incorporated. The results of stable isotope tracer experiments hence give advice to important intermediates.^[124,125] Usually, MS is coupled to a chromatographic system like GC or LC, which allow the separation of compounds that otherwise would be indistinguishable.^[126]

Investigation of Biosynthetic Precursors of 3-Isobutyl-2-methoxypyrazine
Using Stable Isotope Labeling Studies in Bell Pepper Fruits
(*Capsicum annuum* L.)

The research summarized in this chapter has been published as
Zamolo, F.; Wüst, M., *J. Agric. Food Chem.* **2022**, *70*, 6719–6725.
<https://doi.org/10.1021/acs.jafc.2c01747>.

A reprint of this publication is given in **Chapter 8 Appendix E** of this thesis.

Author's contributions: My contributions to this research entail the implementation of the feeding experiments including method development and optimization, data evaluation as well as summarizing the findings and writing the resulting publication. The supervisor of my doctoral thesis *Prof. M. Wüst* provided guidance, gave important suggestions and writing assistance.

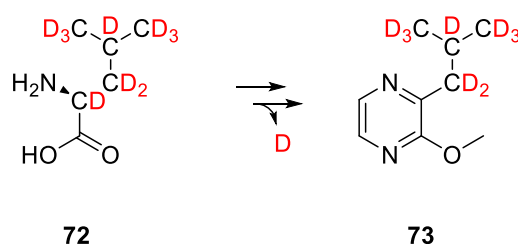
Reprinted with permission from *J. Agric. Food Chem.* **2022**, *70*, 22, 6719–6725.
Copyright 2022 American Chemical Society.

2. Summary

The main topic of this study is the identification of IBMP-precursors. For this purpose, *in vivo* feeding experiments were conducted using stable isotope labeled compounds and the pericarp tissue of bell pepper fruits (*Capsicum annuum* L.). Samples were treated directly after harvesting. Pedicel, calyx, and placenta were removed, and the pericarp was disinfected with a sodium-hypochlorite (NaOCl) solution to avoid microbial contamination. Afterwards, samples were washed with water to remove remaining NaOCl. Samples were incubated for 48 h with a stable isotope labeled compound.

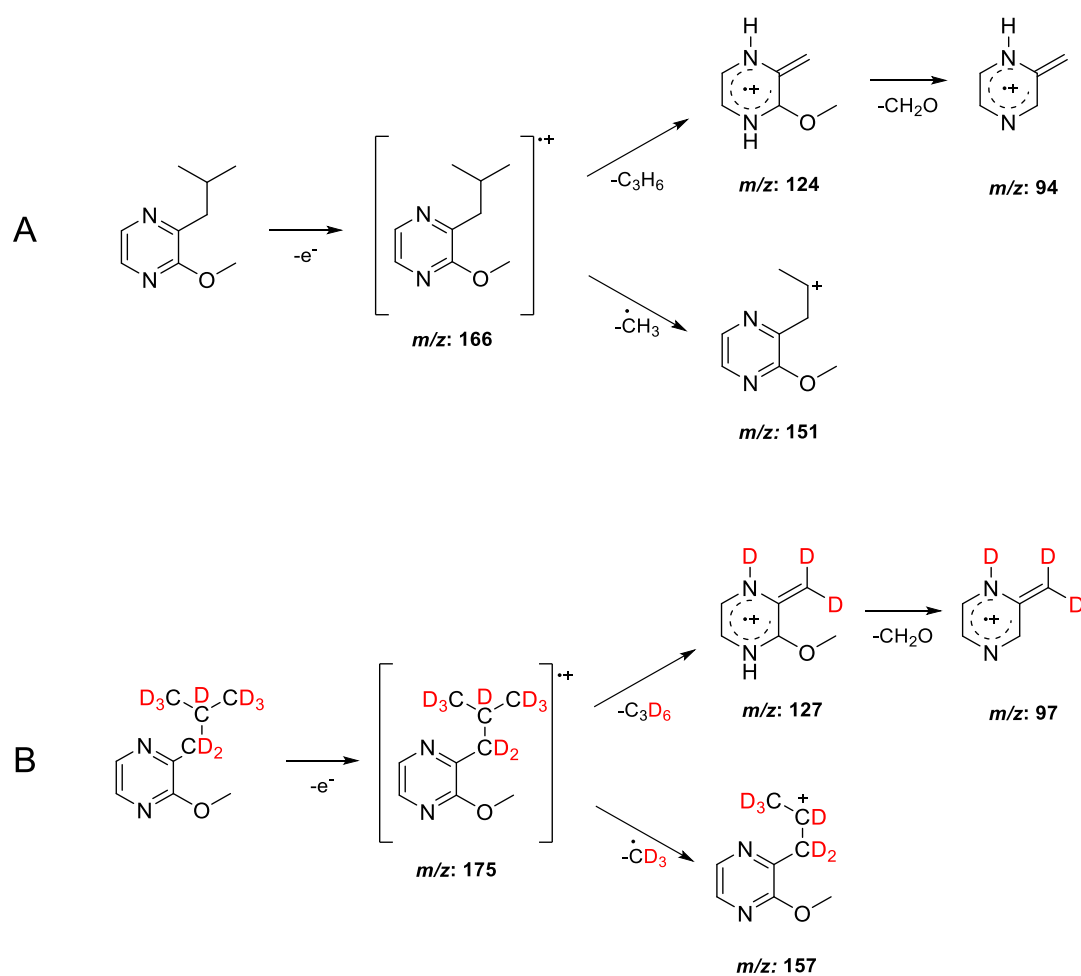
For *in vivo* stable isotope feeding experiments, a method combining HS-SPME with GC×GC and ToF-MS was developed. HS-SPME was carried out using a DVB/CAR/PDMS-coated 2 cm-fiber, which had a good response to IBMP.^[88,92,127] An aqueous solution containing sodium chloride was added to each sample to additionally enhance SPME efficiency (salting-out effect).^[128]

Due to their similarity in the branched side chain, L-leucine has frequently been considered as a potential precursor for IBMP.^[14,51,66] Thus, feeding experiments were conducted using deuterium labeled L-leucine (L-leucine- d_{10}). Since the α -deuterium of L-leucine- d_{10} dissociates during the formation of the pyrazine ring, its incorporation should yield a nine-fold deuterated IBMP (IBMP- d_9). Using pericarp tissue of unripe, green bell pepper pericarp revealed an incorporation of L-leucine (**72**) into IBMP (**73**) (**Scheme 15**). Due to the *inverse isotope effect*, GC×GC-analysis enabled the separation of deuterated IBMP and genuine IBMP. The number of incorporated deuterium atoms was determined based on mass spectral data.



Scheme 15: Incorporation of L-leucine- d_{10} (**72**) generating IBMP- d_9 (**73**). Based on *in vivo* feeding experiments using green, unripe bell pepper pericarp (*Capsicum annuum* L.).

The mass spectrum of deuterated IBMP shows a similar fragmentation pattern to IBMP with shifts to higher masses. The shift of the molecular ion ($M^{+\bullet}$) by nine mass units (m/z 166 to m/z 175) confirmed the incorporation of nine deuterium atoms (IBMP- d_9). In addition, a base peak at m/z 127 resulting from the elimination of deuterated propene (C_3D_6) in turn of a *McLafferty* rearrangement as well as the shift of m/z 151 to m/z 157 due to the methyl radical loss from the isobutyl side chain revealed an incorporation of L-leucine- d_{10} into IBMP (**Scheme 16**).



Scheme 16: Fragmentation pattern of IBMP (**A**) and IBMP-*d*₉ (**B**). Mass shifts in the molecular ion (M^{•+}) *m/z* 166 to *m/z* 175, as well as fragment ions *m/z* 124 to *m/z* 127, *m/z* 151 to *m/z* 157 and *m/z* 94 to *m/z* 97 confirmed the deuteration of the whole isobutyl-moiety of IBMP.

Comparable results were expected when L-leucine-*d*₁₀ was fed to the pericarp of ripe, yellow bell pepper fruits. However, no incorporation of L-leucine-*d*₁₀ into IBMP could be detected. It is known that IBMP-levels decrease during bell pepper and grape ripening. Moreover, a reduced expression of important enzymes involved in MP-biosynthesis was observed in grapes during ripening.^[72] Therefore, it might be that no *de novo* biosynthesis was detectable in ripe fruits due to the down-regulation of important enzymes.

Further experiments were conducted using the pericarp tissue of unripe, green bell pepper fruits. Branched chain amino acids (BCAAs) like L-leucine play an important role in the biosynthesis of several branched-chain volatiles (BCVs), which contribute to the fruity aroma notes of fruits like 2-methylbutanoate esters in strawberries (*Fragaria × ananassa* Duch.) and bananas (*Musa sapientum* L.).^[129] First, it has been suggested that BCVs are biosynthesized as a result of the catabolic degradation of BCAAs in the mitochondria.^[130] Later, the mitochondrial catabolism of BCKAs turned out to be responsible for the biosynthesis of BCVs in fruits like tomatoes.^[131]

To examine the relevance of BCKAs in IBMP-biosynthesis feeding experiments were conducted using α -ketoisocaproic acid (α -KIC), which is the BCKA of L-leucine. Feeding studies revealed an incorporation of α -KIC- d_7 into IBMP. To further investigate which precursor is more efficient, the incorporation rates of α -KIC- d_7 and L-leucine- d_{10} were compared by feeding both compounds simultaneously (co-feeding experiment). In co-feeding experiments, L-leucine showed higher incorporation rates. However, such a higher incorporation rates might also occur due to differences in the cellular uptake, metabolism, and distribution of these compounds. To overcome these differences L-leucine- $^{13}\text{C}_6,^{15}\text{N},2,3,3,4,5,5,5,5',5',5'-d_{10}$ (L-leucine- $^{13}\text{C}_6,^{15}\text{N}, d_{10}$) was used for ensuing investigations. Results proved that the ^{15}N -label is mostly lost during IBMP-biosynthesis, showing that BCKAs are relevant in the biosynthesis of MPs.

Further experiments were conducted to examine which compound serves as the nitrogen donor to IBMP and to identify the C_2 -unit-precursor, which is required to generate the IBMP-heterocycle. However, the *inverse isotope effect* is less effective for stable isotope labeled carbon (^{13}C) and stable isotope labeled nitrogen (^{15}N). So, mixed labeling studies (co-feeding experiments) were performed by feeding L-leucine- d_{10} simultaneously to a putative $^{13}\text{C}/^{15}\text{N}$ -labeled precursor. As displayed in **Figure 13** co-feeding L-leucine- d_{10} and for instance $^{13}\text{C}_2$ -glyoxylic acid should result in the biosynthesis of IBMP- d_9 (A), $^{13}\text{C}_2$ -IBMP- d_9 (B) and $^{13}\text{C}_2$ -IBMP (C).

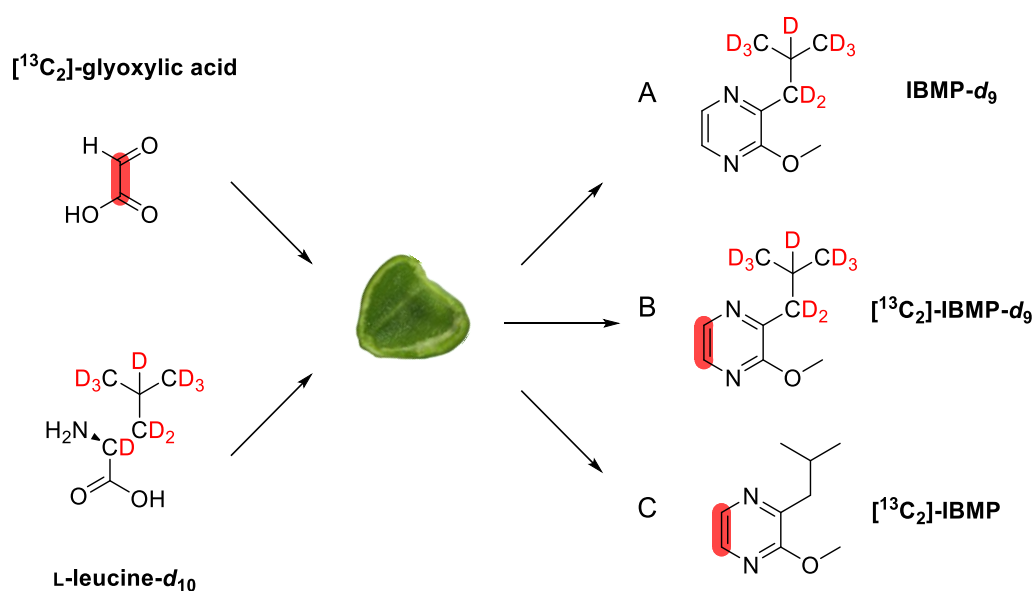


Figure 13: Expected labeling pattern of IBMP in co-feeding studies with $^{13}\text{C}_2$ -glyoxylic acid and L-leucine- d_{10} . Incorporation of (A) L-leucine- d_{10} , (B) L-leucine- d_{10} and $^{13}\text{C}_2$ -glyoxylic acid, (C) $^{13}\text{C}_2$ -glyoxylic acid.

The biosynthesis of $^{13}\text{C}_2$ -IBMP- d_9 and thus an incorporation of $^{13}\text{C}_2$ -glyoxylic acid would be detectable by GC \times GC-ToF-MS. On the one hand, the incorporation of deuterium atoms should

allow the separation of the genuine IBMP and its heavier isotopologue by GCxGC. On the other hand, a chromatographically separation should enable the detection of isotopic enrichments in distinct isotopic mass peaks by ToF-MS.

In fact, the *inverse isotope effect* was enhanced by the incorporation of the deuterium atoms of L-leucine- d_{10} resulting in the separation of the labeled and unlabeled isotopologues by GCxGC. Based on mass spectral data an incorporation of a C₁-unit of glycine and glyoxylic acid as well as one nitrogen atom of glutamine could be confirmed.

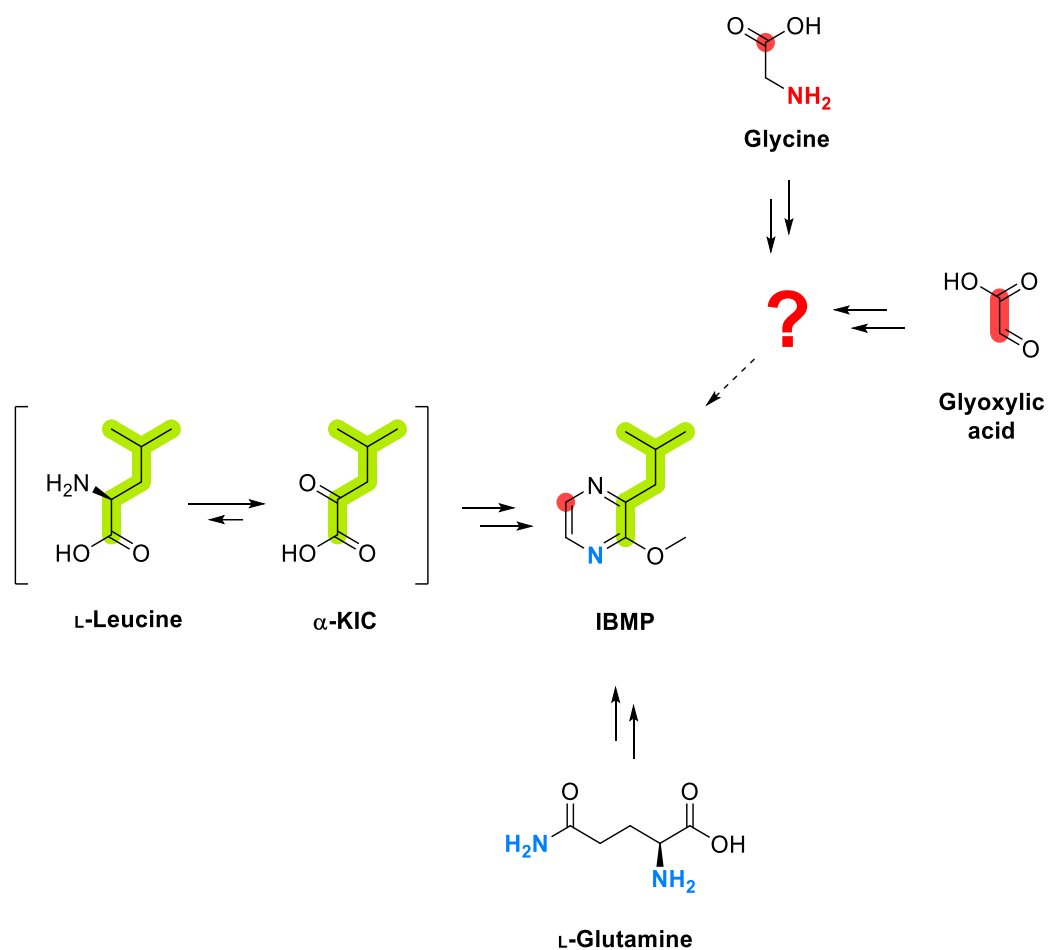


Figure 14: Incorporation of L-leucine and α -KIC as well as glyoxylic acid, glycine, and glutamine into IBMP., based on *in vivo* feeding experiments using green, unripe bell pepper pericarp (*Capsicum annuum* L.). The exact position of the ^{13}C -label in the pyrazine ring (^{13}C -5 or ^{13}C -6; here ^{13}C -5 is shown) cannot be determined at the present stage.

In sum, feeding studies revealed that IBMP is biosynthesized in the pericarp tissue of unripe bell pepper fruits. Feeding experiments showed that L-leucine and α -KIC are important precursors for the biosynthesis of IBMP. Moreover, L-glutamine turned out to serve as a nitrogen source in IBMP-biosynthesis, while glycine as well as glyoxylic acid provide a C₁-building block to IBMP (**Figure 14**).

Chapter 3

1. General Introduction

L-Serine is a proteinogenic amino acid, which plays a key role in plant metabolism. It is an important building block for many biomolecules. L-Serine participates in the biosynthesis of proteins, phospholipids as well as cysteine and glycine. Moreover, it serves as an important C₁-unit donor and participates in the biosynthesis of purines and pyrimidines as well as methionine (**Figure 15**).^[132,133]

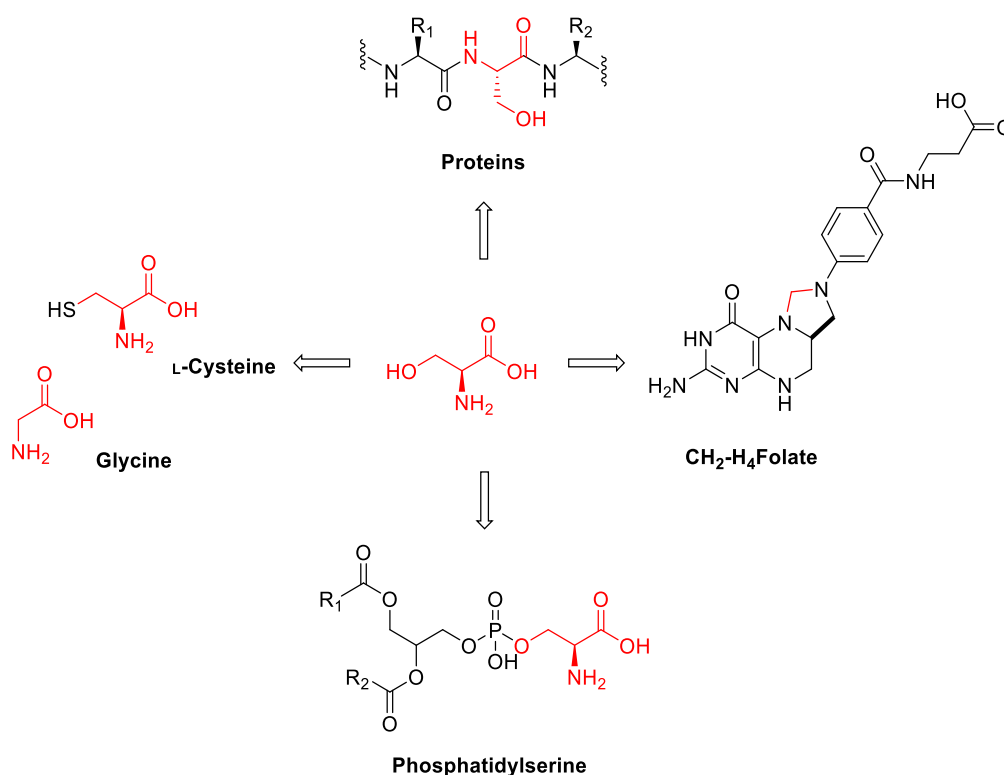
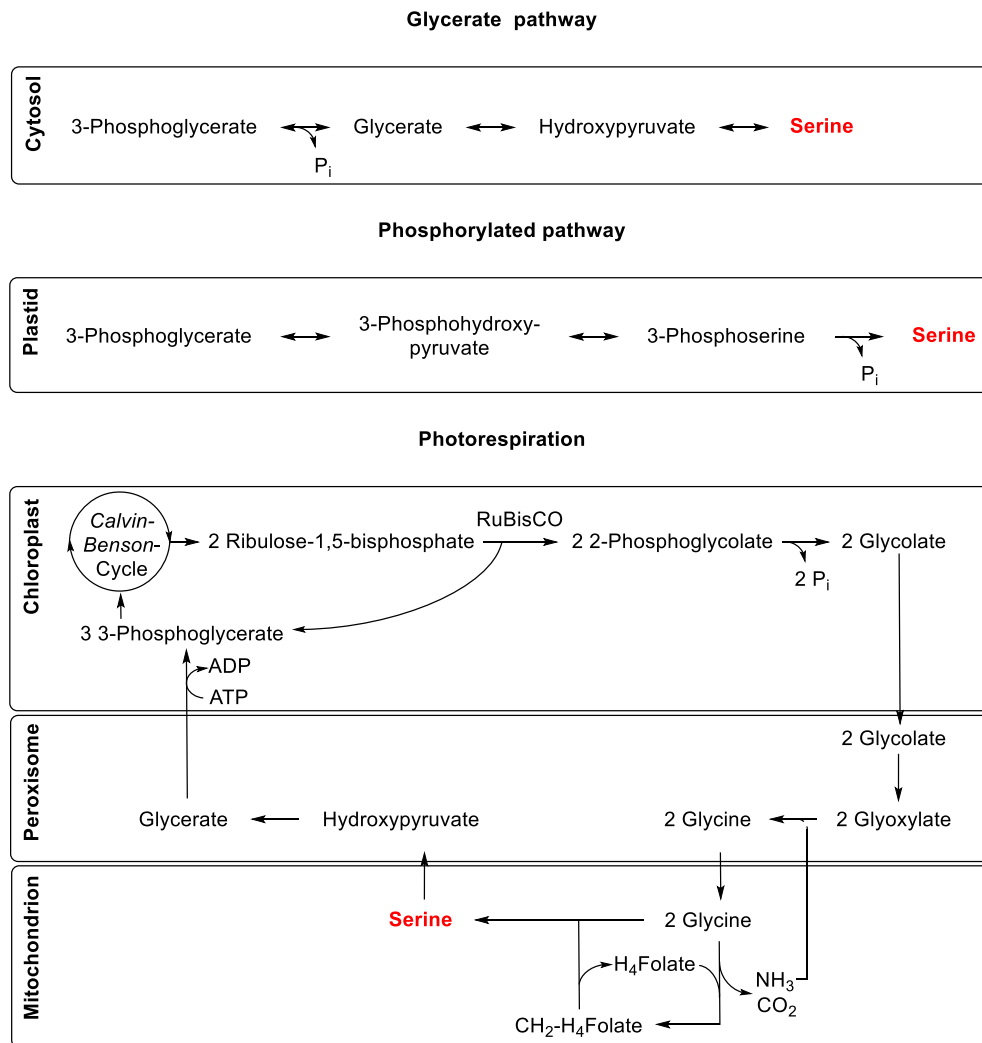


Figure 15: L-Serine as an important building block for several biomolecules.

L-Serine is important for the plant's response to abiotic stresses like flooding, salinity and low temperatures.^[134] Deficiencies in L-serine can result in a higher embryo abortion rate in *Arabidopsis* (*Arabidopsis thaliana*), due to the lack of phosphatidylserine. This can lead to a decrease in embryogenesis, post-embryonic root development, and photorespiration because of a reduced folate metabolism.^[135] To maintain homeostasis, serine-levels in plants need to be strictly regulated.^[133]

In plants are three pathways to L-serine occurring in different cell organelles. While the phosphorylated pathway is located in the plastids, the glycerate pathway occurs in the cytosol and the glycolate pathway in the mitochondrion. As displayed in **Scheme 17** the glycerate pathway starts with a dephosphorylation of 3-phosphoglycerate (3-PGA) to glycerate, which is

oxidized to hydroxypyruvate. In the last step hydroxypyruvate forms serine. During the phosphorylated pathway 3-PGA is first oxidized to 3-phosphohydroxypyruvate which is converted to 3-phosphoserine (PS). Finally, PS is dephosphorylated into serine. While the functional importance of the glycerate pathway is still unknown, the phosphorylated pathway turned out to be essential for the development of plant's embryos, male gametophytes as well as roots. In contrast, the glycolate pathway is the most important L-serine-source in photosynthetic cells where it is associated with the photorespiration pathway.^[136]



Scheme 17: Different biosynthetic pathways to serine in plants.^[133]

Photorespiration is often considered as a wasteful and inefficient process, as it lowers the efficiency of photosynthesis. The main objective of the photorespiratory cycle might be the detoxification of 2-phosphoglycolate (2-PG), which is formed due to the fixation of O₂ catalyzed by the ribulose-1,5-bisphosphate carboxylase/oxygenase (RuBisCO). However, during this detoxification the multi-compartmental cycle interacts with different metabolic processes like nitrogen assimilation and C₁-metabolism.^[136–138]

Photorespiration starts in the chloroplasts. The O_2 -fixation catalyzed by RuBisCO leads to the formation of 3-phosphoglycerate (3-PGA) and 2-PG. While 3-PGA re-enters the *Calvin Benson* cycle, toxic 2-PG needs to be detoxified. In the chloroplast 2-PG forms glycolate, which is transported into the peroxisome where it is irreversibly oxidized to glyoxylate. Following this, glyoxylate is transaminated to glycine, which is transported into the mitochondrion, where two molecules of glycine yield serine. The latter reaction interacts with the plant's nitrogen assimilation and C_1 -metabolism. Catalyzed by the multienzyme glycine decarboxylase complex (GDC) one molecule of glycine is transaminated and decarboxylated to react with one molecule of tetrahydrofolate (H_4 Folate) forming methylene-tetrahydrofolate (CH_2 - H_4 Folate). By combining CH_2 - H_4 Folate and a second molecule of glycine, serine is obtained. Subsequently, serine is transported into the peroxisomes where it is converted to hydroxypyruvate, which in turn is reduced to glycerate. Glycerate is transported back into the chloroplast and forms 3-PGA, which enters the *Calvin Benson* cycle.^[133,136,139]

L-Serine is the Direct Precursor for the Pyrazine Ring Construction in the
Biosynthesis of 3-Isobutyl-2-methoxypyrazine in Bell Pepper Fruits
(*Capsicum annuum* L.)

The research summarized in this chapter has been published as
Zamolo, F.; Wüst, M., *Chem. Eur. J.* **2023**, e202203674.
<https://doi.org/10.1002/chem.202203674>.

A reprint of this publication is given in **Chapter 8 Appendix F** of this thesis.

Author's contributions: My contributions to this research include the implementation of the feeding experiments including the collection, analysis and evaluation of data as well as summarizing the results and preparing the manuscript. The supervisor of my doctoral thesis *Prof. M. Wüst* provided guidance, gave important suggestions and writing assistance.

Reprinted with permission from *Chem. Eur. J.* **2023**, 29, e202203674.

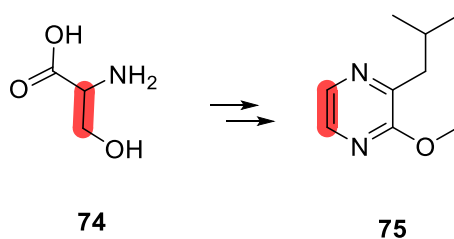
Copyright 2023 Wiley.

2. Summary

Prior feeding experiments proved that glyoxylate and glycine serve as C₁-building blocks in the biosynthesis of IBMP. In plants, glycine and glyoxylate are biochemically linked via photorespiration. During photorespiration, glyoxylate is aminated to glycine. One molecule of glycine undergoes a deamination and decarboxylation generating a C₁-intermediate, which interacts with tetrahydrofolate (H₄Folate) forming 5,10-methylene-tetrahydrofolate (CH₂-H₄Folate). CH₂-H₄Folate in turn reacts with another glycine molecule forming L-serine.^[138,140,141] This metabolic interface of the photorespiratory cycle and the C₁-metabolism via glycine, formed from glyoxylate, gave evidence to L-serine being the direct precursor to the pyrazine ring construction of MPs.

Therefore, the main subject of this paper is to decipher the role of L-serine in the biosynthesis of IBMP in bell pepper pericarp (*Capsicum annuum* L.). For this purpose, *in vivo* feeding experiments were performed with ¹³C- and ¹⁵N-labeled L-serine and unripe, green bell pepper pericarp. After a 48 h-incubation, samples were analyzed using HS-SPME-GC×GC-ToF-MS. However, the *inverse isotope effect* was too weak for a separation of genuine IBMP and ¹³C-/¹⁵N-labeled IBMP by GC×GC. Moreover, the levels of endogenous IBMP were too high to detect an ¹³C-/¹⁵N-incorporation by isotopic enrichments. That is why mixed labeling studies (co-feeding experiments) were performed by feeding a putative ¹³C-/¹⁵N-labeled precursor and a known IBMP-precursor (L-leucine-*d*₁₀) simultaneously.

Co-feeding studies with L-[2-¹³C]-serine proved for the first time that L-serine is incorporated into IBMP. Based on HS-SPME-GC×GC-ToF-MS-analysis it could be shown that L-serine is a precursor in the biosynthesis of the pyrazine ring motif of IBMP. As it was still unclear whether L-serine serves as a C₁- or C₂-building block, further co-feeding experiments were conducted using L-[2,3-¹³C₂]-serine. Isotope mass shifts clearly proved that the two ¹³C-labeled carbon atoms were incorporated into IBMP. Thus, it could be shown that L-serine (**74**) contributes at least a C₂-unit to the pyrazine heterocycle of IBMP (**75**) (**Scheme 18**). The incorporations of the carbon atoms at the positions C-2 and C-3 imply that the carbon atom at position C-1 is lost during the biosynthesis of IBMP. Thus, a decarboxylation of L-serine is conceivable.



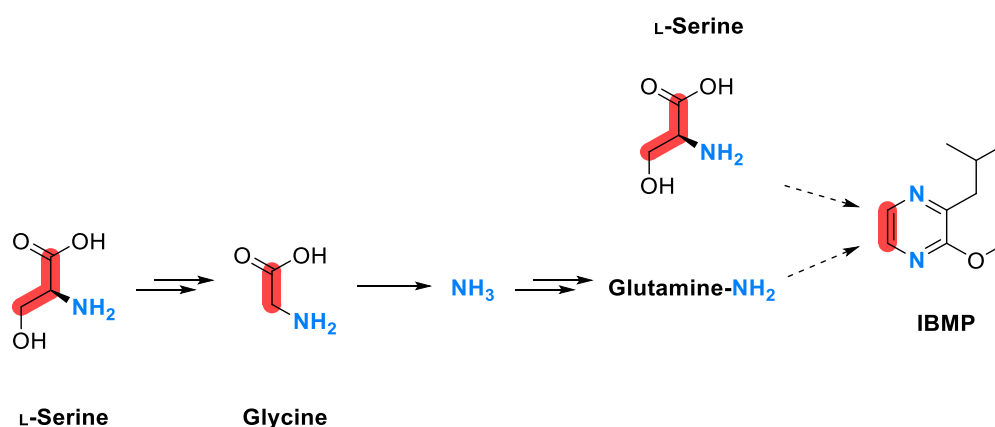
Scheme 18: Incorporation of L-[2,3-¹³C₂]-serine (**74**) generating ¹³C-labeled IBMP (**75**). Based on *in vivo* feeding experiments using green, unripe bell pepper pericarp (*Capsicum annuum* L.).

To investigate whether L-serine serves as a nitrogen donor, further co-feeding studies were performed using L-[¹³C₃, ¹⁵N]-serine. Isotope mass shifts revealed that up to four stable isotopes were incorporated into IBMP. An isotope mass shift by 4 *m/z* signified an incorporation of four stable isotopes, which indicates that both nitrogen atoms of IBMP are L-serine derived.

Considering that the pericarp tissue is still metabolically active during the experiments, the following incorporations of stable isotopes were hypothesized:

- I. Incorporation of one stable isotope: Incorporation of ¹⁵NH₃ into IBMP.
Deamination of L-[¹³C₃, ¹⁵N]-serine.
- II. Incorporation of two stable isotopes: Incorporation of L-[¹³C₂, ¹⁵N]-serine into IBMP.
Reversible conversion of L-serine into glycine:
L-[¹³C₃, ¹⁵N]-serine → [¹³C₂, ¹⁵N]-glycine → L-[¹³C₂, ¹⁵N]-serine.
- III. Incorporation of three stable isotopes: Incorporation of L-[¹³C₃, ¹⁵N]-serine into IBMP.
- IV. Incorporation of four stable isotopes: Incorporation of L-[¹³C₃, ¹⁵N]-serine and ¹⁵NH₃ into IBMP.

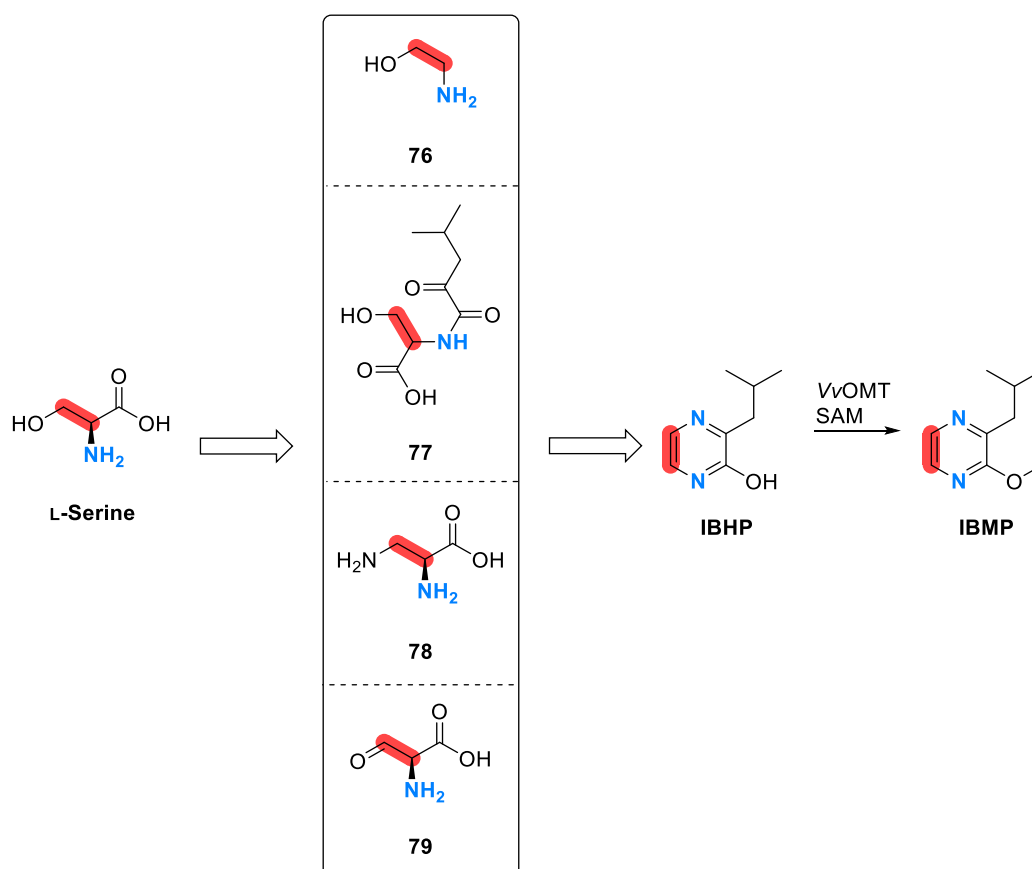
These feeding experiments strengthened the hypothesis of a metabolic link between IBMP-biosynthesis and photorespiration. During photorespiration, NH₃ is released by glycine and reincorporated into glutamine, which in turn aminates α-ketoglutarate to glutamate. Glutamate is transported into the peroxisome and aminates glyoxylate to glycine.^[141] Previous feeding studies revealed that glutamine serves as a nitrogen source. Hence NH₃ released by L-serine might be re-incorporated into IBMP (**Scheme 19**).



Scheme 19: Metabolic fate of stable isotopes during feeding experiments with L-[¹³C₃, ¹⁵N]-serine.

Based on the feeding studies different biosynthetic pathways to IBMP are proposed (**Scheme 20**):

- I. L-Serine is decarboxylated to ethanolamine (**76**), which reacts with α -KIC and NH_3 forming IBHP. In plants, the decarboxylation of L-serine is known to be catalyzed by a serine decarboxylase (SDC).^[142]
- II. L-Serine and α -KIC form a condensation product (**77**), which is transaminated. A cyclization and oxidative decarboxylation leads to the formation of IBHP. A similar oxidative decarboxylation occurs in plants during the conversion of aroenate into tyrosine.^[143]
- III. L-Serine is aminated to 2,3-diaminopropionic acid (DAP, **78**). A condensation of DAP and α -KIC results in IBHP. The non-proteinogenic amino acid DAP is a short-lived intermediate of the neurotoxin β -N-oxalyl- α,β -diaminopropionic acid (ODAP) found in grass pea (*Lathyrus sativus* L.).^[144]
- IV. L-Serine is oxidized to α -formyl-glycine (**79**), which reacts with α -KIC and NH_3 . Cyclization and decarboxylation lead to the formation of IBHP. α -Formyl-glycine is used for the chemical synthesis of cyclic endi amino peptides.^[145]



Scheme 20: Proposed pathways of serine incorporation into IBMP in plants. Putative intermediates are ethanolamine (**76**), a condensation product of L-serine and α -KIC (**77**), 2,3-diaminopropionic acid (DAP, **78**) and α -formyl-glycine (**79**).

In sum, stable isotope tracer experiments clearly proved that L-serine is decarboxylated during the biosynthesis of IBMP. Moreover, this work's results confirmed that both nitrogen atoms of the pyrazine ring originate from L-serine, which in turn supports the hypothesis of a metabolic interface between IBMP-biosynthesis and photorespiration.

Chapter 4

1. General Introduction

MPs belong to the class of alkaloids. Alkaloids are naturally occurring compounds containing at least one nitrogen atom, usually within a heterocyclic ring. Due to their great structural diversity, alkaloids are one of the most manifold group of secondary metabolites.^[146] Alkaloids possess different bioactivities like antimicrobial, anti-inflammatory and cytotoxic activities.^[147] Plant derived alkaloids are often used in medicine as they have pharmacological properties. The probably best-known medical alkaloid is morphine (**80**) biosynthesized by the opium poppy *Papaver somniferum* L. (Papaveraceae) and used as a narcotic analgesic (**Figure 16**).^[146]

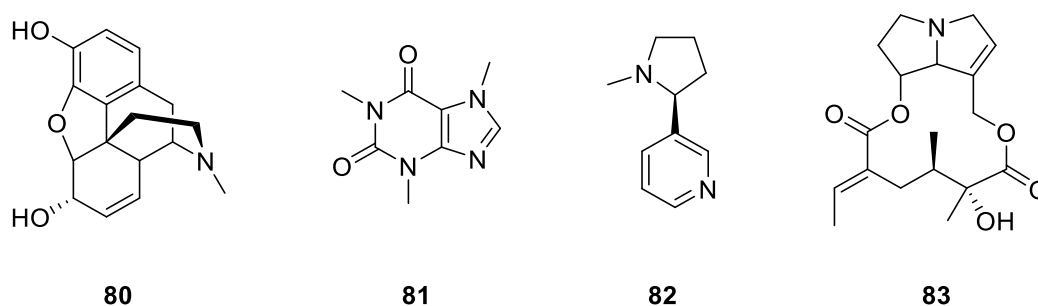


Figure 16: Chemical structures of plant alkaloids. Morphine (**80**), caffeine (**81**), nicotine (**82**), senecionine (**83**).

Alkaloids predominantly accumulate in a particular organ or tissue of plants. Morphine (**80**) for example accumulates in the cytoplasm (latex) of cells designated as laticifers, while another well-known alkaloid namely caffeine (**81**) accumulates in the seeds of *Coffea* fruits.^[148] However, their site of storage is not always their site of origin. A transport of alkaloids and their intermediates through the plant via the vascular system of xylem and phloem is possible. A root-to-shoot transport of solutes occurs usually unidirectional via the xylem into the leaves.^[149] In contrast, the transport of solutes via the phloem is bidirectional from source organs like leaves to sink organs such as fruits or seeds.^[150]

Nicotine (**82**) for example is exclusively biosynthesized in the roots of tobacco plants (*Nicotiana tabacum*) but accumulates in the leaves.^[151] In addition, senecionine (**83**) and its *N*-oxide are biosynthesized in *Senecio vulgaris* L. (Asteraceae) roots and translocated through the shoot to finally accumulate in the inflorescences.^[152]

Physiochemical properties such as the acid dissociation constant (K_a) are crucial parameters for the transportability of a compound via the phloem. Another key factor is its octanol-water partition coefficient (pK_{OW}) i.e. its membrane permeability. Furthermore, plant length, phloem

pH-values and velocities as well as the sieve-tube membrane properties play an important role in the phloem transportability.^[153] Alkaloids usually move through biomembranes, as they are rather lipophilic. Differences in their phloem mobility might mainly occur due to their stability at the phloem's pH-value.^[149]

Over the years several methods like spontaneous exudation through simple incision, exudation facilitated via ethylenediaminetetraacetic acid (EDTA) or aphid stylectomy have been developed for phloem collection. Spontaneous exudation has a limited application, as it is only suitable for plants that exudate spontaneously. If that is not the case, the EDTA-facilitated exudation is used. For this purpose, tips of the petioles for instance are incubated in a solution containing EDTA. EDTA serves as a chelating agent, which prevents undesired phloem sealing.^[154] After incubation, samples are rinsed with water to remove remaining EDTA.^[155] For exudate collection, petiole tips are incubated in water. Humidity must be sufficiently high to avoid loss of exudate by transpiration.^[156] Unfortunately, the use of EDTA can lead to cell damages and thus false-positive results.^[156] That is why control experiments need to be carried out. Samples obtained via the insect stylectomy method, which requires phloem-feeding insects like aphids are less contaminated. For phloem collecting, the aphid's stylet, which is inserted into the sieve tube while the aphid is feeding is cut off. Stylectomy is a less invasive, but more time-consuming and work-intensive phloem collecting technique.^[157]

A long-distance transport of MPs within the grapevine has been discussed controversially. Experiments with stable isotope labeled tracers indicated that IBMP is translocated from the leaves into the grapes.^[158] In contrast, grafting studies showed that there is no IBMP-transport through the shoot into the fruit.^[159] As IBMP-levels increased in the bunch stem (rachis) when they were grown on IBMP-rich rootstocks, a transport through the shoot into the rachis has been suggested instead.^[160]

The occurrence, storage and biosynthetic sites of MPs in grapevines have been widely studied. IPMP for instance seems to accumulate in the roots, while IBMP accumulates in the grape's exocarp.^[72,75,159,161] In contrast, little is known about the distribution and accumulation as well as the biosynthetic sites of MPs within the bell pepper plant.

Sites of Biosynthesis, Distribution and Phloem Transport of 3-Isobutyl-2-methoxypyrazine in *Capsicum annuum* (Bell Pepper) Plants

The research summarized in this chapter has been published as
Zamolo, F.; Heinrichs, J. P.; Wüst, M, *Phytochemistry* **2023**, *205*, 113488.
<https://doi.org/10.1016/j.phytochem.2022.113488>.

A reprint of this publication is given in **Chapter 8 Appendix G** of this thesis.

Author's contributions: My contributions to this research consist of the development and implementation of the feeding experiments and the collection of phloem exudates as well as data analysis and interpretation and manuscript writing. *J. P. Heinrichs* a MSc student, whom I supervised, helped with the validation of the HS-SPME-GC-ToF-MS-method as well as the quantification of IBMP within the plant. The supervisor of my doctoral thesis *Prof. M. Wüst* provided guidance, gave important suggestions and writing assistance.

Reprinted with permission from *Phytochemistry* **2023**, *205*, 113488.

Copyright 2023 Elsevier.







2. Summary

The main issue of this study is the quantification of IBMP within the whole *Capsicum annuum* L. plant. Other key topics are *in vivo* feeding experiments with stable isotope labeled precursors to identify the sites of IBMP-biosynthesis as well as the EDTA-facilitated phloem exudate collection to investigate a possible long-distance transport of IBMP via the phloem system.

For IBMP-quantitation a HS-SPME-GC-ToF-MS-method was developed. IBMP was quantified on a fresh weight (FW) basis using a stable isotope dilution assay (SIDA). IBMP- d_9 was used as a stable isotope labeled, internal standard. The developed method was validated concerning its linearity, its accuracy based on recovery experiments, its precision expressed as RSD (relative standard deviation) as well as its limit of detection (LOD) and limit of quantification (LOQ). In sum, a good linearity ($r^2 = 0.997$ for IBMP 0.1–150 ng/g), appropriate recoveries (97%–102% for IBMP 10–96 ng/g), satisfactory intra-day precision (RSD = 2.57%) and inter-day precision (RSD = 3.98%) as well as LOD (0.16 ng/g) and LOQ (0.28 ng/g) were achieved.

IBMP-levels were examined in all plant parts. Results are shown in **Table 1**. IBMP is distributed within the whole bell pepper plant including roots (7.27 ± 1.18 ng/g FW), stem (4.28 ± 0.56 ng/g FW), leaves (21.29 ± 1.23 ng/g FW), and flowers (31.92 ± 3.16 ng/g FW). Unripe, green fruits and ripe, yellow fruits were examined separately. It could be shown that unripe bell pepper fruits (92.70 ± 4.00 ng/g FW) possess higher IBMP-contents than ripe fruits (45.97 ± 2.24 ng/g FW).

Table 1: IBMP-contents in different organs and tissues of bell pepper plants (*Capsicum annuum* L.). Data are means \pm standard deviations ($n = 5-11$) expressed as ng/g fresh weight (FW).

					
Roots	Stems	Leaves	Flowers	Fruit (ripe)	Fruit (unripe)
7.27 ± 1.18	4.28 ± 0.56	21.29 ± 1.23	31.92 ± 3.16	45.97 ± 2.24	92.70 ± 4.00

As IBMP seems to be predominantly stored in the fruits, the major site of IBMP-accumulation within the fruit was examined. The highest IBMP-values were found in the pericarp tissues. Unripe, green bell pepper pericarp contains 78.51 ± 6.65 ng/g (FW) IBMP, while yellow, ripe bell pepper contains less (65.70 ± 3.44 ng/g FW IBMP). Additionally, IBMP was detected in the fruit's placenta (unripe: 20.61 ± 1.14 ng/g; ripe: 18.87 ± 2.29 ng/g FW), pedicel

(unripe: 21.00 ± 3.72 ng/g; ripe: 19.07 ± 1.92 ng/g FW) as well as in the seeds (unripe: 36.80 ± 3.16 ng/g; ripe: 7.23 ± 0.14 ng/g FW) (**Figure 17**). This work's results show that IBMP-levels decrease in all fruit tissues during bell pepper ripening and that IBMP is mainly stored in the pericarp tissue of unripe fruits.

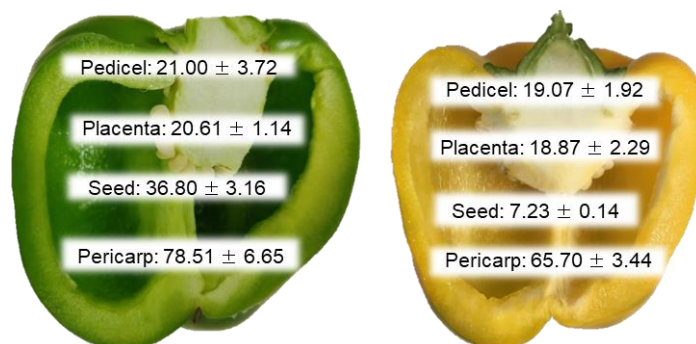


Figure 17: IBMP-content in various parts of unripe, green bell pepper fruits and ripe, yellow bell pepper fruits (*Capsicum annuum* L.). Data are means \pm standard deviations ($n = 5-8$) expressed as ng/g fresh weight (FW).

Subsequently, the biosynthetic sites of IBMP within the bell pepper plant were examined. For this purpose, *in vivo* feeding experiments were performed using different plant organs and fruit tissues. Samples were incubated for 48 h with deuterium labeled L-leucine (L-leucine- d_{10}) and analyzed by HS-SPME-GC \times GC-ToF-MS. Interestingly, feeding experiments revealed that apart from roots and unripe fruit tissues, all plant parts biosynthesize IBMP *de novo*.

A translocation of IBMP through the plant was examined, as IBMP was detected in the roots and ripe fruits, even though these tissues turned out to not biosynthesize IBMP *de novo*. To investigate a possible translocation of IBMP through the bell pepper plant, phloem sap of excised leaves was collected using the EDTA-facilitated exudation technique. The obtained phloem exudates were then analyzed using HS-SPME-GC-ToF-MS. Unfortunately, IBMP-levels in phloem exudates were not significantly higher than in water control samples. Thus, a transport of IBMP via the phloem was considered as unlikely.

In sum, IBMP turned out to be present in the whole bell pepper plant. IBMP-concentrations in reproductive plant parts (flowers and fruits) exceed those of the vegetative organs (roots, stems, leaves). The highest IBMP-concentrations were detected in the pericarp tissue of unripe bell pepper fruits. In general, it could be shown that IBMP-levels of unripe fruit tissues exceeded those in ripe fruit tissues. Additionally, *in vivo* feeding experiments with deuterium labeled L-leucine revealed that all aerial plant parts apart from ripe fruits can biosynthesize IBMP *de novo*. As IBMP-containing roots showed no incorporation of labeled L-leucine into IBMP, a long-distance transport of IBMP through the plant was considered possible. However, no IBMP could be observed in the petiole phloem sap.

Chapter 5 Summary and Outlook

MPs are extremely potent odorants associated with a green and earthy aroma. MPs are responsible for the distinctive flavor and aroma properties of numerous fruits and vegetables. The most prominent MPs are IPMP, the most abundant MP in peas (*Pisum sativum*), sBMP mainly present in beetroot (*Beta vulgaris*) and IBMP predominantly biosynthesized in bell pepper fruits (*Capsicum annuum* L.).^[48] While the occurrence of MPs has been widely studied, little is known about their biosynthesis. The identification of four genes encoding *Vitis vinifera* O-methyltransferases (VvOMT1-VvOMT4) gave important insights into the final step of MP-biosynthesis.^[73–75] However, earlier biosynthetic steps and precursors remained unknown. Since 1970 different pathways and precursors have been proposed and controversially discussed in the literature.^[51,66,71,72] So far, none of them could be confirmed.

This thesis aimed to identify MP-precursors by *in vivo* stable isotope feeding experiments (**Chapter 2** and **Chapter 3**). Feeding studies were conducted focusing on the biosynthesis of IBMP in *Capsicum annuum* plants. For this purpose, pericarp tissue of bell pepper fruits was incubated for 48 h with an aqueous solution of a stable isotope labeled compound. After incubation and homogenization, samples were analyzed using HS-SPME-GC×GC-ToF-MS. In GC, an incorporation of deuterium atoms is detectable by a decrease in the retention time of the heavier (deuterated) isotopologue (*inverse isotope effect*). This is due to a shorter carbon-hydrogen bond, which reduces the molar volume and boiling point of the deuterated compound.^[108] Deuterated and unlabeled compounds can therefore be separated by GC. Moreover, GC-MS-hyphenation allows the calculation of the number of incorporated deuterium atoms by the mass shifts of the molecular ion peak ($M^{+\bullet}$). Based on mass spectral fragmentation positional labeling information can be obtained.^[120]

Feeding experiments using unripe, green pericarp tissue revealed an incorporation of the branched-chain amino acid (BCAA) L-leucine into IBMP. As expected by the *inverse isotope effect* in GC a new peak eluting just before endogenous IBMP appeared in samples incubated with L-leucine- d_{10} . Based on mass spectral data the incorporation of nine deuterium atoms (IBMP- d_9) could be confirmed. Subsequently, the relevance of branched-chain keto acids (BCKAs) in the biosynthesis of IBMP was examined by feeding deuterated α -ketoisocaproic acid (α -KIC- d_7) to unripe, green pericarp tissue. An incorporation of α -KIC into IBMP could be confirmed. In fact, feeding experiments with L-leucine- $^{13}\text{C}_6,^{15}\text{N},2,3,3,4,5,5,5',5',5'-d_{10}$ (L-leucine- $^{13}\text{C}_6,^{15}\text{N},d_{10}$) revealed that the ^{15}N -label is mainly lost during IBMP-biosynthesis. Thus, feeding studies proved that BCKAs participate in the biosynthesis of MPs.

So far, L-leucine and α -KIC were identified as precursors to IBMP. However, to form a pyrazine motif, another nitrogen source and C₂-unit are required. Therefore, further investigations were performed using ¹³C- and ¹⁵N-labeled compounds. Unfortunately, the *inverse isotope effect* becomes weaker for ¹³C-/¹⁵N-atoms, as the decrease in molar volume, and boiling point is lower for a ¹³C/¹⁵N-incorporation than for a deuterium-incorporation.^[108] As this results in coeluting isotopologues, ¹³C-/¹⁵N-incorporations are detected by isotopic enrichments in distinct isotopic mass peaks instead. Higher levels of the genuine compound, however, can mask these isotopic enrichments, making the detection of ¹³C-/¹⁵N-incorporation hard or even impossible. To avoid undesired coelutions, mixed labeling studies were performed (co-feeding experiments). For this purpose, a known deuterated precursor and the potential ¹³C/¹⁵N-labeled compound were fed simultaneously. A ¹³C-/¹⁵N-incorporation should result in a deuterated and ¹³C/¹⁵N-labeled reaction product that can be separated from the unlabeled compound by GC. GC-separation in turn enables the mass spectral detection of isotopic enrichments that occur due to ¹³C/¹⁵N-incorporations.

Subsequently, co-feeding studies were conducted using L-leucine-*d*₁₀ as a known precursor. While an incorporation of L-aspartic acid and L-glutamic acid into IBMP could not be detected, the involvement of L-glutamine as a nitrogen donor to IBMP was proven. Further co-feeding experiments revealed that glycine and glyoxylic acid serve as C₁-building blocks in the IBMP-biosynthesis. It has been hypothesized that glycine and glyoxylic acid are first metabolized forming a C₁-intermediate, which is then incorporated into the pyrazine heterocycle of IBMP. Hence, the aim of the following study was to elucidate the underlying metabolic pathway of the metabolization of glycine and glyoxylic acid to a C₁-intermediate (**Chapter 3**).

L-Serine, as the final product of the metabolic interface of glycine and the C₁-metabolism, was considered as a putative precursor for IBMP. To examine its relevance in the biosynthesis of IBMP, co-feeding experiments were conducted using L-leucine-*d*₁₀ and stable isotope labeled L-serine. Indeed, *in vivo* feeding experiments showed that a C₂-unit of L-serine is incorporated into IBMP. The fragmentation and isotope labeling pattern of the labeled product confirmed a decarboxylation of L-serine during its incorporation into IBMP. In addition, it could be shown that both nitrogen atoms of the pyrazine ring are L-serine derived.

In sum, stable isotope tracer experiments gave an important insight into the biosynthesis of IBMP in plants. Feeding experiments turned out to be an efficient technique for tracking precursors of IBMP. It could be shown for the first time that L-leucine and α -KIC are important IBMP-precursors that glutamine serves as a nitrogen donor and that L-serine acts as a C₂-building block and nitrogen source in the IBMP-biosynthesis. Based on these findings, different biosynthetic pathways for the formation of IBMP were proposed. The identification of

precursors increases the knowledge of MP-biosynthesis significantly. Knowing the precursors of IBMP helps to elucidate its biosynthetic pathway.

So far, feeding experiments were focused only on the edible pericarp tissue of bell pepper fruits. The main objective of the following study (**Chapter 4**) was therefore, to examine the distribution, translocation, and biosynthetic sites of IBMP in plants. First, a SIDA-HS-SPME-GC-ToF-MS-method was developed for the IBMP-quantification. The analytical performance of this method was validated concerning its linearity, accuracy, precision, limit of detection (LOD) and limit of quantification (LOQ). Then, the distribution of IBMP was analyzed by quantifying the value of IBMP in all plant parts. It could be shown that IBMP is distributed within the whole shoot system including all aerial parts like leaves, the stem, flowers, and fruits as well as in the root system. The highest IBMP-levels were detected in the reproductive organs. In contrast, roots contained the highest IPMP-levels. The results showed that IBMP is predominantly accumulated in the fruits. A distinction between ripe and unripe fruits proved that IBMP-levels decrease during fruit ripening. The unripe pericarp tissue turned out to be the main site of IBMP-accumulation as a result of the analysis of different fruit tissues.

It has been assumed that the IBMP-distribution within the plant might be caused by either a long-distance transport of IBMP through the plant or multiple sites of *de novo* biosynthesis. To examine different plant organs concerning their activity to biosynthesize IBMP, *in vivo* feeding experiments were conducted with L-leucine- d_{10} . Apart from roots and ripe fruit tissues including seeds, placenta, pericarp and pedicel, all plant compartments showed an incorporation of L-leucine- d_{10} into IBMP. Subsequently, a long-distance transport of IBMP via the phloem was analyzed. Therefore, petiole phloem exudates of bell pepper plant leaves were collected using the EDTA-facilitated exudation technique. However, no IBMP was detected in the phloem exudates of bell pepper plant leaves. It has been hypothesized that MPs themselves may not be phloem-mobile, and need to be chemically modified first by for example a glycoconjugation. A glycoconjugate of MP would be soluble in the phloem. In fact, glycosylated IBHP has already been considered to be a degradation product of IBMP.^[84]

IBMP-storage in bell pepper plants is comparable to IBMP-accumulation in grapevines. In both cases, IBMP is distributed throughout the plant and fruits turned out to be the main IBMP-accumulation site.^[75,159,161] The reasons for IBMP-accumulation in the vegetative plant parts are so far unknown. Knowing the sites of IBMP-accumulation in plants may help to figure out its biological function. Different biological functions of IBMP have been discussed in the literature. Volatile organic compounds are often released by plants to interact with other organisms.^[162] Hence, it has been suggested that IBMP serves as a semiochemical. IPMP has been shown to attract the knot nematode *Meloidogyne incognita*.^[163] In contrast, IBMP and sBMP were found to be biosynthesized for chemical defense in aposematic insects like the

wood tiger moths (*Arctia plantaginis*).^[13] It has been suggested that IBMP may act as warning signal to defend the unripe fruits from being eaten.^[75] An antimicrobial activity of IBMP against yeast and bacteria was tested, but not could not be confirmed (1 ppb–1 ppm).^[164]

Moreover, knowing the site of MP-accumulation and biosynthesis may help to understand MP-regulation in plants. Several factors and metabolic processes are responsible for the regulation of MP-levels in plants. As elevated MP-concentrations in grapes can cause an unpleasant, earthy, green bell pepper-like aroma in wine, knowledge about horticultural treatments and environmental factors to reduce MPs in grapes is gaining in importance.^[165] It is known that IBMP-levels in grapes are influenced by viticultural and environmental factors such as climate and soil type.^[56] Additionally, it has been shown that temperature and sunlight exposure reduce IBMP-levels.^[55,57] Deciphering the biosynthetic pathway and metabolic regulation of MPs, may allow to identify, which processes are responsible for decreasing MP-contents in response to abiotic and biotic stresses.

Besides, this work's results indicated that there might be a biosynthetic link between photorespiration and the biosynthesis of MPs. A metabolic link may explain why less IBMP is detectable in ripe fruits. It might be that the inactivation of IBMP-biosynthesis in ripe fruits occurs due to the lack of photorespiratory-derived L-serine. Photorespiration starts in the chloroplasts, which undergo an irreversible transition into chromoplasts during bell pepper fruit ripening. The photorespiratory pathway of chloroplasts is thus dismantled in ripe fruits. A decrease during bell pepper ripening has also been observed in activity of peroxisomal, photorespiratory enzymes.^[166] However, it is still unknown whether only photorespiratory-derived L-serine is incorporated into IBMP since two non-photorespiratory (glycerate and phosphorylated pathway) pathways of serine biosynthesis coexist. The involvement of these biosynthetic pathways of serine in the biosynthesis of MPs cannot be ruled out currently. So far, little is known about IBMP-degradation. Due to a correlation between decreasing IBMP-levels and increasing IBHP-levels in ripe fruits, it has been hypothesized that IBMP degrades to IBHP.^[84] However, the down-regulation of VvOMT-expressions observed in ripe grapes might as well be responsible for an IBHP-accumulation.^[77] A metabolic interface between photorespiration and MP-biosynthesis might help to understand the pathway of the biological breakdown of IBMP.

Additional work is needed, to examine whether photorespiration is the only L-serine-source in the IBMP-biosynthesis. Moreover, for pathway delineation important intermediates and enzymes, which participate in the biosynthesis of MPs need to be identified.

Chapter 6 References

- [1] M. Lökov, S. Tshepelevitsh, A. Heering, P. G. Plieger, R. Vianello, I. Leito, *Eur. J. Org. Chem.* **2017**, 2017, 4475–4489.
- [2] N. Sato in *Science of Synthesis, 16: Category 2, Hetarenes and Related Ring Systems. Six-Membered Hetarenes with Two Identical Heteroatoms*, Georg Thieme Verlag, **2004**.
- [3] H. L. Snape, A. Brooke, *J. Chem. Soc., Trans.* **1897**, 71, 528–532.
- [4] R. G. Jones, *J. Am. Chem. Soc.* **1949**, 71, 78–81.
- [5] a) K. T. Ong, Z.-Q. Liu, M. G. Tay, *BJRST* **2017**, 7, 60–75; b) G. Vernin *Ellis Horwood Series in chemical science*, Ellis Horwood, **1982**; c) J. A. Joule, K. Mills, *Heterocyclic chemistry*, Wiley, **2010**.
- [6] I. J. Krems, P. E. Spoerri, *Chem. Rev.* **1947**, 40, 279–358.
- [7] M. Dolezal, K. Kralov in *Herbicides, Theory and Applications*, InTech, **2011**.
- [8] a) P. B. Miniyar, P. R. Murumkar, P. S. Patil, M. A. Barmade, K. G. Bothara, *Mini Rev. Med. Chem.* **2013**, 13, 1607–1625; b) R. L. Yeager, W. G. C. Munroe, F. I. Dessau, *Am. Rev. Tuberc.* **1952**, 65, 523–546.
- [9] R. F. Skrentny, J. A. Ellis, *Pestic. Sci.* **1970**, 1, 45–48.
- [10] J. S. Dickschat, S. Wickel, C. J. Bolten, T. Nawrath, S. Schulz, C. Wittmann, *Eur. J. Org. Chem.* **2010**, 2010, 2687–2695.
- [11] a) R. L. Buchanan, W. M. Houston, *J. Food Sci.* **1982**, 47, 779–782; b) J. C. MacDonald, *Biochem. J.* **1965**, 96, 533–538.
- [12] B. P. Moore, W. V. Brown, M. Rothschild, *Chemoecology* **1990**, 1, 43–51.
- [13] E. Burdfield-Steel, H. Pakkanen, B. Rojas, J. A. Galarza, J. Mappes, *J. Insect Sci.* **2018**, 18.
- [14] K. E. Murray, F. B. Whitfield, *J. Sci. Food Agric.* **1975**, 26, 973–986.
- [15] J. C. MacDonald, *JBC (Journal of Biological Chemistry)* **1961**, 236, 512–514.
- [16] a) L. Lindström, C. Rowe, T. Guilford, *Proc. Biol. Sci.* **2001**, 268, 159–162; b) J. H. Law, F. E. Regnier, *Annu. Rev. Biochem.* **1971**, 40, 533–548; c) M. Dicke, M. W. Sabelis, *Funct. Ecol.* **1988**, 2, 131.
- [17] B. Bohman, L. Jeffares, G. Flematti, L. T. Byrne, B. W. Skelton, R. D. Phillips, K. W. Dixon, R. Peakall, R. A. Barrow, *J. Nat. Prod.* **2012**, 75, 1589–1594.

- [18] E. A. Silva-Junior, A. C. Ruzzini, C. R. Paludo, F. S. Nascimento, C. R. Currie, J. Clardy, M. T. Pupo, *Sci. Rep.* **2018**, *8*, 2595.
- [19] J. H. Cross, R. C. Byler, U. Ravid, R. M. Silverstein, S. W. Robinson, P. M. Baker, J. S. de Oliveira, A. R. Jutsum, J. M. Cherrett, *J. Chem. Ecol.* **1979**, *5*, 187–203.
- [20] A. T. Dossey, M. Gottardo, J. M. Whitaker, W. R. Roush, A. S. Edison, *J. Chem. Ecol.* **2009**, *35*, 861–870.
- [21] B. Bohman, R. D. Phillips, M. H. M. Menz, B. W. Berntsson, G. R. Flematti, R. A. Barrow, K. W. Dixon, R. Peakall, *New Phytol.* **2014**, *203*, 939–952.
- [22] a) L. K. Murungi, H. Kirwa, D. Coyne, P. E. A. Teal, J. J. Beck, B. Torto, *J. Agric. Food Chem.* **2018**, *66*, 7328–7336; b) S. Al Abassi, M. A. Birkett, J. Pettersson, J. A. Pickett, C. M. Woodcock, *Cell. Mol. Life Sci.* **1998**, *54*, 876–879.
- [23] F. B. Mortzfeld, C. Hashem, K. Vranková, M. Winkler, F. Rudroff, *Biotechnol. J.* **2020**, *15*, 2000064.
- [24] M. Rothe, B. Thomas, *Eur. Food Res. Technol.* **1963**, *119*, 302–310.
- [25] P. Marcinek, F. Haag, C. Geithe, D. Krautwurst, *FASEB J.* **2021**, *35*, e21638.
- [26] P. E. Koehler, M. E. Mason, G. V. Odell, *J. Food Sci.* **1971**, *36*, 816–818.
- [27] T. Shibamoto, *J. Food Sci.* **1986**, *51*, 1098–1099.
- [28] R. M. Seifert, R. G. Buttery, D. G. Guadagni, D. R. Black, J. G. Harris, *J. Agric. Food Chem.* **1972**, *20*, 135–137.
- [29] E. Ortner, M. Granvogl, P. Schieberle, *J. Agric. Food Chem.* **2016**, *64*, 8179–8190.
- [30] I. Chetschik, M. Granvogl, P. Schieberle, *J. Agric. Food Chem.* **2010**, *58*, 11018–11026.
- [31] M. Czerny, W. Grosch, *J. Agric. Food Chem.* **2000**, *48*, 868–872.
- [32] H. Masuda, S. Mihara, *J. Agric. Food Chem.* **1988**, *36*, 584–587.
- [33] S. S. Schiffman, J. C. Leffingwell, *Pharmacol. Biochem. Behav.* **1981**, *14*, 787–798.
- [34] R. Wagner, M. Czerny, J. Bielohradsky, W. Grosch, *ZLUF (Zeitschrift für Lebensmittel-Untersuchung und -Forschung)* **1999**, *208*, 308–316.
- [35] S. Mihara, H. Masuda, *J. Agric. Food Chem.* **1988**, *36*, 1242–1247.
- [36] T. Nawrath, J. S. Dickschat, B. Kunze, S. Schulz, *Chem. Biodivers.* **2010**, *7*, 2129–2144.
- [37] a) C. Cerny, W. Grosch, *Eur. Food Res. Technol.* **1993**, *196*, 417–422; b) W. Grosch, *Trends Food Sci. Technol.* **1993**, *4*, 68–73; c) J. Serra Bonvehí, F. Ventura Coll, *J. Agric. Food Chem.* **2002**, *50*, 3743–3750; d) I. Blank, A. Sen, W. Grosch, *Eur. Food Res.*

- Technol.* **1992**, *195*, 239–245; e) R. G. Buttery, D. G. Guadagni, L. C. Ling, *J. Sci. Food Agric.* **1973**, *24*, 1125–1131; f) P. Schieberle, W. Grosch, *Eur. Food Res. Technol.* **1985**, *180*, 474–478.
- [38] a) I. Besson, C. Creuly, J. B. Gros, C. Larroche, *Appl. Microbiol. Biotechnol.* **1997**, *47*, 489–495; b) K. S. Kim, H. J. Lee, D. H. Shon, D. K. Chung, *J. Microbiol. Biotechnol.* **1994**, *4*, 327–332; c) T. Kosuge, H. Zenda, K. Tsuji, T. Yamamoto, H. Narita, *Agric. Biol. Chem.* **1971**, *35*, 693–696; d) T. Kosuge, T. Adachi, H. Kamiya, *Nature* **1962**, *195*, 1103; e) N. Nunomura, M. Sasaki, Y. Asao, T. Yokotsuka, *Agric. Biol. Chem.* **1978**, *42*, 2123–2128.
- [39] S. M. Fors, B. K. Olofsson, *Chem. Senses* **1986**, *11*, 65–77.
- [40] a) G. L. L. Scalone, T. Cucu, N. de Kimpe, B. de Meulenaer, *J. Agric. Food Chem.* **2015**, *63*, 5364–5372; b) J. E. Hodge, *J. Agric. Food Chem.* **1953**, *1*, 928–943.
- [41] L. C. Maillard, *Compte-rendu de l'academie des sciences* **1912**, *154*, 66–68.
- [42] P. V. Guerra, V. A. Yaylayan, *J. Agric. Food Chem.* **2010**, *58*, 12523–12529.
- [43] H. Yu, R. Zhang, F. Yang, Y. Xie, Y. Guo, W. Yao, W. Zhou, *Trends Food Sci. Technol.* **2021**, *112*, 795–807.
- [44] S. Schulz, J. S. Dickschat, *Nat. Prod. Rep.* **2007**, *24*, 814–842.
- [45] G. P. Rizzi in *ACS Symposium Series*, American Chemical Society, Washington, DC, **1998**, 132–149.
- [46] R. G. Buttery, R. M. Seifert, D. G. Guadagni, L. C. Ling, *J. Agric. Food Chem.* **1969**, *17*, 1322–1327.
- [47] C. Legrum, P. Slabizki, H.-G. Schmarr, *Anal. Bioanal. Chem.* **2015**, *407*, 253–263.
- [48] D. Mutarutwa, L. Navarini, V. Lonzarich, D. Compagnone, P. Pittia, *J. Mass Spectrom.* **2018**, *53*, 871–881.
- [49] C. Zhou, Z. Xu, H. Shi, G. Zhang, W. Cao, X. Xu, *J. Agric. Food Chem.* **2022**, *70*, 6247–6252.
- [50] D. Mutarutwa, L. Navarini, V. Lonzarich, P. Crisafulli, D. Compagnone, P. Pittia, *J. Agric. Food Chem.* **2020**, *68*, 4743–4751.
- [51] K. E. Murray, J. Shipton, F. B. Whitfield, *Chem. Ind.* **1970**, *27*, 897–898.
- [52] A. F. Bramwell, J. Burrell, G. Riezebos, *Tetrahedron Lett.* **1969**, *10*, 3215–3216.
- [53] a) Q. Sun, M. J. Gates, E. H. Lavin, T. E. Acree, G. L. Sacks, *J. Agric. Food Chem.* **2011**, *59*, 10657–10664; b) A. Botezatu, Y. Kotseridis, D. Inglis, G. J. Pickering, *J. Food Agric.*

- Environ.* **2016**, *14*, 24–29; c) A. Belancic, E. Agosin, *Am. J. Enol. Vitic.* **2007**, *58*, 462–469; d) B. Liu, X.-Q. Xu, J. Cai, Y.-B. Lan, B.-Q. Zhu, J. Wang, *Eur. Food Res. Technol.* **2015**, *240*, 985–997.
- [54] Bayonove C., Cordonnier R., Dubois P., *C. R. Acad. Sci. Gen.* **1975**, 75–78.
- [55] M. J. Lacey, M. S. Allen, R. L. N. Harris, V. W. Brown, *Am. J. Enol. Vitic.* **1991**, *42*, 103–108.
- [56] D. Roujou de Boubée, C. van Leeuwen, D. Dubourdiou, *J. Agric. Food Chem.* **2000**, *48*, 4830–4834.
- [57] M. S. Allen, M. J. Lacey, R. L. N. Harris, W. V. Brown, *Am. J. Enol. Vitic.* **1991**, *42*, 109–112.
- [58] Y. Kotseridis, R. L. Baumes, A. Bertrand, G. K. Skouroumounis, *J. Chromatogr. A* **1999**, *841*, 229–237.
- [59] M. S. Allen, M. J. Lacey, S. Boyd, *J. Agric. Food Chem.* **1994**, *42*, 1734–1738.
- [60] R. M. Seifert, R. G. Buttery, D. G. Guadagni, D. R. Black, J. G. Harris, *J. Agric. Food Chem.* **1970**, *18*, 246–249.
- [61] W. V. Parr, J. A. Green, K. G. White, R. R. Sherlock, *Food Qual. Preference* **2007**, *18*, 849–861.
- [62] a) A. I. Botezatu, Y. Kotseridis, D. Inglis, G. J. Pickering, *J. Sci. Food Agric.* **2013**, *93*, 803–810; b) G. J. Pickering, Y. Lin, A. Reynolds, G. Soleas, R. Riesen, I. Brindle, *J. Food Sci.* **2005**, *70*, 128–135; c) G. J. Pickering, M. Spink, Y. Kotseridis, I. D. Brindle, M. Sears, D. Inglis, *Vitis* **2008**, *47*, 227–230.
- [63] M. S. Allen, M. J. Lacey, S. J. Boyd, *J. Agric. Food Chem.* **1995**, *43*, 769–772.
- [64] a) P. Slabizki, C. Legrum, P. Wegmann-Herr, C. Fischer, H.-G. Schmarr, *Eur. Food Res. Technol.* **2016**, *242*, 977–986; b) P. Slabizki, C. Fischer, C. Legrum, H.-G. Schmarr, *J. Agric. Food Chem.* **2015**, *63*, 7840–7848.
- [65] a) A. Gallois, P. A. Grimont, *Appl. Environ. Microbiol.* **1985**, *50*, 1048–1051; b) M. E. Alañón, M. Alarcón, I. J. Díaz-Maroto, M. S. Pérez-Coello, M. C. Díaz-Maroto, *J. Sci. Food Agric.* **2021**, *101*, 4735–4742.
- [66] T. B. Cheng, G. A. Reineccius, J. A. Bjorklund, E. Leete, *J. Agric. Food Chem.* **1991**, *39*, 1009–1012.
- [67] A. Gallois, A. Kergomard, J. Adda, *Food Chem.* **1988**, *28*, 299–309.
- [68] a) B. Bouyjou, G. Fourny, D. Perreaux in *Proceedings of the 15th International Scientific Colloquim on Coffee*, **1993**, 357–369; b) D. Gueule, G. Fourny, E. Ageron, A. Le Flèche-

References

- Matéos, M. Vandenbogaert, P. A. D. Grimont, C. Cilas, *Int. J. Syst. Evol. Microbiol.* **2015**, *65*, 23–29.
- [69] R. Becker, B. Dohla, S. Nitz, O. G. Vitzthum in *Proceedings of the 12th International Scientific Colloquim of Coffee*, **1987**, 203–215.
- [70] K. E. Frato, *J. Agric. Food Chem.* **2019**, *67*, 341–351.
- [71] H. E. Nursten, M. R. Sheen, *J. Sci. Food Agric.* **1974**, *25*, 643–663.
- [72] Y. Lei, S. Xie, H. Chen, X. Guan, Z. Zhang, *Food Chem.* **2019**, *277*, 609–616.
- [73] K. Hashizume, K. Tozawa, M. Endo, I. Aramaki, *Biosci. Biotechnol. Biochem.* **2001**, *65*, 795–801.
- [74] K. Hashizume, K. Tozawa, Y. Hiraga, I. Aramaki, *Biosci. Biotechnol. Biochem.* **2001**, *65*, 2213–2219.
- [75] J. D. Dunlevy, K. L. Soole, M. V. Perkins, E. G. Dennis, R. A. Keyzers, C. M. Kalua, P. K. Boss, *Plant Mol. Biol.* **2010**, *74*, 77–89.
- [76] S. Guillaumie, A. Ilg, S. Réty, M. Brette, C. Trossat-Magnin, S. Decroocq, C. Léon, C. Keime, T. Ye, R. Baltenweck-Guyot et al., *Plant Physiol.* **2013**, *162*, 604–615.
- [77] J. D. Dunlevy, E. G. Dennis, K. L. Soole, M. V. Perkins, C. Davies, P. K. Boss, *Plant J.* **2013**, *75*, 606–617.
- [78] J. G. Vallarino, X. A. Lopez-Cortes, J. D. Dunlevy, P. K. Boss, F. D. Gonzalez-Nilo, Y. M. Moreno, *J. Agric. Food Chem.* **2011**, *59*, 7310–7316.
- [79] C. M. Tan, C.-H. Li, N.-W. Tsao, L.-W. Su, Y.-T. Lu, S. H. Chang, Y. Y. Lin, J.-C. Liou, L.-C. Hsieh, J.-Z. Yu et al., *J. Exp. Bot.* **2016**, *67*, 4415–4425.
- [80] a) M. S. Allen, *Austr. Grapegr. Winem.* **1993**, 10–12; b) X. Zhao, Y. Ju, X. Wei, S. Dong, X. Sun, Y. Fang, *Molecules* **2019**, *24*, 4598; c) C. Sala, O. Busto, J. Guasch, F. Zamora, *J. Agric. Food Chem.* **2004**, *52*, 3492–3497; d) C. M. Plank, E. W. Hellman, T. Montague, *HortScience* **2019**, *54*, 282–288; e) R. A. Arnold, A. M. Bledsoe, *Am. J. Enol. Vitic.* **1990**, *41*, 74–76; f) M. S. Allen, M. J. Lacey, *Vitic. Enol. Sci.* **1993**, *48*, 211–213.
- [81] I. Ryona, B. S. Pan, D. S. Intrigliolo, A. N. Lakso, G. L. Sacks, *J. Agric. Food Chem.* **2008**, *56*, 10838–10846.
- [82] K. Hashizume, T. Samuta, *Am. J. Enol. Vitic.* **1999**, *50*, 194–198.
- [83] a) R. E. Smart, T. R. Sinclair, *Agric. Meteorol.* **1976**, *17*, 241–259; b) H. Heymann, A. C. Noble, R. B. Boulton, *J. Agric. Food Chem.* **1986**, *34*, 268–271.
- [84] I. Ryona, S. Leclerc, G. L. Sacks, *J. Agric. Food Chem.* **2010**, *58*, 9723–9730.

- [85] a) O. Augustyn, A. Rapp, C. J. van Wyk, *S. Afr. J. Enol. Vitic.* **1982**, 3, 53–59; b) R. W. Slingsby, R. E. Kepner, C. J. Muller, A. D. Webb, *Am. J. Enol. Vitic.* **1980**, 31, 360–363.
- [86] a) P. J. Hartmann, H. M. McNair, B. W. Zoecklein, *Am. J. Enol. Vitic.* **2002**, 285–288; b) C. Sala, M. Mestres, M. P. Martí, O. Busto, J. Guasch, *J. Chromatogr. A* **2000**, 880, 93–99; c) D. Roujou de Boubée, A. M. C. M. Pons, D. Dubourdieu, *Am. J. Enol. Vitic.* **2002**, 53, 1–5; d) C. Franc, F. David, G. de Revel, *J. Chromatogr. A* **2009**, 1216, 3318–3327.
- [87] K. Hashizume, N. Umeda, *Biosci. Biotechnol. Biochem.* **1996**, 60, 802–805.
- [88] A. K. Hjelmeland, P. L. Wylie, S. E. Ebeler, *Talanta* **2016**, 148, 336–345.
- [89] P. Alberts, M. Kidd, M. A. Stander, H. H. Nieuwoudt, A. Tredoux, A. de Villiers, *S. Afr. J. Enol. Vitic.* **2016**, 34, 54–67.
- [90] P. J. Hartmann, H. M. McNair, B. W. Zoecklein, *Am J Enol Vitic.* **2002**, 53, 285–288.
- [91] D. Ryan, P. Watkins, J. Smith, M. Allen, P. Marriott, *J. Sep. Sci.* **2005**, 28, 1075–1082.
- [92] I. Ryona, B. S. Pan, G. L. Sacks, *J. Agric. Food Chem.* **2009**, 57, 8250–8257.
- [93] H.-G. Schmarr, S. Ganss, S. Koschinski, U. Fischer, C. Riehle, J. Kinnart, T. Potouridis, M. Kutyrev, *J. Chromatogr. A* **2010**, 1217, 6769–6777.
- [94] C. N. Cain, N. J. Haughn, H. J. Purcell, L. C. Marney, R. E. Synovec, C. T. Thoumsin, S. C. Jackels, K. J. Skogerboe, *J. Agric. Food Chem.* **2021**, 69, 2253–2261.
- [95] C. L. Arthur, J. Pawliszyn, *Anal. Chem.* **1990**, 62, 2145–2148.
- [96] G. Vas, K. Vékey, *J. Mass Spectrom.* **2004**, 39, 233–254.
- [97] J. Pawliszyn, B. Pawliszyn, M. Pawliszyn, *Chem. Educator* **1997**, 2, 1–7.
- [98] a) J. Pawliszyn *Applications of solid phase microextraction*, Royal Society of Chemistry, **1999**; b) J. Pawliszyn, *Handbook of solid phase microextraction*, Elsevier, **2012**.
- [99] J. Pawliszyn, *Solid phase microextraction. Theory and practice*, Wiley-VCH, **1997**.
- [100] S. Balasubramanian, S. Panigrahi, *Food Bioproc. Tech.* **2011**, 4, 1–26.
- [101] a) K. Schmidt, I. Podmore, *J. Mol. Biomark. Diagn.* **2015**, 6; b) X. Yang, T. Peppard, *J. Agric. Food Chem.* **1994**, 42, 1925–1930.
- [102] L. Tuduri, V. Desauziers, J. L. Fanlo, *J. Chromatogr. Sci.* **2001**, 39, 521–529.
- [103] G. Ouyang in *Handbook of Solid Phase Microextraction*, Elsevier, 167–199.
- [104] a) J. Ai, *Anal. Chem.* **1997**, 69, 1230–1236; b) G. Ouyang, R. Jiang *Solid Phase Microextraction. Recent Developments and Applications*, Springer, **2017**.
- [105] P. Schieberle, W. Grosch, *J. Agric. Food Chem.* **1987**, 35, 252–257.

- [106] M. Rychlik, S. Asam, *Umweltwiss. Schadst. Forsch.* **2009**, *21*, 470–482.
- [107] J. Wieling, *Chromatographia* **2002**, *55*, 107–113.
- [108] M. Matucha, W. Jockisch, P. Verner, G. Anders, *J. Chromatogr. A* **1991**, *588*, 251–258.
- [109] J. B. Phillips, J. Beens, *J. Chromatogr. A* **1999**, *856*, 331–347.
- [110] J. C. Giddings, *Anal. Chem.* **1984**, *56*, 1258–1270.
- [111] P. Q. Tranchida, G. Purcaro, P. Dugo, L. Mondello, *TrAC (Trends in Analytical Chemistry)* **2011**, *30*, 1437–1461.
- [112] C. Meinert, U. J. Meierhenrich, *Angew. Chem. Int. Ed.* **2012**, *51*, 10460–10470; *Angew. Chem.* **2012**, *124*, 10610–10621.
- [113] a) L. Mondello, A. C. Lewis, K. D. Bartle, *Multidimensional chromatography*, John Wiley, **2002**; b) C. Vendeuvre, R. Ruiz-Guerrero, F. Bertoncini, L. Duval, D. Thiébaud, *Oil & Gas Science and Technology - Rev. IFP* **2007**, *62*, 43–55; c) P. Q. Tranchida, P. Donato, F. Cacciola, M. Beccaria, P. Dugo, L. Mondello, *TrAC (Trends in Analytical Chemistry)* **2013**, *52*, 186–205; d) H.-G. Janssen, E. Kaal, S. de Koning in *Comprehensive Analytical Chemistry*, Elsevier, **2009**, 123–145.
- [114] Z. Liu, J. B. Phillips, *J. Chromatogr. Sci.* **1991**, *29*, 227–231.
- [115] R. C. Y. Ong, P. J. Marriott, *J. Chromatogr. Sci.* **2002**, *40*, 276–291.
- [116] a) P.-H. Stefanuto, J.-F. Focant in *Basic Multidimensional Gas Chromatography*, **2020**, 69–88; b) G. Semard, M. Adahchour, J.-F. Focant in *Comprehensive Analytical Chemistry*, Elsevier, **2009**, 15–48.
- [117] P. Q. Tranchida, G. Purcaro, D. Sciarrone, P. Dugo, G. Dugo, L. Mondello, *J. Sep. Sci.* **2010**, *33*, 2791–2795.
- [118] J. H. Gross, *Mass spectrometry. A textbook*, Springer International Publishing, **2017**.
- [119] H. Aguirre-Becerra, M. C. Vazquez-Hernandez, D. La Saenz de O, A. Alvarado-Mariana, R. G. Guevara-Gonzalez, J. F. Garcia-Trejo, A. A. Feregrino-Perez in *Bioactive Natural Products for Pharmaceutical Applications*, Springer, **2021**, 151–195.
- [120] N. J. Kruger, R. G. Ratcliffe, A. Roscher, *Phytochem. Rev.* **2003**, *2*, 17–30.
- [121] T. Mahmud, *J. Labelled Compd. Radiopharm.* **2007**, *50*, 1039–1051.
- [122] M. Rohmer, M. Knani, P. Simonin, B. Sutter, H. Sahm, *Biochem. J.* **1993**, *295*, 517–524.
- [123] T. Mahmud, S. C. Wenzel, E. Wan, K. W. Wen, H. B. Bode, N. Gaitatzis, R. Müller, *Chembiochem* **2005**, *6*, 322–330.
- [124] E. Pichersky, N. A. Dudareva *Biology of plant volatiles*, CRC Press, **2020**.

- [125] D. J. Creek, A. Chokkathukalam, A. Jankevics, K. E. V. Burgess, R. Breitling, M. P. Barrett, *Anal. Chem.* **2012**, *84*, 8442–8447.
- [126] S. Klein, E. Heinzle, *WIREs Syst. Biol. Med.* **2012**, *4*, 261–272.
- [127] D. M. Chapman, J. H. Thorngate, M. A. Matthews, J.-X. Guinard, S. E. Ebeler, *J. Agric. Food Chem.* **2004**, *52*, 5431–5435.
- [128] Y. S. Kotseridis, M. Spink, I. D. Brindle, A. J. Blake, M. Sears, X. Chen, G. Soleas, D. Inglis, G. J. Pickering, *J. Chromatogr. A* **2008**, *1190*, 294–301.
- [129] a) S. G. Wyllie, J. K. Fellman, *J. Agric. Food Chem.* **2000**, *48*, 3493–3496; b) D. D. Rowan, H. P. Lane, J. M. Allen, S. Fielder, M. B. Hunt, *J. Agric. Food Chem.* **1996**, *44*, 3276–3285; c) M. J. Myers, P. Issenberg, E. L. Wick, *Phytochemistry* **1970**, *9*, 1693–1700.
- [130] S. Binder, *The arabidopsis book* **2010**, *8*.
- [131] a) A. Kochevenko, W. L. Araújo, G. S. Maloney, D. M. Tieman, P. T. Do, M. G. Taylor, H. J. Klee, A. R. Fernie, *Mol. Plant* **2012**, *5*, 366–375; b) I. Gonda, E. Bar, V. Portnoy, S. Lev, J. Burger, A. A. Schaffer, Y. Tadmor, S. Gepstein, J. J. Giovannoni, N. Katzir et al., *J. Exp. Bot.* **2010**, *61*, 1111–1123.
- [132] J. M. Mouillon, S. Aubert, J. Bourguignon, E. Gout, R. Douce, F. Rébeillé, *Plant J.* **1999**, *20*, 197–205.
- [133] R. Ros, J. Muñoz-Bertomeu, S. Krueger, *Trends Plant Sci.* **2014**, *19*, 564–569.
- [134] C. L. Ho, K. Saito, *Amino acids* **2001**, *20*, 243–259.
- [135] a) E. Collakova, A. Goyer, V. Naponelli, I. Krassovskaya, J. F. Gregory, A. D. Hanson, Y. Shachar-Hill, *Plant Cell* **2008**, *20*, 1818–1832; b) A. C. Srivastava, P. A. Ramos-Parra, M. Bedair, A. L. Robledo-Hernández, Y. Tang, L. W. Sumner, R. I. La Díaz de Garza, E. B. Blancaflor, *Plant Physiol.* **2011**, *155*, 1237–1251; c) Y. Yamaoka, Y. Yu, J. Mizoi, Y. Fujiki, K. Saito, M. Nishijima, Y. Lee, I. Nishida, *Plant J.* **2011**, *67*, 648–661.
- [136] H. Bauwe, M. Hagemann, A. R. Fernie, *Trends Plant Sci.* **2010**, *15*, 330–336.
- [137] S. Timm, M. Hagemann, *J. Exp. Bot.* **2020**, *71*, 3955–3965.
- [138] C. Peterhansel, I. Horst, M. Niessen, C. Blume, R. Kebeish, S. Kürkcüoglu, F. Kreuzaler, *The arabidopsis book* **2010**, *8*, e0130.
- [139] X. Shi, A. Bloom, *Plants* **2021**, *10*.
- [140] a) R. M. Benstein, K. Ludewig, S. Wulfert, S. Wittek, T. Gigolashvili, H. Frerigmann, M. Gierth, U.-I. Flügge, S. Krueger, *Plant Cell* **2013**, *25*, 5011–5029; b) S. Timm, A. Nunes-Nesi, A. Florian, M. Eisenhut, K. Morgenthal, M. Wirtz, R. Hell, W. Weckwerth, M.

References

- Hagemann, A. R. Fernie et al., *Metabolites* **2021**, *11*, 391–412; c) R. Douce, J. Bourguignon, M. Neuburger, F. Rébeillé, *Trends Plant Sci.* **2001**, *6*, 167–176.
- [141] B. B. Buchanan, W. Gruissem, R. L. Jones *Biochemistry & molecular biology of plants*, American Society of Plant Biologists; Wiley Blackwell, **2015**.
- [142] a) D. Rontein, I. Nishida, G. Tashiro, K. Yoshioka, W. I. Wu, D. R. Voelker, G. Basset, A. D. Hanson, *JBC (Journal of Biological Chemistry)* **2001**, *276*, 35523–35529; b) S. H. Mudd, A. H. Datko, *Plant Physiol.* **1989**, *91*, 587–597.
- [143] E. Jung, L. O. Zamir, R. A. Jensen, *PNAS* **1986**, *83*, 7231–7235.
- [144] Y.-H. Kuo, F. Lambein, *Phytochemistry* **1991**, *30*, 3241–3244.
- [145] D. Pappo, M. Vartanian, S. Lang, Y. Kashman, *J. Am. Chem. Soc.* **2005**, *127*, 7682–7683.
- [146] M. F. Roberts, M. Wink, *Alkaloids*, Springer, **1998**.
- [147] a) B. Weniger, L. Italiano, J. P. Beck, J. Bastida, S. Bergoñon, C. Codina, A. Lobstein, R. Anton, *Planta medica* **1995**, *61*, 77–79; b) L. Othman, A. Sleiman, R. M. Abdel-Massih, *Front. Microbiol.* **2019**, *10*, 911; c) A. L. Souto, J. F. Tavares, M. S. Da Silva, M. d. F. F. M. Diniz, P. F. de Athayde-Filho, J. M. Barbosa Filho, *Molecules* **2011**, *16*, 8515–8534.
- [148] a) Y. Koshiro, X.-Q. Zheng, M.-L. Wang, C. Nagai, H. Ashihara, *Plant Sci.* **2006**, *171*, 242–250; b) T. M. Kutchan, S. Ayabe, C. J. Coscia in *Proceedings in Life Sciences*, Springer, **1985**, 281–294.
- [149] M. Nowak, D. Selmar, *Plant Biol.* **2016**, *18*, 879–882.
- [150] P. J. White in *Marschner's Mineral Nutrition of Higher Plants*, Elsevier, **2012**, 49–70.
- [151] R. F. Dawson, *Am. J. Bot.* **1942**, *29*, 813.
- [152] T. Hartmann, A. Ehmke, U. Eilert, K. von Borstel, C. Theuring, *Planta* **1989**, *177*, 98–107.
- [153] F. C. Hsu, D. A. Kleier, *J. Exp. Bot.* **1996**, *47*, 1265–1271.
- [154] R. W. King, J. A. Zeevaart, *Plant Physiol.* **1974**, *53*, 96–103.
- [155] B. S. Guelette, U. F. Benning, S. Hoffmann-Benning, *J. Exp. Bot.* **2012**, *63*, 3603–3616.
- [156] O. Tetyuk, U. F. Benning, S. Hoffmann-Benning, *Journal of visualized experiments : JoVE* **2013**, e51111.
- [157] a) S. Dinant, J. Kehr, *Methods Mol. Biol.* **2013**, *953*, 185–194; b) D. B. Fisher, J. M. Frame, *Planta* **1984**, *161*, 385–393.

-
- [158] A. Koch, C. L. Doyle, M. A. Matthews, L. E. Williams, S. E. Ebeler, *Phytochemistry* **2010**, *71*, 2190–2198.
- [159] D. Roujou de Boubée, *Research on 2-methoxy-3-isobutylpyrazine in grapes and wines*, **2003**, 1–21.
- [160] a) D. L. Capone, I. L. Francis, P. R. Clingeleffer, S. M. Maffei, P. K. Boss, *Aust. J. Grape Wine Res.* **2022**, *28*, 304–315; b) D. L. Capone, A. Barker, W. Pearson, I. L. Francis, *Aust. J. Grape Wine Res.* **2021**, *27*, 348–359.
- [161] K. Hashizume, T. Samuta, *J. Agric. Food Chem.* **1997**, *45*, 1333–1337.
- [162] F. Negre-Zakharov, M. C. Long, N. Dudareva in *Plant-derived Natural Products*, Springer, New York, **2009**, 405–431.
- [163] R. Kihika, L. K. Murungi, D. Coyne, M. Ng'ang'a, A. Hassanali, P. E. A. Teal, B. Torto, *Sci. Rep.* **2017**, *7*, 2903.
- [164] S. Kögel, A. Eben, C. Hoffmann, J. Gross, *J. Chem. Ecol.* **2012**, *38*, 854–864.
- [165] G. J. Pickering, A. Karthik, D. Inglis, M. Sears, K. Ker, *J. Food Sci.* **2007**, *72*, 468–72.
- [166] R. M. Mateos, A. M. León, L. M. Sandalio, M. Gómez, L. A. Del Río, J. M. Palma, *J. Plant Physiol.* **2003**, *160*, 1507–1516.

Chapter 7 Abbreviations

$[M]^{+\bullet}$	molecular ion
^{13}C	heavy carbon/carbon isotope
^{15}N	heavy nitrogen/nitrogen isotope
^1D	first dimension
^2D	second dimension
3-HMG-CoA	3-hydroxy-3-methylglutaryl-CoA
3-PGA	3-phosphoglycerate
AMPA	2-amino-4-methylpentanamide
BCAA	branched-chain amino acid
BCKA	branched-chain keto acid
BCV	branched-chain volatile
c_0	initial concentration of the analyte in the matrix
C_1	one carbon atom
C-1	carbon at position 1
CAR	carboxen
$\text{CH}_2\text{-H}_4\text{Folate}$	methylene-tetrahydrofolate
d	deuterium/hydrogen isotope
DAP	2,3-diaminopropionic acid
DB/CAR/PDMS	divinylbenzol/carboxen/polydimethylsiloxan
d_f	film thickness
DI-SPME	direct immersion solid-phase microextraction

DMAPP	dimethylallyl-diphosphate
DVB	divinylbenzene
DXP	1-desoxy-D-xylulose-5-phosphat
EDTA	ethylenediaminetetraacetic acid
EI	electron impact ionization
EIC	extracted ion chromatogram
<i>et al.</i>	et alii
FID	flame ionization detection
FW	fresh weight
GC	gas chromatography
GCxGC	comprehensive two-dimensional gas chromatography
GDC	glycine decarboxylase complex
H ₄ Folate	tetrahydrofolate
HP	3-alkyl-2-hydroxypyrazine
HPLC	high performance liquid chromatography
HS	headspace
HS-SPME	headspace solid-phase microextraction
I.D.	inner diameter
IBMP	3-isobutyl-2-methoxypyrazine
IBMP- <i>d</i> ₉	nine-fold deuterated IBMP
IPMP	3-isopropyl-2-methoxypyrazine
IPP	isopentenyl-diphosphate

Abbreviations

IUPAC	<i>International Union of Pure and Applied Chemistry</i>
K_a	acid dissociation constant
K_{fs}	distribution coefficient of analyte between coating and sample
K_{hs}	distribution coefficient of analyte between headspace and sample
LBT	ladybug taint
LC	liquid chromatography
LLE	liquid-liquid extraction
L-leucine- d_{10}	tenfold deuterated L-leucine
LOD	limit of detection
LOQ	limit of quantification
m/z	mass-to-charge ratio
MDGC	multidimensional gas chromatography
MEP	2-C-methyl-D-erythritol-4-phosphate
MPs	3-Alkyl-2-methoxypyrazine
MS	mass spectrometry
n_{eq}	mass analyte adsorbed by the fiber coating
<i>NbOMT</i>	<i>Nicotiana benthamiana O-methyltransferase</i>
NIST	National Institute of Standards and Technology
NMR	nuclear magnetic resonance
NPD	nitrogen phosphorus detection
OAV	odor activity value
ODAP	β -N-oxalyl- α,β -diamino propionic acid

OMT	O-methyltransferase
OR	olfactory receptor
OR5K1	pyrazine-selective olfactory receptor
OT	odor detection threshold
PA	polyacrylate
PDMS	polydimethylsiloxane
P _i	phosphate
pK _{ow}	octanol-water partition coefficient
P _M	modulation period
ppb	parts per billion
ppt	parts per trillion
PS	3-phosphoserine
PTD	potato-taste defect
RE	relative error
RuBisCO	ribulose 1,5-bisphosphate carboxylase/oxygenase
SAM	S-adenosyl-L-methionine
sBMP	3-sec-butyl-2-methoxypyrazine
SBSE	stir bar sorptive extraction
SDE	simultaneous distillation-extraction
SDC	serine decarboxylase
SIDA	stable isotope dilution assay
SPE	solid-phase extraction

Abbreviations

SPME	solid-phase microextraction
TIC	total ion chromatogram
ToF-MS	time-of-flight–mass spectrometer
V_f	volume of the fiber coating
V_h	volume of the headspace
V_s	volume of the sample
VvOMT	<i>Vitis vinifera</i> O-methyltransferase
α -KIC	α -ketoisocaproic acid

Chapter 8 Appendix

A. List of Figures

Figure 1: Chemical structure and numbering of pyrazine.	1
Figure 2: Chemical structure of 2,3,5,6-tetraphenylpyrazine.	1
Figure 3: Chemical structures of pyrazines used as pharmaceuticals or pesticides.	2
Figure 4: Chemical structure of aspergillilic acid.	2
Figure 5: Chemical structures of semiochemically active pyrazines.	3
Figure 6: Structure-odor relationship of alkylpyrazines I.	4
Figure 7: Structure-odor relationship of alkylpyrazines II.	4
Figure 8: Structure-odor relationship of alkoxy pyrazines I.	8
Figure 9: Structure-odor relationship of alkoxy pyrazines II.	8
Figure 10: Structure-odor relationship of alkoxy pyrazines III.	9
Figure 11: Chemical structures of 3-isopropyl-2-methoxy pyrazine (IPMP, 44), 3-sec-butyl-2-methoxy pyrazine (sBMP, 45), 3-isobutyl-2-methoxy pyrazine (IBMP, 46).	9
Figure 12: Principle of HS-SPME extraction.	15
Figure 13: Expected labeling pattern of IBMP in co-feeding studies with [¹³ C ₂]-glyoxylic acid and L-leucine- <i>d</i> ₁₀ .	27
Figure 14: Incorporation of L-leucine and α-KIC as well as glyoxylic acid, glycine, and glutamine into IBMP.	28
Figure 15: L-Serine as an important building block for several biomolecules.	29
Figure 16: Chemical structures of plant alkaloids.	37
Figure 17: IBMP-content in various parts of unripe, green bell pepper fruits and ripe, yellow bell pepper fruits (<i>Capsicum annuum</i> L.).	41

B. List of Tables

Table 1: IBMP-contents in different organs and tissues of bell pepper plants (<i>Capsicum annuum</i> L.).	40
-------------------------------------------------------------------------------------------------------------------	----

C. List of Schemes

Scheme 1: Synthetic routes to pyrazines.	1
Scheme 2: Pyrazine generation from the <i>Maillard</i> reaction.	5
Scheme 3: Pyrazine generation via azomethine ylides (20) under <i>Maillard</i> reaction conditions.	6
Scheme 4: Proposed pathway of alkylpyrazines via acyloin (23).	6
Scheme 5: Proposed pathway of 3-ethyl-2,5-dimethylpyrazine (32) via L-threonine (27) and aminoacetone (28).	7
Scheme 6: Proposed pathway of 2,5-diisopropylpyrazine (36) via valine (33) and valinal (34).	7
Scheme 7: Postulated biosynthesis of 3-isopropyl-2-methoxypyrazine (IPMP, 50) in <i>Pseudomonas</i> species.	10
Scheme 8: Postulated biosynthesis of 3-isopropyl-2-methoxypyrazine (IPMP, 54) in plants.	11
Scheme 9: Postulated biosynthesis of 3-isobutyl-2-methoxypyrazine (IBMP, 57) via leucinamide (AMPA, 56).	11
Scheme 10: Proposed incorporation of L-isoleucine (58) into (S)-sBMP (59).	11
Scheme 11: Final enzyme-catalyzed step in the biosynthesis of 3-alkyl-2-methoxypyrazines (MPs).	12
Scheme 12: Supposed degradation of IBMP (63) back to IBHP (62).	13
Scheme 13: Glyceraldehyde-3-phosphate (64) and pyruvate (65) as precursors of dimethylallyl-diphosphate (DMAPP, 66) and isopentenyl-diphosphate (IPP, 67).	22
Scheme 14: Shunt pathway that connects the mevalonate pathway and branched-chain fatty acids via 3-hydroxy-3-methylglutaryl-CoA (3-HMG-CoA, 69).	23
Scheme 15: Incorporation of L-leucine- d_{10} (72) generating IBMP- d_9 (73).	25
Scheme 16: Fragmentation pattern of IBMP (A) and IBMP- d_9 (B).	26
Scheme 17: Different biosynthetic pathways to serine in plants. ^[133]	30
Scheme 18: Incorporation of L-[2,3- $^{13}\text{C}_2$]-serine (74) generating ^{13}C -labeled IBMP (75).	33
Scheme 19: Metabolic fate of stable isotopes during feeding experiments with L-[$^{13}\text{C}_3$, ^{15}N]-serine.	34
Scheme 20: Proposed pathways of serine incorporation into IBMP in plants.	35

D. List of Equations

Equation 1

16

E. Publication 1

Investigation of Biosynthetic Precursors of 3-Isobutyl-2-Methoxypyrazine Using Stable Isotope Labeling Studies in Bell Pepper Fruits (*Capsicum annuum* L.)

Francesca Zamolo and Matthias Wüst*



Cite This: *J. Agric. Food Chem.* 2022, 70, 6719–6725



Read Online

ACCESS |



Metrics & More



Article Recommendations



Supporting Information

ABSTRACT: The biosynthesis of 3-isobutyl-2-methoxypyrazine (IBMP) in bell pepper fruits (*Capsicum annuum* L.) was investigated by *in vivo* feeding experiments with stable isotope-labeled precursors. Volatiles were extracted using headspace solid-phase microextraction (HS-SPME) and analyzed by comprehensive two-dimensional gas chromatography (GC×GC) coupled to a time-of-flight mass spectrometer (ToF-MS). Feeding experiments revealed incorporation of L-leucine and α -ketoisocaproic acid (α -KIC) as well as glycine and glyoxylic acid into IBMP. Furthermore, it has been shown that *de novo* biosynthesis of IBMP occurs in pericarp tissues of unripe bell pepper fruits, whereas pericarp tissues of ripe bell pepper fruits showed no capability of IBMP biosynthesis.

KEYWORDS: 3-alkyl-2-methoxypyrazine (MP), *Capsicum annuum*, headspace solid-phase microextraction (HS-SPME), comprehensive two-dimensional gas chromatography (GC×GC), time-of-flight mass spectrometry (ToF-MS)

INTRODUCTION

3-Alkyl-2-methoxypyrazines (MPs) are aroma-active volatiles. MPs occur in many raw vegetables and several grape varieties.^{1–6} The most studied MP derivatives are 3-isobutyl-2-methoxypyrazine (IBMP), 3-*sec*-butyl-2-methoxypyrazine (*s*BMP), and 3-isopropyl-2-methoxypyrazine (IPMP). Usually, all three derivatives are present, with one being predominant.³ In capsicum fruits, the most abundant MP is IBMP.⁶ In fact, it is one of the most important volatile compounds of unripe, green pepper fruits, in which it was first identified in 1969.⁷ IBMP concentration decreases during bell pepper ripening. Thus, levels are lower in ripe fruits than in unripe fruits.⁸

Although MPs have often been discussed in the literature, their biosynthesis in plants is still unknown. So far, only the final enzymatically catalyzed step has been confirmed. It involves the O-methylation of 3-alkyl-2-hydroxypyrazines (HPs), catalyzed by *Vitis vinifera*-O-methyltransferases (*Vv*OMTs).^{9–11} In contrast, little is known about precursors and metabolic intermediates. Different biosynthetic pathways have been proposed, but none of them has been clearly confirmed. First, condensation of an α -amino acid amide of leucine, isoleucine, or valine with glyoxal has been suggested.¹ However, both amino acids forming α -amino acid amides and free glyoxal have never been detected in plants. That is why either glyoxylic acid or a nitrogen derivative of glyoxylate has been considered instead.^{2,3} Later, condensation of leucine, isoleucine, or valine and a second amino acid has been supposed, according to the bacterial MP biosynthesis.¹²

All suggested pathways have incorporation of leucine, isoleucine, or valine in common. This is due to their structural similarity to the branched side chain. Leucine, isoleucine, and valine are called branched-chain amino acids (BCAAs). They play an important role in the biosynthesis of several branched-

chain volatiles, which in turn are relevant aroma-active compounds in fruits.^{13–15} BCAAs were thought to be direct precursors for branched-chain volatiles, until *in vivo* feeding studies revealed branched-chain keto acids (BCKAs) as even more efficient precursors.^{16,17} Whereas the influence of BCKAs on MP biosynthesis has only been observed in bacteria so far,¹⁸ feeding experiments with grape cell cultures and intact grapes indicated the relevance of BCAA in MP biosynthesis.^{19,20} However, neither *in vitro* nor *in vivo* experiments demonstrated incorporation of stable isotope-labeled precursors into MPs.

To investigate the plant MP biosynthesis, *in vivo* feeding experiments were conducted with bell pepper fruits (*Capsicum annuum* L. cv. Allrounder). Furthermore, feeding experiments were performed to compare the relevance of amino acids and their respective keto acids in MP-biosynthesis.

MATERIALS AND METHODS

Plant Material. Feeding experiments were performed with green (unripe) and yellow (ripe) bell pepper fruits (*Capsicum annuum* L. cv. Allrounder) (*Rijk Zwaan*, De Lier, the Netherlands) obtained from the Institute of Crop Science and Resource Conservation (INRES), Chair of Horticultural Sciences of the University of Bonn, Germany. Fruits were harvested and incubated the same day.

Chemicals. 3-Isobutyl-2-methoxypyrazine (IBMP) (97%), glycine-1-¹³C,¹⁵N (99 atom% ¹³C, 98 atom% ¹⁵N), L-leucine-¹³C₆,¹⁵N,_{2,3,4,5,5,5',S',S',S'-d}₁₀ (L-leucine-¹³C₆,¹⁵N,_d₁₀) (99 atom

Received: March 11, 2022

Revised: May 11, 2022

Accepted: May 16, 2022

Published: May 27, 2022



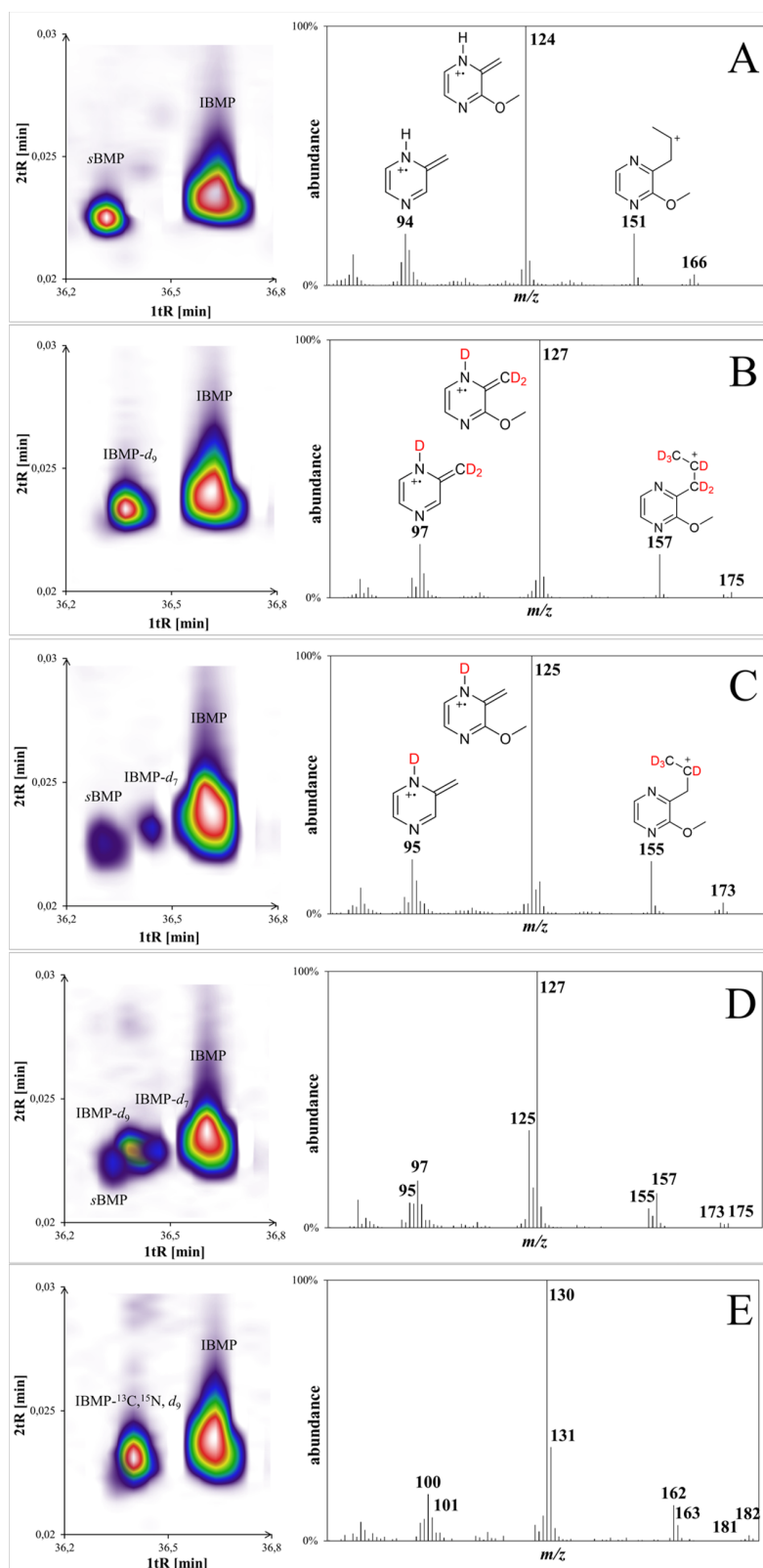


Figure 1. Extracted-ion chromatograms (EIC), electron ionization (EI) mass spectra, and structures of fragment ions of genuine IBMP (EIC m/z 124) (A) and after feeding *L*-leucine-*d*₁₀ (EIC m/z 124, 127) (B), α -KIC-*d*₇ (EIC m/z 124, 125) (C) after co-feeding *L*-leucine-*d*₁₀ and α -KIC-*d*₇ (EIC m/z 124, 125, 127) (D) and after feeding *L*-leucine-¹³C₆, ¹⁵N, *d*₁₀ (EIC m/z 124, 130, 131) (E) to pericarp tissue of unripe bell peppers (*Capsicum annuum* L. cv. Allrounders).

% ^{13}C , 98 atom% ^{15}N , 98 atom% D, 95% (CP)), L-aspartic acid- ^{15}N (98 atom% ^{15}N), L-glutamic acid- ^{15}N (98 atom% ^{15}N), and L-glutamine- $^{15}\text{N}_2$ (98 atom% ^{15}N) were purchased from Sigma Aldrich (St Louis, Missouri). L-Leucine -2,3,3,4,5,5,5,5',5',5'- d_{10} (L-leucine- d_{10}) (99%) was purchased from C/D/N isotopes (Pointe-Claire, Quebec, Canada). Glyoxylic acid- $^{13}\text{C}_2$, monohydrate (95.7%) was obtained from Toronto Research Chemical Inc. (Toronto, Canada). α -Ketoisocaproic acid- d_7 (α -KIC- d_7) (99.7%) was purchased as a sodium salt from Cambridge Isotope Laboratories (Andover, Massachusetts). 3-Isobutyl- d_9 -2-methoxypyrazine (IBMP- d_9) ($\geq 95\%$) was obtained from AromaLab (Martinsried, Germany). Sodium chloride was purchased from Merck GmbH (Darmstadt, Germany). Methanol ($>99.99\%$) was obtained from Honeywell (Muskegon, Michigan). Water (HPLC, LC-MS grade) was obtained from VWR International S.A.S. (Fontenay-sous-Bois, Ile-de-France, France).

HS-SPME. Headspace solid-phase microextraction (HS-SPME) was carried out using a divinylbenzene/carboxen/polydimethylsiloxane fiber (DVB/CAR/PDMS, 50/30 μm , 2 cm) (Supelco, Bellefonte, Pennsylvania). Samples were incubated at 50 $^\circ\text{C}$ for 10 min with agitation (500 rpm; 30 s on time; 10 s off time) followed by sample extraction at 50 $^\circ\text{C}$ for 30 min. After incubation and extraction, the analytes were desorbed in the injection port at 250 $^\circ\text{C}$ for 10 min.

GC \times GC-TOF-MS. Chromatographic separation was carried out on an Agilent 7890B gas chromatograph (Agilent Technologies, Palo Alto, California) equipped with an OPTIMA 5 MS (30 m, 0.25 mm i.d. \times 0.1 μm df) primary column, a MEGA WAX FAST (2 m, 0.1 mm i.d. \times 0.1 μm df) secondary column, and a liquid nitrogen cryogenic modulator (Consumable-Free ZX2 thermal modulator). Helium was used as the carrier gas at a constant flow of 1 mL/min. The temperature program started at 35 $^\circ\text{C}$ for 5 min, was increased at 3 $^\circ\text{C}/\text{min}$ to 160 $^\circ\text{C}$, then ramped at 20 $^\circ\text{C}/\text{min}$ to 220 $^\circ\text{C}$, and kept at 220 $^\circ\text{C}$ for 5 min. The modulation period was set to 4 s with hot jet duration of 350 ms and with a shift of +20 $^\circ\text{C}$ regarding the temperature program of the GC oven. Detection was performed on a time-of-flight mass spectrometer (Markes International Ltd., Llantrisant, RCT, UK) operating in the electron-ionization (EI) mode with an ionizing voltage set at -70 eV. The transfer line was set to 250 $^\circ\text{C}$. The ion source temperature was 250 $^\circ\text{C}$. Data analysis was performed using the software ChromSpace (Markes International Ltd., Llantrisant, RCT, UK). The software was used to remove unwanted background noise and for spectrum deconvolution. Analytes were identified by comparing the retention times and mass spectra with standard substances and using the NIST Mass Spectral Library (National Institute of Standards and Technology, Gaithersburg, Maryland). IBMP and IBMP- d_9 were identified by comparing retention times and mass spectra with standard substances.

Feeding Experiments. Feeding experiments were carried out using bell pepper fruits (*Capsicum annuum* L. cv. Allrounder). Samples were treated directly after harvesting. Feeding experiments focused on the edible part of the fruit to study the biosynthesis of IBMP. That is why the calyx, pedicel as well as seeds, and placenta were removed before feeding experiments were carried out. The pericarp was cut into pieces (2 cm^2) and soaked in 1% NaOCl (sodium-hypochlorite) to avoid microbial contamination. Afterward, samples were rinsed with water to remove the remaining NaOCl. Samples were incubated on a sterile Petri dish with 200 μL of an aqueous solution containing a stable isotope-labeled precursor (1 mg/mL), whereas control samples were incubated with water. Co-feeding experiments were performed with a solution containing equal concentrations of both stable isotope-labeled precursors (1 mg/mL). After a 48 h incubation at room temperature, the samples were frozen using liquid nitrogen and crushed with a mortar. The homogenized sample (1 g) was weighed into a 10 mL headspace vial. To enhance SPME-efficiency, due to the salting-out effect, 2 mL of NaCl solution (20%, w/v) was added. Each experiment was repeated at least three times.

RESULTS AND DISCUSSION

Feeding Experiments. *In vivo* feeding experiments with stable isotope-labeled precursors were performed to investigate the biosynthesis of MPs, focusing on the biosynthesis of IBMP in the bell pepper pericarp (*Capsicum annuum* L. cv. Allrounder). Therefore, samples were incubated with stable isotope-labeled precursors before volatiles were extracted by HS-SPME and analyzed by GC \times GC-ToF-MS. Genuine IBMP was identified by comparing retention times and mass spectra with standard substances. As shown in Figure 1A, the EI mass spectrum of IBMP contains a molecular ion peak (M^+) at m/z 166 and intense mass peaks at m/z 124, m/z 151, and m/z 94. According to the literature, a mass peak at m/z 151 results from a methyl loss of the isobutyl chain, whereas m/z 124 results from a McLafferty rearrangement and the loss of propene (C_3H_6) (Figure 1A).²¹ The subsequent loss of formaldehyde (CH_2O) leads to m/z 94 (see Figure S1).²² High-resolution mass spectra (see Table S1) and mass spectra of the labeled reference compound 3-isobutyl- d_9 -2-methoxypyrazine (IBMP- d_9) (see below) confirmed the assignments of the mass fragments and the postulated fragmentation reactions.

For feeding experiments, the pericarp tissues of green, unripe and yellow, ripe bell pepper fruits were incubated with an aqueous solution of deuterated L-leucine (L-leucine- d_{10}). As displayed in Figure 1B, feeding experiments using the unripe bell pepper pericarp revealed incorporation of L-leucine- d_{10} into IBMP. As expected by the inverse isotope effect in GC,²³ a new peak, eluting a few seconds before genuine IBMP, appeared in samples incubated with L-leucine- d_{10} . Based on its mass spectrum, the number of incorporated deuterium atoms was determined. As shown in Figure 1B, M^+ is shifted by nine mass units (u) to m/z 175, which indicates incorporation of nine deuterium atoms (IBMP- d_9). Thus, apart from one deuterium at the α -C atom of L-leucine- d_{10} , which is lost during biosynthesis, all deuterium atoms of L-leucine- d_{10} are incorporated into IBMP. This is confirmed by mass shifts of m/z 124 to m/z 127, m/z 94 to m/z 97, and m/z 151 to m/z 157 (Figure 1B).

Similar findings were expected when feeding L-leucine- d_{10} to the ripe bell pepper pericarp. Interestingly, no incorporation of L-leucine- d_{10} into IBMP could be observed in pericarp tissue of ripe bell pepper fruits. As a reduced expression of the important enzymes *Vv*OMTs has been observed during grape ripening,²⁰ down-regulated enzymes might also explain why no incorporation of L-leucine- d_{10} into IBMP was detectable in the ripe bell pepper pericarp. Based on this observation, the following experiments were carried out with the unripe fruit.

As BCKAs might have an influence on MP biosynthesis as well, their relevance in plant MP biosynthesis was examined by additional feeding experiments using deuterated α -ketoisocaproic acid (α -KIC- d_7), the BCKA of L-leucine. As shown in Figure 1C, feeding experiments revealed incorporation of α -KIC- d_7 into IBMP in the unripe bell pepper pericarp. The degree of deuterium incorporation was deduced from the M^+ peaks. A shift up to seven mass units indicates incorporation of α -KIC- d_7 without a loss of a deuterium. In addition, fragment ions at m/z 125 and m/z 155 confirm incorporation of α -KIC- d_7 leading to the formation of IBMP- d_7 (Figure 1C).

To compare the efficiency of BCAAs and BCKAs in MP biosynthesis, further co-feeding experiments were performed.

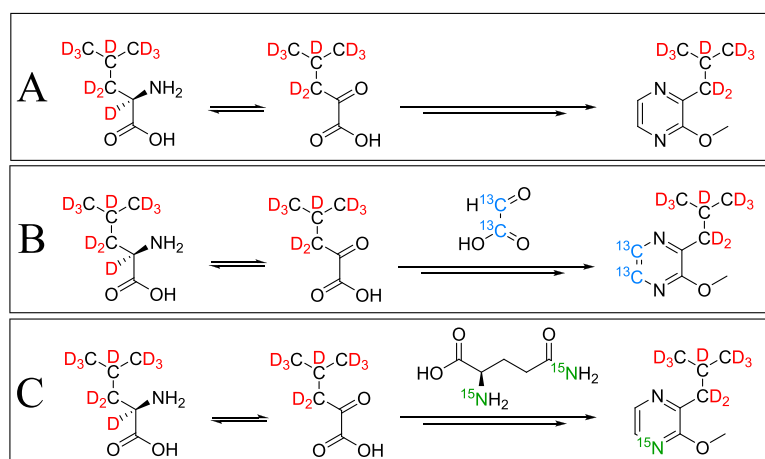


Figure 2. Possible structures of biosynthetic intermediates and products after incorporation of stable isotope-labeled L-leucine- d_{10} (A), L-leucine- d_{10} + glyoxylic acid- $^{13}\text{C}_2$ (B), and L-leucine- d_{10} + glutamine- $^{15}\text{N}_2$ (C) into IBMP.

First, pericarp tissue was incubated with a solution containing equal concentrations of L-leucine- d_{10} and α -KIC- d_7 . As the inverse isotope effect increases with the degree of deuteration,²³ not only IBMP and its deuterated analogues but also differentially labeled IBMP- d_7 and IBMP- d_9 could be partially separated by GC \times GC-ToF-MS. By comparing the peak areas of biosynthesized IBMP- d_7 and IBMP- d_9 , higher incorporation rates were detected for L-leucine- d_{10} (Figure 1D). This indicates that BCAAs might be more important precursors of MPs. However, higher BCAA incorporation rates might also occur due to differences between BCAAs and BCKAs regarding their cellular uptake, metabolism, and distribution. To address these possible differences in intracellular behavior, additional feeding experiments were carried out with L-leucine- $^{13}\text{C}_6$, $^{15}\text{N}_2$, 3,3,4,4,5,5,5,5',5'- d_{10} (L-leucine- $^{13}\text{C}_6$, $^{15}\text{N}_2$, d_{10}). Due to ^{15}N -labelling, a preceding biosynthetic deamination should be detectable using mass spectrometry data. Without preceding deamination, M^+ would be shifted up by 16 u (m/z 166 \rightarrow m/z 182), while a McLafferty rearrangement and elimination of isotope-labeled propene ($^{13}\text{C}_3\text{D}_6$) would result in a mass peak at m/z 131. Subsequent loss of deuterated formaldehyde (CD_2O) would lead to m/z 101. The fragment ion peak at m/z 151 would result in m/z 163. In contrast, a preceding deamination would shift M^+ up by 15 u (m/z 166 \rightarrow m/z 181) and further m/z ratios would be shifted up to m/z 162, m/z 130, and m/z 100. As shown in Figure 1E, feeding L-leucine- $^{13}\text{C}_6$, $^{15}\text{N}_2$, d_{10} to pericarp tissue of unripe bell peppers showed incorporation of both aminated and deaminated precursors. Nevertheless, m/z -ratios related to a preceding deamination show higher intensities than those related to the incorporation of the aminated precursor. Thus, incorporation of BCKAs appears to be preferred (Figure 2A). The results of these co-feeding experiments clearly demonstrate that BCKAs are involved in MP biosynthesis because a large portion of the ^{15}N -labels is lost during biosynthesis.

Additionally, it is still unknown which compound provides the second C2 unit to generate the IBMP heterocycle. As glycine and glyoxylic acid are often discussed in the literature, feeding experiments were performed using glycine-1- ^{13}C , ^{15}N and glyoxylic acid- $^{13}\text{C}_2$. Since the inverse isotope effect is more effective for deuterium than for isotope-labeled carbon,²⁴ no new peaks appear upon incorporation of ^{15}N and ^{13}C atoms and the peaks of the isotopomers are overlapping. Instead, ^{15}N

and ^{13}C incorporation should lead to larger intensities in distinct isotopic mass peaks in the mass spectrum of IBMP (isotope mass shift). Previously performed feeding experiments with L-leucine-1- ^{13}C , ^{15}N demonstrated that the incorporation rates are too low to show an isotopic mass shift (data not shown). To still reveal ^{15}N and ^{13}C incorporation, co-feeding experiments were conducted. To this end, samples were fed with solutions of L-leucine- d_{10} and either glyoxylic acid- $^{13}\text{C}_2$ or glycine-1- ^{13}C , ^{15}N , whereas control samples were fed with L-leucine- d_{10} only. In co-fed samples, the biosynthesis of three IBMP-isotopologues is possible. Besides the incorporation of only one precursor, also $^{13}\text{C}/^{15}\text{N}$ -labeled IBMP- d_9 as mixed reaction products of L-leucine- d_{10} and either glyoxylic acid- $^{13}\text{C}_2$ or glycine-1- ^{13}C , ^{15}N was expected (Figure 2B). Due to the incorporated deuterium atoms, the inverse isotope effect should occur for the mixed reaction products, leading to a clear separation from the unlabeled genuine IBMP and to a co-elution of IBMP- d_9 and $^{13}\text{C}/^{15}\text{N}$ -labeled IBMP- d_9 . This should allow the sensitive detection of isotopic enrichments due to ^{13}C and ^{15}N incorporation, which would be otherwise masked by the huge amount of unlabeled genuine IBMP. However, the abundances of M^+ , $[\text{M}^+ + 1]$, and $[\text{M}^+ + 2]$ were too low to compare. Instead, m/z 127 was chosen due to its high abundance, as well as m/z 157, as it includes most of the incorporable isotopes. Incorporation of one labeled atom would result in higher intensities of m/z 128 (m/z 127 + 1) and m/z 158 (m/z 157 + 1), whereas abundances of m/z 129 (m/z 127 + 2) and m/z 159 (m/z 157 + 2) would increase, if two labeled atoms are incorporated. The intensities of m/z 128 and m/z 129 were examined in relation to the intensity of m/z 127, while the intensities of m/z 158 and m/z 159 were examined in relation to the intensity of m/z 157 (Figure 4).

As shown in Figure 3B, intensities increased significantly in examined m/z ratios after feeding samples with L-leucine- d_{10} and glycine-1- ^{13}C , ^{15}N . The intensity of m/z 128 is 9% of the m/z 127 intensity in control samples because of the natural stable isotope abundance. This ratio increases significantly up to 32% in samples treated with L-leucine- d_{10} and glycine-1- ^{13}C , ^{15}N (Figure 4). Similarly, the abundance of m/z 158 is significantly higher (39%) in L-leucine- d_{10} and glycine-1- ^{13}C , ^{15}N -fed samples than it is in control samples (20%) (Figure 4). The abundance of m/z 129 is 2% in samples fed with L-leucine- d_{10} , while it is significantly higher (6%) in

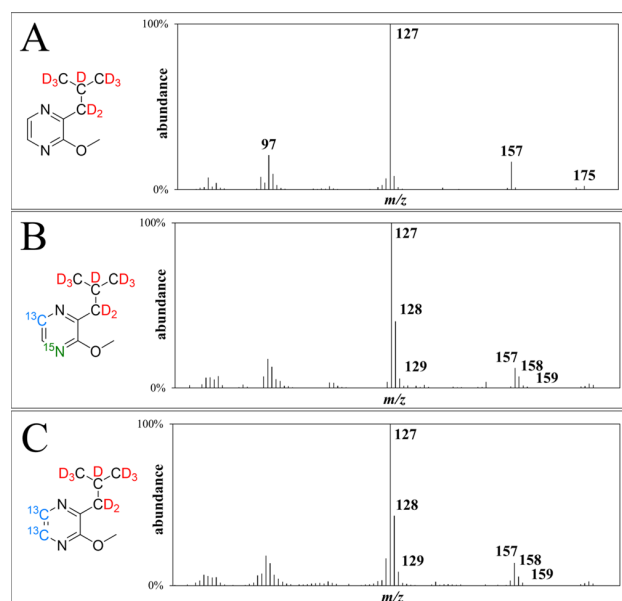


Figure 3. Electron ionization (EI) mass spectra of biosynthetic products after feeding L-leucine- d_{10} (A), L-leucine- d_{10} + glycine- $1-^{13}\text{C},^{15}\text{N}$ (B), and L-leucine- d_{10} + glyoxylic acid- $^{13}\text{C}_2$ (C) to pericarp tissue of unripe bell peppers (*Capsicum annuum* L. cv. Allrounder).

samples fed with L-leucine- d_{10} and glycine- $1-^{13}\text{C},^{15}\text{N}$. Significant increases (3% \rightarrow 10%) can also be observed in m/z 159 (Figure 4). In summary, samples fed with L-leucine- d_{10} and glycine- $1-^{13}\text{C},^{15}\text{N}$ show significant intensity increases by a factor of 3.6 in m/z 128 (9% \rightarrow 32%) and 2.3 in m/z 158 (20% \rightarrow 45%) as well as by factors of 3.0 in m/z 129 (2% \rightarrow 6%) and 3.3 in m/z 159 (3% \rightarrow 10%) (Figure 4). While the enrichments in m/z 129 and m/z 159 indicate incorporation of both ^{13}C and ^{15}N , enrichments in m/z 128 and m/z 158 indicate incorporation of only one labeled atom. On the one hand, only the ^{15}N atom could be incorporated, so glycine would serve as a nitrogen (N) source in IBMP biosynthesis. On the other hand, a preceding deamination of glycine and thus the loss of the ^{15}N atom would be possible. Deamination of glycine would lead to glyoxylic acid. In this case, higher incorporation rates were expected for glyoxylic acid.

In fact, co-feeding experiments with L-leucine- d_{10} and glyoxylic acid- $^{13}\text{C}_2$ show significant intensity increases in examined m/z ratios (Figure 3C). In short, abundances increase by a factor of 3.8 in m/z 128 (9% \rightarrow 34%) and 1.9 in m/z 158 (20% \rightarrow 39%) as well as by 5.5 in m/z 129 (2% \rightarrow 11%) and 4.7 in m/z 159 (3% \rightarrow 14%) when feeding L-leucine- d_{10} and glyoxylic acid- $^{13}\text{C}_2$ to the pericarp of unripe bell pepper fruits (Figure 4). An increase in m/z 128 and m/z 158 abundances demonstrates that the C2 unit of glyoxylic acid- $^{13}\text{C}_2$ is not incorporated into IBMP and that glyoxylic acid is not a direct precursor to IBMP. Considering that the fruit tissue is still metabolically active, other metabolic processes must have taken place during incubation. Thus, it is conceivable and in line with the labeling pattern that glyoxylic is first metabolized forming a C1 intermediate, which is then incorporated into IBMP. Nevertheless, intensity increases in relevant mass fragments as indicated by the detected m/z ratios clearly demonstrate incorporation of a C1 unit from labeled glycine and glyoxylic acid into IBMP, but at

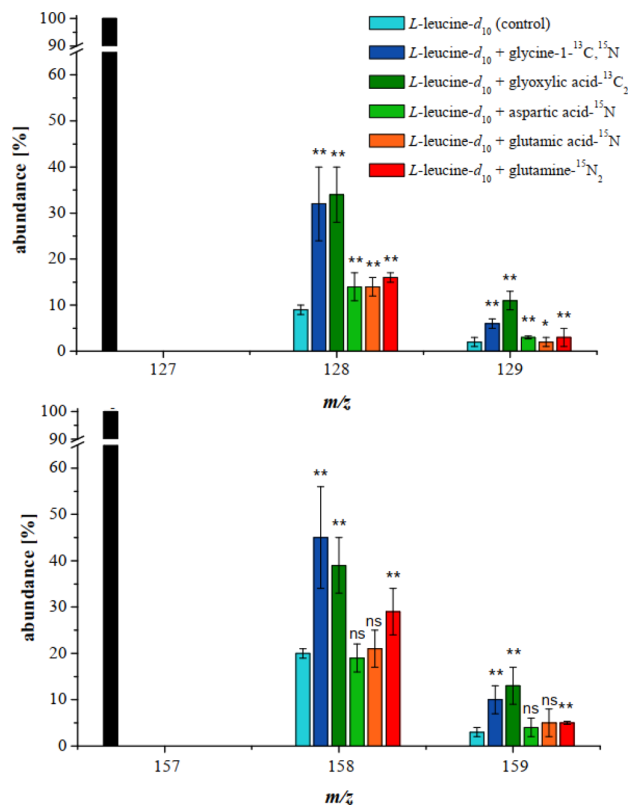


Figure 4. Ratio between the fragment ions of IBMP- d_9 (m/z 127, 157) and $^{13}\text{C}/^{15}\text{N}$ -labeled IBMP- d_9 (m/z 128, 158) and $^{13}\text{C}_2/^{13}\text{C},^{15}\text{N}$ -labeled IBMP- d_9 (m/z 129, 159) after feeding L-leucine- d_{10} , L-leucine- d_{10} + glycine- $1-^{13}\text{C},^{15}\text{N}$, L-leucine- d_{10} + glyoxylic acid- $^{13}\text{C}_2$, L-leucine- d_{10} + L-aspartic acid- ^{15}N , L-leucine- d_{10} + L-glutamic acid- ^{15}N , and L-leucine- d_{10} + L-glutamine- $^{15}\text{N}_2$ to unripe bell pepper pericarp (*Capsicum annuum* L. cv. Allrounder). Error bars indicate standard deviation. Statistical significance based on the t test (* $p \leq 0,05$; ** $p \leq 0,01$; ns: not significant).

the present stage, it is not yet possible to identify this C1 precursor in MP biosynthesis.

The incorporation of at least one keto acid (α -KIC or glyoxylic acid) implies the involvement of another precursor as the N source. Co-feeding experiments were conducted, with L-leucine- d_{10} and either L-aspartic acid- ^{15}N or L-glutamic acid- ^{15}N or L-glutamine- $^{15}\text{N}_2$, known as N-donors in plant metabolism (Figure 2C). Results for samples treated with L-leucine- d_{10} and either L-aspartic acid- ^{15}N or L-glutamic acid- ^{15}N show significant intensity increases in m/z 128 (9% \rightarrow 14%) and m/z 129 (2% \rightarrow 3%) but not in m/z 158 and m/z 159 abundances (Figure 4). In contrast, significant differences were observed for L-glutamine- $^{15}\text{N}_2$ by a factor of 1.8 in m/z 128 (9% \rightarrow 16%), 1.5 in m/z 158 (20% \rightarrow 29%) as well as m/z 129 (2% \rightarrow 3%), and 1.7 in m/z 159 (3% \rightarrow 5%) abundances (Figure 4). Thus, L-aspartic acid and L-glutamic acid seem to be less associated with the biosynthesis of MPs, whereas an involvement of L-glutamine as a N donor in MP biosynthesis appears to be of importance.

In conclusion, *in vivo* feeding experiments offered insights into the biosynthesis of MPs. A correlation between biosynthetic activity of MPs and the stage of maturity of bell pepper fruits has been observed. Whereas a *de novo* biosynthesis of IBMP was detectable in the unripe bell pepper pericarp, no incorporation of stable isotope-labeled precursors

into IBMP was detected in the ripe bell pepper pericarp. A correlation between the decreasing IBMP content and a reduced expression of *Vv*OMT during ripening seems to be possible. Furthermore, feeding experiments with the unripe bell pepper pericarp revealed for the first time incorporation of L-leucine and glycine as well as their respective keto acids, α -KIC and glyoxylic acid, into IBMP. The relevance of amino acids and their respective keto acids in MP biosynthesis was verified by comparing incorporation rates of labeled precursors. The feeding experiments with glycine and glyoxylic acid, co-feeding experiments with L-leucine and α -KIC, and feeding experiments with ^{15}N -labeled L-leucine gave insights into the biosynthesis of these potent odorants with clear hints for the involvement of C1 units as “building blocks” of the pyrazine heterocycle.

■ ASSOCIATED CONTENT

Supporting Information

The Supporting Information is available free of charge at <https://pubs.acs.org/doi/10.1021/acs.jafc.2c01747>.

Figure S1: Fragmentation mechanism leading to the mass peak at m/z 94; Table S1: HRMS data of 3-isobutyl-2-methoxy pyrazine (IBMP) (reference compound): nominal masses, exact masses, and chemical formula of characteristic fragment ions (PDF)

■ AUTHOR INFORMATION

Corresponding Author

Matthias Wüst – Institute of Nutritional and Food Sciences, Food Chemistry, University of Bonn, Bonn 53115, Germany; orcid.org/0000-0001-6808-5555; Phone: +49-228-73-2964; Email: matthias.wuest@uni-bonn.de; Fax: +49-228-73-3499

Author

Francesca Zamolo – Institute of Nutritional and Food Sciences, Food Chemistry, University of Bonn, Bonn 53115, Germany; orcid.org/0000-0002-0721-4162

Complete contact information is available at: <https://pubs.acs.org/doi/10.1021/acs.jafc.2c01747>

Notes

The authors declare no competing financial interest.

■ ACKNOWLEDGMENTS

We thank the Institute of Crop Science and Resource Conservation (INRES), Chair of Horticultural Sciences of the University of Bonn, Germany for providing bell pepper fruits.

■ ABBREVIATIONS

HS-SPME, headspace solid-phase microextraction; GC×GC, comprehensive two-dimensional gas chromatography; ToF-MS, time-of-flight mass spectrometer; MPs, 3-alkyl-2-methoxy pyrazines; HPs, 3-alkyl-2-hydroxy pyrazines; IBMP, 3-isobutyl-2-methoxy pyrazine; IBMP-*d*, 3-isobutyl-*d*₉-2-methoxy pyrazine; IBMP-*d*₇, 3-isobutyl-*d*₇-2-methoxy pyrazine; sBMP, 3-sec-butyl-2-methoxy pyrazine; IPMP, 3-isopropyl-2-methoxy pyrazine; *Vv*OMTs, *Vitis vinifera*-O-methyltransferases; BCAA, branched-chain amino acid; BCKA, branched-chain keto acid; α -KIC, α -ketoisocaproic acid

■ REFERENCES

- (1) Murray, K. E.; Shipton, J.; Whitfield, F. B. 2-methoxy pyrazines and the flavour of green peas (*Pisum sativum*). *Chem. Ind.* **1970**, 27, 897–898.
- (2) Nursten, H. E.; Sheen, M. R. Volatile flavour components of cooked potato. *J. Sci. Food Agric.* **1974**, 25, 643–663.
- (3) Murray, K. E.; Whitfield, F. B. The occurrence of 3-alkyl-2-methoxy pyrazines in raw vegetables. *J. Sci. Food Agric.* **1975**, 26, 973–986.
- (4) Augustyn, O. P. H.; Rapp, A.; van Wyk, C. J. Some Volatile Aroma Components of *Vitis Vinifera* L. cv. Sauvignon blanc. *SAJEV* **1982**, 3, 53–59.
- (5) Legrum, C.; Slabizki, P.; Schmarr, H.-G. Enantiodifferentiation of 3-sec-butyl-2-methoxy pyrazine in different species using multi-dimensional and comprehensive two-dimensional gas chromatographic approaches. *Anal. Bioanal. Chem.* **2015**, 407, 253–263.
- (6) Mutarutwa, D.; Navarini, L.; Lonzarich, V.; Compagnone, D.; Pittia, P. GC-MS aroma characterization of vegetable matrices: Focus on 3-alkyl-2-methoxy pyrazines. *J. Mass Spectrom.* **2018**, 53, 871–881.
- (7) Buttery, R. G.; Seifert, R. M.; Guadagni, D. G.; Ling, L. C. Characterization of some volatile constituents of bell peppers. *J. Agric. Food Chem.* **1969**, 17, 1322–1327.
- (8) Ryona, I.; Leclerc, S.; Sacks, G. L. Correlation of 3-isobutyl-2-methoxy pyrazine to 3-isobutyl-2-hydroxy pyrazine during maturation of bell pepper (*Capsicum annum*) and wine grapes (*Vitis vinifera*). *J. Agric. Food Chem.* **2010**, 58, 9723–9730.
- (9) Dunlevy, J. D.; Soole, K. L.; Perkins, M. V.; Dennis, E. G.; Keyzers, R. A.; Kalua, C. M.; Boss, P. K. Two O-methyltransferases involved in the biosynthesis of methoxy pyrazines: grape-derived aroma compounds important to wine flavour. *Plant Mol. Biol.* **2010**, 77–89.
- (10) Dunlevy, J. D.; Dennis, E. G.; Soole, K. L.; Perkins, M. V.; Davies, C.; Boss, P. K. A methyltransferase essential for the methoxy pyrazine-derived flavour of wine. *Plant J.* **2013**, 75, 606–617.
- (11) Guillaumie, S.; Ilg, A.; Réty, S.; Brette, M.; Trossat-Magnin, C.; Decroocq, S.; Léon, C.; Keime, C.; Ye, T.; Baltenweck-Guyot, R.; Claudel, P.; Bordenave, L.; Vanbrabant, S.; Duchêne, E.; Delrot, S.; Darriet, P.; Huguene, P.; Gomès, E. Genetic analysis of the biosynthesis of 2-methoxy-3-isobutyl pyrazine, a major grape-derived aroma compound impacting wine quality. *Plant Physiol.* **2013**, 162, 604–615.
- (12) Cheng, T. B.; Reineccius, G. A.; Bjorklund, J. A.; Leete, E. Biosynthesis of 2-methoxy-3-isopropyl pyrazine in *Pseudomonas perolens*. *J. Agric. Food Chem.* **1991**, 39, 1009–1012.
- (13) Wyllie, S. G.; Fellman, J. K. Formation of volatile branched chain esters in bananas (*Musa sapientum* L.). *J. Agric. Food Chem.* **2000**, 48, 3493–3496.
- (14) Rowan, D. D.; Lane, H. P.; Allen, J. M.; Fielder, S.; Hunt, M. B. Biosynthesis of 2-Methylbutyl, 2-Methyl-2-butenyl, and 2-Methylbutanoate Esters in Red Delicious and Granny Smith Apples Using Deuterium-Labeled Substrates. *J. Agric. Food Chem.* **1996**, 44, 3276–3285.
- (15) Myers, M. J.; Issenberg, P.; Wick, E. L. L-Leucine as a precursor of isoamyl alcohol and isoamyl acetate, volatile aroma constituents of banana fruit discs. *Phytochemistry* **1970**, 9, 1693–1700.
- (16) Kochevenko, A.; Araújo, W. L.; Maloney, G. S.; Tieman, D. M.; Do, P. T.; Taylor, M. G.; Klee, H. J.; Fernie, A. R. Catabolism of branched chain amino acids supports respiration but not volatile synthesis in tomato fruits. *Mol. Plant* **2012**, 5, 366–375.
- (17) Gonda, I.; Bar, E.; Portnoy, V.; Lev, S.; Burger, J.; Schaffer, A. A.; Tadmor, Y.; Gepstein, S.; Giovannoni, J. J.; Katzir, N.; Lewinsohn, E. Branched-chain and aromatic amino acid catabolism into aroma volatiles in *Cucumis melo* L. fruit. *J. Exp. Bot.* **2010**, 61, 1111–1123.
- (18) Gallois, A.; Kergomard, A.; Adda, J. Study of the biosynthesis of 3-isopropyl-2-methoxy pyrazine produced by *Pseudomonas taetrolens*. *Food Chem.* **1988**, 28, 299–309.
- (19) Roujou de Boubée, D. *Research on 2-methoxy-3-isobutyl pyrazine in grapes and wines*; Academie Amorim: Paris, France, 2003.

(20) Lei, Y.; Xie, S.; Chen, H.; Guan, X.; Zhang, Z. Behavior of 3-isobutyl-2-methoxypyrazine biosynthesis related to proposed precursor and intermediate in wine grape. *Food Chem.* **2019**, *277*, 609–616.

(21) Gerritsma, D. A.; Brindle, I. D.; Jones, T. R.; Capretta, A. Preparation of labelled 2-methoxy-3-alkylpyrazines: synthesis and characterization of deuterated 2-methoxy-3-isopropylpyrazine and 2-methoxy-3-isobutylpyrazine. *J. Labelled Compd. Radiopharm.* **2003**, *46*, 243–253.

(22) Gross, J. H. *Mass spectrometry: A textbook*; Third edition; Springer International Publishing, 2017, DOI: 10.1007/978-3-319-54398-7.

(23) Matucha, M.; Jockisch, W.; Verner, P.; Anders, G. Isotope effect in gas—liquid chromatography of labelled compounds. *J. Chromatogr. A* **1991**, *588*, 251–258.

(24) Elmore, J. S. Extraction techniques for analysis of aroma compounds. In *Flavour Development, Analysis and Perception in Food and Beverages // Flavour development, analysis and perception in food and beverages*; Parker, J. K., Elmore, J. S., Methven, L., Eds.; Woodhead Publishing series in food science, technology and nutrition, Vol. 273; Elsevier; WP Woodhead Publ./Elsevier, 2015; pp 31–46, DOI: 10.1016/B978-1-78242-103-0.00002-3.

Recommended by ACS

Furan Fatty Acids in Some 20 Fungi Species: Unique Profiles and Quantities

Franziska Müller, Walter Vetter, *et al.*

SEPTEMBER 26, 2022
JOURNAL OF AGRICULTURAL AND FOOD CHEMISTRY

READ 

Characterization of the Oxylipin Pattern and Other Fatty Acid Oxidation Products in Freshly Pressed and Stored Plant Oils

Elisabeth Koch, Nils Helge Schebb, *et al.*

SEPTEMBER 29, 2022
JOURNAL OF AGRICULTURAL AND FOOD CHEMISTRY

READ 

ROS Stress and Cell Membrane Disruption are the Main Antifungal Mechanisms of 2-Phenylethanol against *Botrytis cinerea*

Xiurong Zou, Xingfeng Shao, *et al.*

NOVEMBER 02, 2022
JOURNAL OF AGRICULTURAL AND FOOD CHEMISTRY

READ 

Identification of a Novel 2,4-D Metabolic Detoxification Pathway in 2,4-D-Resistant Waterhemp (*Amaranthus tuberculatus*)

Marcelo R. A. de Figueiredo, Todd A. Gaines, *et al.*

DECEMBER 01, 2022
JOURNAL OF AGRICULTURAL AND FOOD CHEMISTRY

READ 

Get More Suggestions >

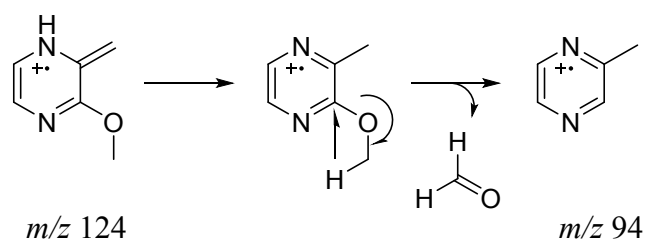
SUPPORTING INFORMATION

Investigation of Biosynthetic Precursors of 3-Isobutyl-2-Methoxypyrazine using Stable Isotope Labelling Studies in Bell Pepper Fruits (*Capsicum annuum* L.)

Francesca Zamolo¹, Matthias Wüst^{1,*}

¹ *University of Bonn, Institute of Nutritional and Food Sciences, Food Chemistry,
Friedrich-Hirzebruch-Allee 7, 53115 Bonn, Germany*

* **Corresponding author:** Prof. Dr. Matthias Wüst, University of Bonn, Institute of Nutritional and
Food Sciences, Food Chemistry, Friedrich-Hirzebruch-Allee 7, 53115 Bonn, Germany;
Phone: +49-228-73-2964, Fax: +49-228-73-3499, E-mail: matthias.wuest@uni-bonn.de

Figure S-1 Fragmentation mechanism leading to the mass peak at m/z 94.**Table S-1** Nominal masses, exact masses, and chemical formula of characteristic fragment ions of 3-isobutyl-2-methoxypyrazine (IBMP) (reference compound) detected by EI-MS using a MAT 95 XL high resolution mass spectrometer (*Thermo Finnigan*, Bremen, Germany)

Nominal mass (m/z)	Measured mass (m/z)	Formula
166	-	$[\text{C}_9\text{H}_{14}\text{N}_2\text{O}]^{+\bullet}$
151	151.0869	$[\text{C}_8\text{H}_{11}\text{N}_2\text{O}]^+$
124	124.0632	$[\text{C}_6\text{H}_8\text{N}_2\text{O}_9]^{+\bullet}$
94	94.0525	$[\text{C}_5\text{H}_6\text{N}_2]^{+\bullet}$

F. Publication 2



Chemistry—A European Journal

Research Article
doi.org/10.1002/chem.202203674

 Chemistry
Europe
European Chemical
Societies Publishing

www.chemeurj.org

L-Serine is the Direct Precursor for the Pyrazine Ring Construction in the Biosynthesis of 3-Isobutyl-2-Methoxypyrazine in Bell Pepper Fruits (*Capsicum annuum* L.)

Francesca Zamolo^[a] and Matthias Wüst^{*[a]}

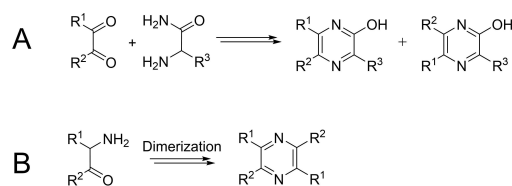
Abstract: 3-Isobutyl-2-methoxypyrazine (IBMP) is an extremely potent odorant and responsible for the specific aroma of many fruits and vegetables. Especially bell pepper contains high levels of IBMP, which is the character impact compound of its typical aroma. However, since the discovery of methoxypyrazines in plants in the 1960s the biosynthesis of their pyrazine ring motif remained so far unknown.

Therefore, the biosynthetic pathway to IBMP was investigated by feeding experiments with stable-isotope labeled precursors. For the first time it could be shown that L-serine plays a key role in the pyrazine ring construction of 3-alkyl-2-methoxypyrazines (MPs). Based on HS-SPME-GC-TOF-MS analysis, it is shown that the biosynthetic pathway to IBMP is closely linked to photorespiratory derived L-serine.

Introduction

Pyrazines are six-membered heterocycles possessing two nitrogen atoms in the 1,4-positions. Pyrazine and its derivatives are ubiquitous in nature, biosynthesized by microorganisms, insects and plants, serving as odor signals or repellents against pathogens, pests and herbivores.^[1–3] As many pesticides, pharmaceuticals and flavorings are pyrazine-based, they are also synthesized chemically in industry.^[4–6] The pyrazine ring can be synthesized using various routes mainly by direct ring closure such as the two-step synthesis starting with a condensation of a 1,2-diketone with a 1,2-diamine (Scheme 1A) or the spontaneous intramolecular α -aminoketone-cyclization (Scheme 1B).^[4,5,7,8]

Pyrazines contribute to different aromas; their aroma properties depend on their substitution pattern. Alkyl-substituted pyrazines have a roasted, nutty, or earthy flavour.^[10] They occur in thermally processed foods for example peanuts or coffee synthesized in non-enzymatic processes as typical Maillard reaction products, but also in fermented food as products biosynthesized enzymatically by microorganisms.^[11] In contrast, alkoxy-pyrazines such as 3-alkyl-2-methoxypyrazines (MPs) are associated with a green and earthy flavor.^[3] MPs are

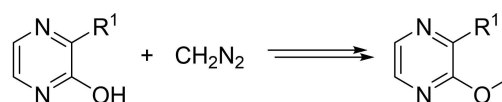


Scheme 1. Synthesis of (A) 2-hydroxypyrazines by a condensation of a 1,2-diketone with a 1,2-diamine by Jones^[4] and (B) pyrazines by a self-cyclization of two α -aminoketones by Gutknecht.^[8]

chemically synthesized by a methylation of the respective 2-hydroxypyrazine (see Scheme 1A) with diazomethane, as displayed in Scheme 2 or methyl iodide.^[12–14]

The most studied MPs are 3-isobutyl-2-methoxypyrazine (IBMP, **1**), 3-sec-butyl-2-methoxypyrazine (sBMP, **2**) and 3-isopropyl-2-methoxypyrazine (IPMP, **3**) (Scheme 3).^[1,15] They are found in many raw vegetables^[15,16] as well as in several grape varieties and their corresponding wines.^[17]

As higher MP-levels in wines are undesired and associated with immaturity^[18] the interest of unravelling the biosynthetic pathway of MPs in plants has increased. The mechanism of MP-formation has long been questioned and controversially discussed in the literature. First, a condensation of an α -amino

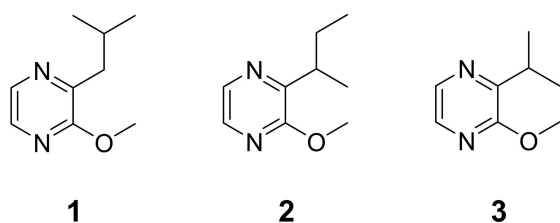


Scheme 2. Synthesis of 3-alkyl-2-methoxypyrazines (MPs) according to Seifert et al.^[12]

[a] F. Zamolo, Prof. Dr. M. Wüst
Institute of Nutritional and Food Sciences, Chair of Food Chemistry
University of Bonn
Friedrich-Hirzebruch-Allee 7, 53115 Bonn (Germany)
E-mail: matthias.wuest@uni-bonn.de

Supporting information for this article is available on the WWW under <https://doi.org/10.1002/chem.202203674>

© 2022 The Authors. Chemistry - A European Journal published by Wiley-VCH GmbH. This is an open access article under the terms of the Creative Commons Attribution Non-Commercial NoDerivs License, which permits use and distribution in any medium, provided the original work is properly cited, the use is non-commercial and no modifications or adaptations are made.

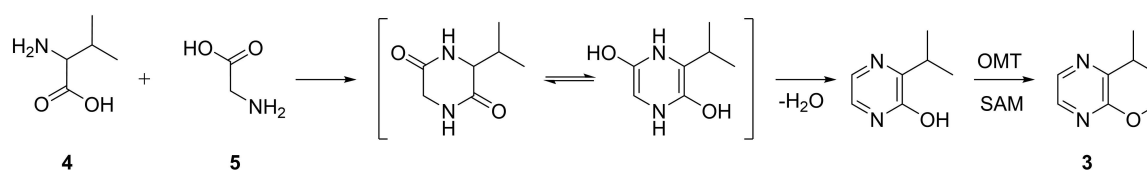


Scheme 3. Structures of the most studied 3-alkyl-2-methoxy-pyrazines MPs: 3-isobutyl-2-methoxy-pyrazine (IBMP, **1**), 3-sec-butyl-2-methoxy-pyrazine (sBMP, **2**) and 3-isopropyl-2-methoxy-pyrazine (IPMP, **3**).

acid amide of a branched chain amino acid and glyoxal has been proposed.^[13,19] However, neither α -amino acid amides nor free glyoxal have been detected in plants.^[3,20] Alternatively, a biosynthetic pathway as described in microorganism has been suggested including the formation of a cyclic dipeptide from valine (**4**) and glycine (**5**) followed by the elimination of water and an enzymatic *O*-methylation (Scheme 4).^[21]

Recent research provided new insight into the biosynthesis of MPs. First, *S*-adenosylmethionine (SAM)-dependent *O*-methyltransferases (*Vitis vinifera O*-methyltransferases, VvOMTs) catalyzing the *O*-methylation have been identified.^[22] Then, feeding studies proved an incorporation of L-leucine (**6**) and α -ketoisocaproic acid (α -KIC, **7**) into **1** and revealed glycine (**5**) and glyoxylic acid (**8**) as C_1 -building blocks and L-glutamine (**9**) as N-donor in the biosynthesis of **1**.^[23]

However, the direct precursor providing the C_2 -unit for the pyrazine ring construction remained unknown. To investigate the origin of the C_2 -unit in the biosynthesis of **1** feeding experiments using ^{13}C -compounds were conducted and analyzed. Therefore, volatiles were extracted using headspace solid-phase microextraction (HS-SPME), analyzed by comprehensive two-dimensional gas chromatography (GCxGC) and detected using time-of-flight mass spectrometry (TOF-MS). Since low rates of ^{13}C -incorporations were masked by the huge amount of unlabeled genuine IBMP and thus difficult to detect by HS-SPME-GCxGC-TOF-MS, we took advantage of the inverse isotope effect of deuterium labeled compounds in GC and the concomitant shift in retention time in $^{13}\text{C}/^2\text{H}$ -mixed labeling experiments to detect the incorporation of ^{13}C -labeled precursor, even at trace levels.



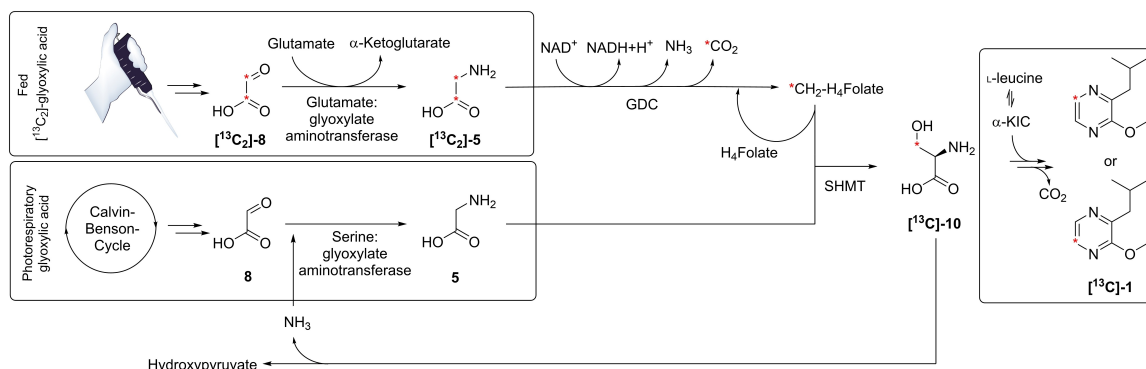
Scheme 4. Proposed biosynthetic pathway to **3** in *Pseudomonas perolens* according to Cheng et al.^[21]

Results and Discussion

Prior investigations clearly demonstrated that glycine (**5**) and glyoxylic acid (**8**) do not serve as direct precursors to 3-isobutyl-2-methoxy-pyrazine (IBMP, **1**). Instead, they are deemed to act as C_1 -building blocks, suggesting that they are first metabolized before they are incorporated into **1**.^[23] However, the underlying metabolic pathway remained unknown in this previously performed labeling study. We have therefore reanalyzed these previous results taking into account that in plants **5** and **8** are biochemically linked. During photorespiration two molecules of **8** are aminated to two molecules of **5**, of which one undergoes a deamination and decarboxylation catalyzed by the glycine decarboxylase complex (GDC), which is composed of four enzymes, one catalyzes the decarboxylation of **5** to methylamine, another interacts with tetrahydrofolate (H_4Folate) catalyzing the reaction of methylamine with H_4Folate resulting in 5,10-methylenetetrahydrofolate ($\text{CH}_2\text{-H}_4\text{Folate}$).^[24,25] Subsequently H_4Folate is recycled and L-serine (**10**) is formed by combining $\text{CH}_2\text{-H}_4\text{Folate}$ and a second molecule of **5** catalyzed by the serine-hydroxymethyltransferase (SHMT).^[26–28]

The metabolic interface of C_1 -metabolism and photorespiratory cycle via **8** and **5** points to a potential biosynthetic link between photorespiration and the biosynthesis of **1**. As displayed in Scheme 5, [$^{13}\text{C}_2$]-**8** can be metabolized to [$3\text{-}^{13}\text{C}$]-**10**, as well as [$^{13}\text{C}_3$]-**10** and [$1,2\text{-}^{13}\text{C}_2$]-**10**, depending on the position of incorporated ^{13}C -atoms and the number of incorporated [$^{13}\text{C}_2$]-**8** (one- or twofold). The decarboxylation and incorporation of ^{13}C -labeled **10** into **1** would lead to two ^{13}C -labeled **1** explaining the incorporation of a C_1 -unit into **1** rather than a C_2 -unit when feeding [$^{13}\text{C}_2$]-**8**,^[23] which would indicate that **10** serves as a direct precursor to **1**.

To investigate the relevance of **10** in the biosynthesis of **1**, feeding experiments were conducted in this study using stable-isotope labeled **10**. Usually, stable-isotope labeled analytes can be identified as new peaks eluting before their unlabeled analogue, as the inverse isotope effect leads to a shortened retention time of the stable-isotope labeled analyte.^[29] This leads to pure mass spectra of the labeled and unlabeled compounds. The degree of stable-isotope incorporation can thus be deduced based on the mass spectral data. However, the inverse isotope effect is less effective for stable-isotopes like ^{15}N and ^{13}C than for deuterium atoms.^[29] Unlabeled and ^{15}N - or ^{13}C -labeled compounds are therefore generally co-eluting and only detectable by intensity increases in distinct isotopic mass peaks (isotope mass shift). Nonetheless, a large amount of the unlabeled isotopologue masks these intensity increases, making



Scheme 5. Possible incorporation of [^{13}C]-glyoxylic acid into **1** during photorespiration. GDC, glycine decarboxylase complex; SHMT, serine hydroxymethyltransferase; H_4Folate , tetrahydrofolate.

low incorporation rates of ^{15}N - or ^{13}C -labeled precursors difficult to detect. To prevent this, we have performed mixed labeling studies that avoid undesired co-elutions, as it leads to the separation of the isotope labeled from the genuine, unlabeled analyte. For this purpose, the formation of a deuterated and ^{15}N , ^{13}C -labeled reaction product is forced by co-feeding experiments with a known deuterated precursor and a putative ^{15}N , ^{13}C -labeled precursor. The incorporation of deuterium atoms leads to the inverse isotope effect, allowing to separate labeled and unlabeled isotopologues by GC, which in turn enables the mass spectral detection of isotopic enrichments, occurring due to ^{15}N - or ^{13}C -incorporations.

In following co-feeding experiments L-[$^2\text{H}_{10}$]-leucine ($[^2\text{H}_{10}]$ -**6**) was used as the known deuterated precursor, as prior biosynthetic investigations clearly demonstrated that **6** serves as a precursor to **1**.^[23] Feeding $[^2\text{H}_{10}]$ -**6** to bell pepper pericarp leads to the deuteration of the whole isobutyl-moiety and thus to the incorporation of nine deuterium atoms ($[^2\text{H}_9]$ -**1**).^[23] A chromatographic separation of **1** and $[^2\text{H}_9]$ -**1** as well as the detection of shifts of distinctive fragment ions to higher masses are detectable by HS-SPME-GC/GC-TOF-MS (Figure 1). The electron impact (EI) mass spectra of **1** and $[^2\text{H}_9]$ -**1** are displayed in Figure 2.^[23]

The mass spectral fragmentation pattern of $[^2\text{H}_9]$ -**1** shows a molecular ion peak ($\text{M}^{+\bullet}$) at m/z 175 and intense mass peaks at

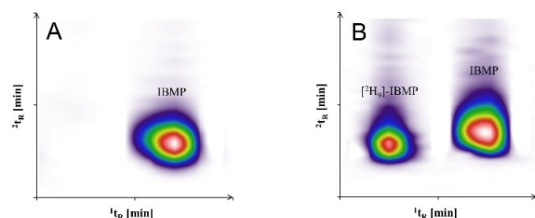


Figure 1. Extracted-ion chromatograms (EIC) of (A) genuine **1** (EIC m/z 124) and (B) **1** and $[^2\text{H}_9]$ -**1** after feeding L-[$^2\text{H}_{10}$]-leucine to pericarp tissue of unripe bell peppers (*Capsicum annuum* L. cv. Allrounder).

m/z 127, m/z 157, and m/z 97. According to Scheme 6 the mass peak at m/z 157 [$\text{C}_8\text{H}_5\text{D}_3\text{N}_2\text{O}$] $^{+\bullet}$ is formed by a loss of a deuterated methyl radical of the isobutyl chain, whereas m/z 127 [$\text{C}_6\text{H}_5\text{D}_3\text{N}_2\text{O}$] $^{+\bullet}$ results from a *McLafferty* rearrangement and the loss of deuterated propene (C_3D_6). The fragment ion m/z 97 [$\text{C}_5\text{H}_3\text{D}_3\text{N}_2$] $^{+\bullet}$ is formed by a neutral loss of formaldehyde (CH_2O) via a four-membered transition state, similar to the formaldehyde loss during the fragmentation of arylalkyl ethers.^[23,30]

Feeding experiments with L-[2 - ^{13}C]-serine

First, co-feeding experiments with $[^2\text{H}_{10}]$ -**6** and $[2$ - ^{13}C]-**10** were carried out. An incorporation of labeled precursors into **1** would lead to the formation of the following differentially labeled methoxypyrazines: $[^2\text{H}_9]$ -**1** (incorporation of $[^2\text{H}_{10}]$ -**6**, Scheme 7A), ^{13}C -labeled $[^2\text{H}_9]$ -**1** ($[^2\text{H}_9, ^{13}\text{C}]$ -**1**) (incorporation of $[^2\text{H}_{10}]$ -**6** and $[2$ - $^{13}\text{C}]$ -**10**, Scheme 7B) and $[^{13}\text{C}]$ -**1** (incorporation of $[2$ - $^{13}\text{C}]$ -**10**, Scheme 7C).

The co-feeding prevented a co-elution of unlabeled genuine and $^{13}\text{C}/^2\text{H}$ -isotope labeled **1**. Instead, the desired co-elution of $[^2\text{H}_9]$ -**1** and $[^2\text{H}_9, ^{13}\text{C}]$ -**1** was achieved. Based on the mass spectra, an incorporation of $[2$ - $^{13}\text{C}]$ -**10** into **1** could be confirmed. The incorporation of $[2$ - $^{13}\text{C}]$ -**10** leads to mass shifts to higher mass ranges and results in increases of the mass peaks m/z 176, 158, 128 and 98 (Figure 3A).

To examine whether the intensities increase significantly, abundances of highly diagnostic fragment ions of control samples ($[^2\text{H}_{10}]$ -**6**) were compared to those in co-fed samples ($[^2\text{H}_{10}]$ -**6** + $[2$ - $^{13}\text{C}]$ -**10**). For this purpose, the fragment ion containing most of the incorporable isotopes (m/z 157) and the most abundant base peak ion (m/z 127) were chosen, as the $\text{M}^{+\bullet}$ (m/z 175) abundance was too low, even when using soft ionization (-15 eV). Since the abundances vary depending on the incorporation rate, relative intensities were considered instead. For this purpose, the highly diagnostic mass peaks implying only the incorporation of $[^2\text{H}_{10}]$ -**6** (m/z 127, 157) were set equal to 100% and the respective intensities of the mass

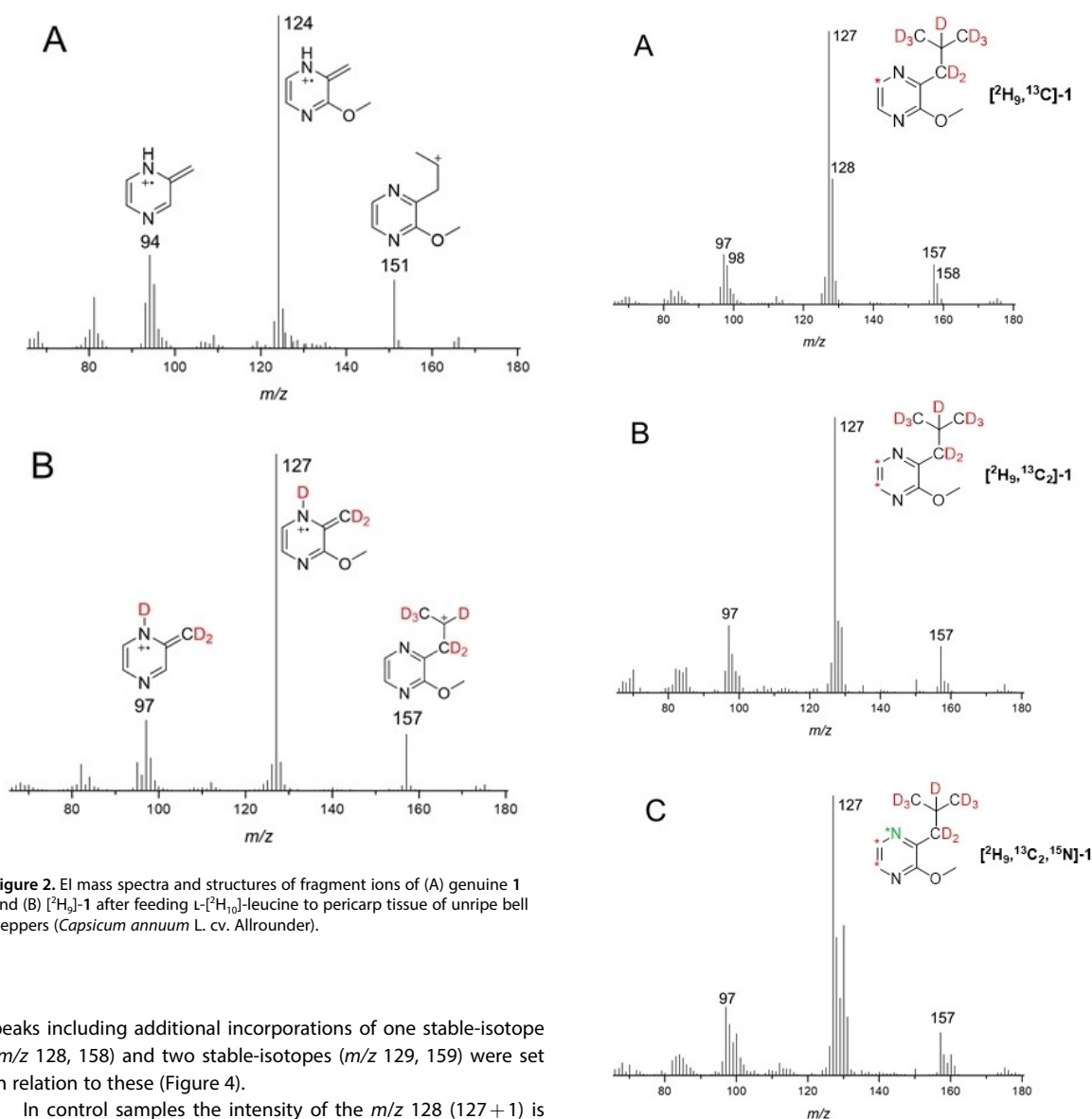


Figure 2. EI mass spectra and structures of fragment ions of (A) genuine **1** and (B) $[\text{2H}_9]\text{-1}$ after feeding L- $[\text{2H}_{10}]$ -leucine to pericarp tissue of unripe bell peppers (*Capsicum annuum* L. cv. Allrounder).

peaks including additional incorporations of one stable-isotope (m/z 128, 158) and two stable-isotopes (m/z 129, 159) were set in relation to these (Figure 4).

In control samples the intensity of the m/z 128 ($127 + 1$) is 8% of the base peak m/z 127 intensity, due to the natural stable-isotope abundance. In contrast, in samples fed with $[\text{2H}_{10}]\text{-6}$ and $[\text{2-}^{13}\text{C}]\text{-10}$ it increases up to 40%. Similarly, m/z 158 ($157 + 1$) increases up to 44% in samples fed with $[\text{2H}_{10}]\text{-6}$ and $[\text{2-}^{13}\text{C}]\text{-10}$. Consequently, intensities increase significantly by a factor of 4.9 for m/z 128 in samples fed with $[\text{2H}_{10}]\text{-6}$ and $[\text{2-}^{13}\text{C}]\text{-10}$ compared to abundances of m/z 128 in control samples and by a factor of 3.2 for m/z 158. Therefore, these feeding experiments clearly demonstrate that **10** is incorporated into **1**.

Nevertheless, significant intensity increases can also be detected in m/z 129 ($127 + 2$) by a factor of 4.7 (2% to 7%) as well as in m/z 159 ($157 + 2$) by a factor of 4.6 (3% to 15%). These intensity increases can be rationalized by the catabolism of **10** occurring in the metabolically active fruit tissue during feeding experiments. As it is known, serine (**10**) and glycine (**5**) are interconvertible.^[31] Absorbed **10** is catabolized to $[\text{2-}^{13}\text{C}]\text{-5}$,

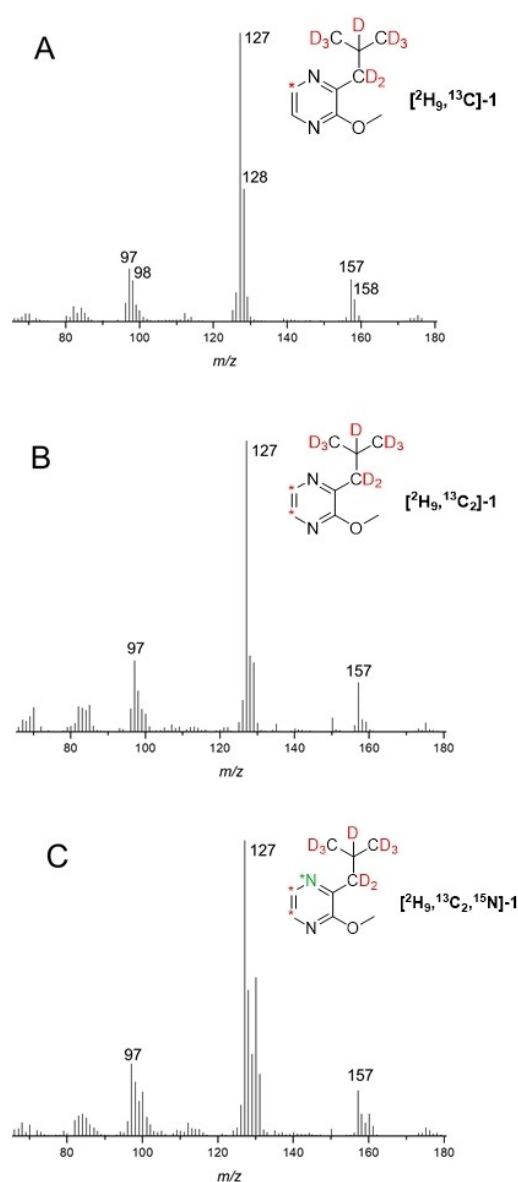
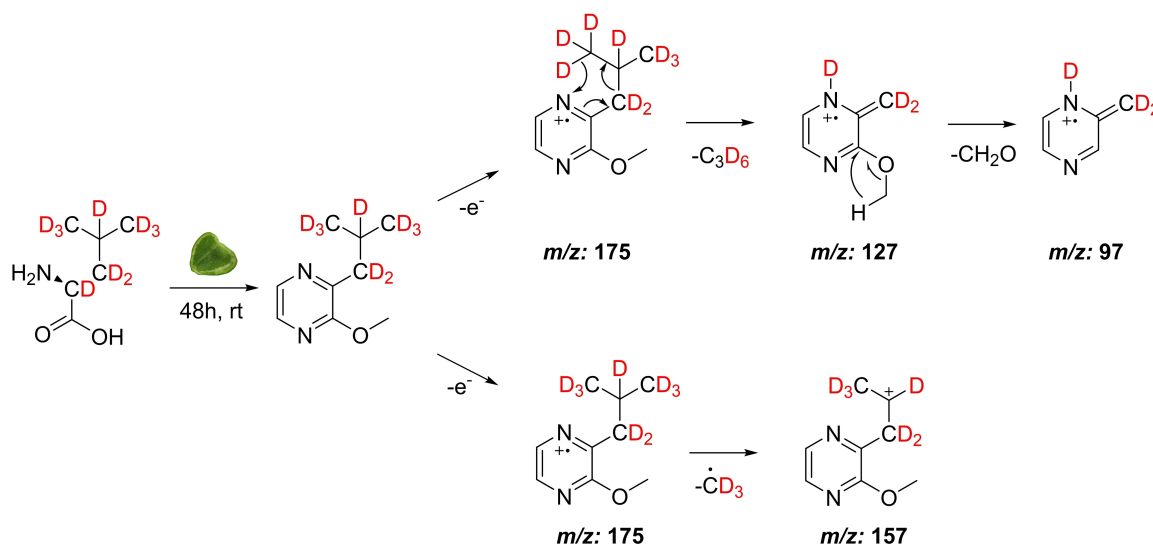


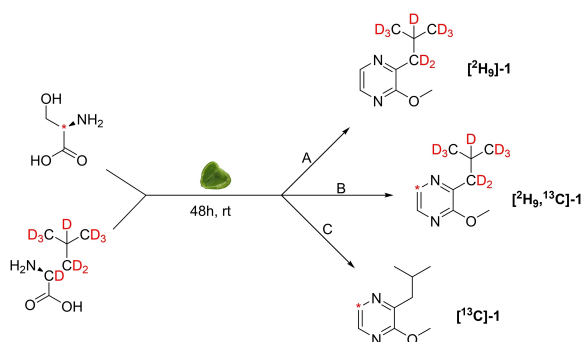
Figure 3. Mass spectra of (A) $[\text{2H}_9,^{13}\text{C}]\text{-1}$ after feeding L- $[\text{2H}_{10}]$ -leucine + L- $[\text{2-}^{13}\text{C}]\text{-serine}$, (B) $[\text{2H}_9,^{13}\text{C}_2]\text{-1}$ after feeding L- $[\text{2H}_{10}]$ -leucine + L- $[\text{2,3-}^{13}\text{C}_2]\text{-serine}$ and (C) $[\text{2H}_9,^{13}\text{C}_2,^{15}\text{N}]\text{-1}$ after feeding L- $[\text{13C}_3,^{15}\text{N}]\text{-serine}$. The exact position of the ^{15}N -label in the pyrazine ring ($^{15}\text{N-1}$ or $^{15}\text{N-4}$; here $^{15}\text{N-4}$ is shown) cannot be determined at the present stage.

which in turn is metabolized to $^{13}\text{CH}_2\text{-H}_4\text{Folate}$. As shown in Scheme 8, the catabolism of $[\text{2-}^{13}\text{C}]\text{-10}$ to $[\text{2-}^{13}\text{C}]\text{-5}$ and $^{13}\text{CH}_2\text{-H}_4\text{Folate}$ and their re-incorporation into **10** leads to $[\text{2,3-}^{13}\text{C}_2]\text{-10}$. An incorporation of $[\text{2,3-}^{13}\text{C}_2]\text{-10}$ into **1** results in intensity increases in m/z 129 and m/z 159, providing that the C-2 and C-3 of **10** are incorporated into **1**.

In summary, feeding experiments revealed that **10** is incorporated into **1**. However, the exact position of ^{13}C -



Scheme 6. Labeling pattern and fragmentation of $[\text{2H}_9]\text{-1}$ after feeding $\text{L-}[\text{2H}_{10}]\text{-leucine}$ to unripe bell pepper pericarp (*Capsicum annuum* L. cv. Allrounder).^[23]



Scheme 7. Labeling pattern of IBMP after the incorporation of (A) $\text{L-}[\text{2H}_{10}]\text{-leucine}$, (B) $\text{L-}[\text{2H}_{10}]\text{-leucine}$ and $\text{L-}[\text{2-}^{13}\text{C}]\text{-serine}$ and (C) $\text{L-}[\text{2-}^{13}\text{C}]\text{-serine}$. The exact position of the ^{13}C -label in the pyrazine ring ($^{13}\text{C-5}$ or $^{13}\text{C-6}$; here $^{13}\text{C-5}$ is shown) cannot be determined at the present stage (see also Scheme 5).

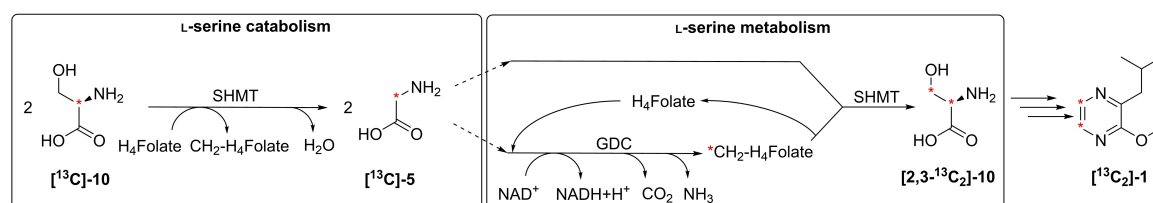
incorporation into **1** remained unknown. To determine the position of ^{13}C -incorporation the fragmentation patterns of the pyrazine ring was examined by direct-injection ESI/MSⁿ analyses using a stock solution of **1** (data not shown), but the

abundances of the fragment ions $\text{C}_4\text{H}_4\text{N}^+$ (m/z 66), $\text{C}_3\text{H}_4\text{N}^+$ (m/z 54) and $\text{C}_3\text{H}_3\text{N}^{*+}$ (m/z 53) indicating the degradation of the pyrazine ring (Scheme 9), were too low (see Supporting Information Table S1. for high-resolution EI mass spectra (HR-EL-MS)).

Feeding experiments with $\text{L-}[\text{2,3-}^{13}\text{C}_2]\text{-serine}$

Moreover, it is still unclear whether serine (**10**) provides a C_1 - or a C_2 -unit to **1**. To examine if **10** serves as a C_2 -donor in the biosynthesis of **1**, further co-feeding experiments were conducted using $\text{L-}[\text{2H}_{10}]\text{-leucine}$ ($[\text{2H}_{10}]\text{-6}$) and $[\text{2,3-}^{13}\text{C}_2]\text{-10}$. As displayed in Figure 3 B, feeding experiments strongly suggested that C-2 and C-3 of **10** are incorporated into **1**. Mass spectral data show significant increases in fragment ion peaks m/z 129 ($127+2$) (2% to 19%) and m/z 159 ($157+2$) (3% to 20%) (Figure 4).

However, increases are also detectable in m/z 128 (8% to 25%) and m/z 158 (14% to 25%), which can be rationalized by the catabolism of $[\text{2,3-}^{13}\text{C}_2]\text{-10}$ during incubation experiments. As mentioned above, $[\text{2,3-}^{13}\text{C}_2]\text{-10}$ is degraded to $[\text{2-}^{13}\text{C}]\text{-glycine}$



Scheme 8. The catabolism of $\text{L-}[\text{2-}^{13}\text{C}]\text{-serine}$ to $[\text{2-}^{13}\text{C}]\text{-glycine}$ and $^{13}\text{CH}_2\text{-H}_4\text{Folate}$ and their re-incorporation into $\text{L-}[\text{2,3-}^{13}\text{C}_2]\text{-serine}$. GDC, glycine decarboxylase complex; SHMT, serine hydroxymethyltransferase, H_4Folate , tetrahydrofolate.

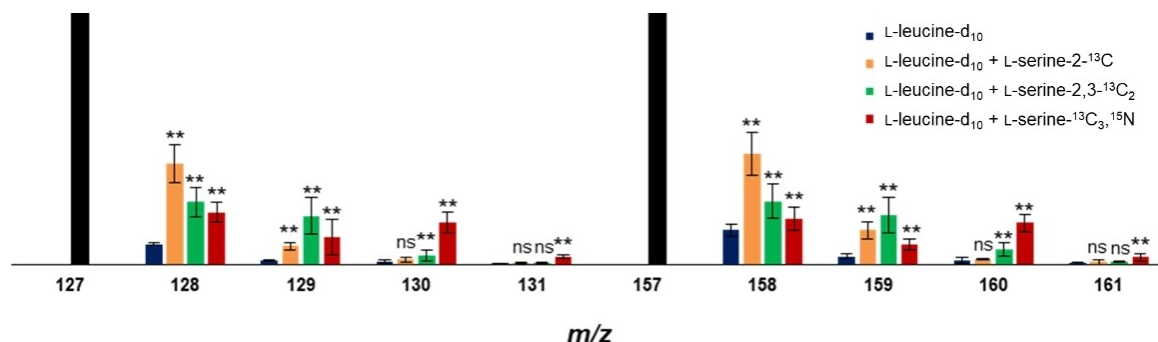
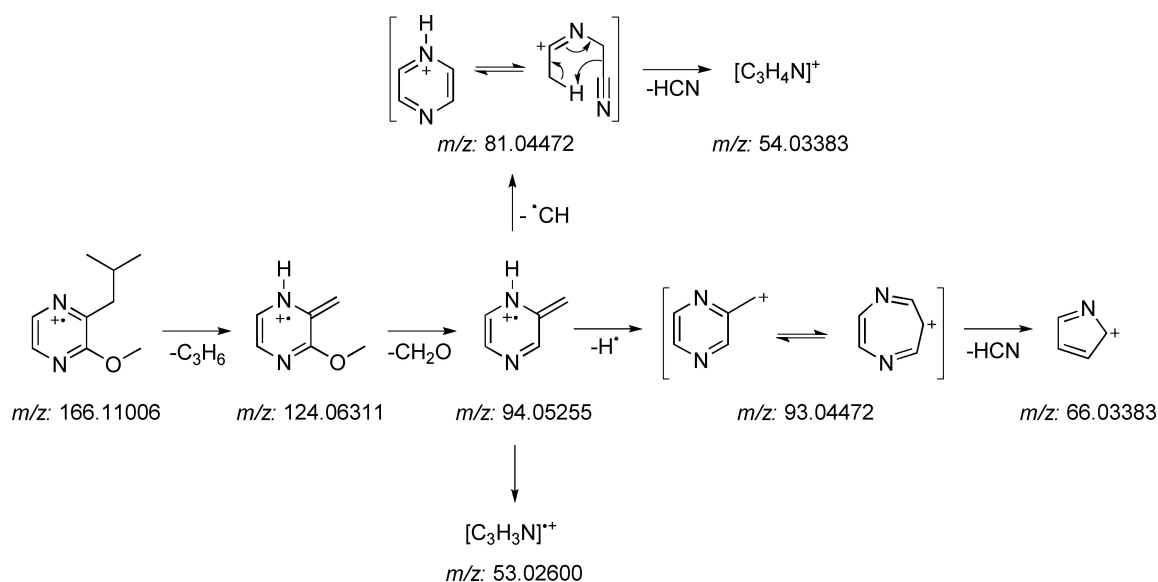


Figure 4. Ratio between the fragment ions of $[\text{H}_9]$ -IBMP (m/z 127, 157) and $^{13}\text{C}/^{15}\text{N}$ -labeled $[\text{H}_9]$ -IBMP (m/z 128, 158) and $^{13}\text{C}_2/^{13}\text{C},^{15}\text{N}$ -labeled $[\text{H}_9]$ -IBMP (m/z 129, 159) after feeding L- $[\text{H}_{10}]$ -leucine, L- $[\text{H}_{10}]$ -leucine + L- $[\text{C}_2\text{-}^{13}\text{C}]$ -serine-2- ^{13}C , L- $[\text{H}_{10}]$ -leucine + L- $[\text{C}_2\text{-}^{13}\text{C}]$ -serine-2,3- $^{13}\text{C}_2$, L- $[\text{H}_{10}]$ -leucine + L- $[\text{C}_3,^{15}\text{N}]$ -serine to unripe bell pepper pericarp (*Capsicum annuum* L. cv. Allrounder). Error bars indicate standard deviation. Statistical significance based on the *t* test (**: $p \leq 0.01$; ns: not significant).



Scheme 9. Proposed fragmentation mechanism of IBMP.

($[\text{C}_2\text{-}^{13}\text{C}]$ -5) and $^{13}\text{CH}_2\text{-H}_4$ Folate, which in turn is metabolized to $[\text{C}_2\text{-}^{13}\text{C}]$ -10 and $[\text{C}_3\text{-}^{13}\text{C}]$ -10, whose incorporation into **1** results in intensity increases of m/z 128 ($127 + 1$) and m/z 158 ($157 + 1$). Thus, intensity increases in m/z 128 and m/z 158 are explainable by an incorporation of $[\text{C}_3\text{-}^{13}\text{C}]$ -10 and $[\text{C}_2\text{-}^{13}\text{C}]$ -10. Increases are relatively large as both ($[\text{C}_3\text{-}^{13}\text{C}]$ -10 and $[\text{C}_2\text{-}^{13}\text{C}]$ -10) lead to intensity increases in the same m/z -ratios.

In conclusion, intensity increases by 2 amu clearly demonstrate that C-2 and C-3 of **10** are incorporated into **1**, indicating that **10** is involved in the pyrazine ring formation of **1**. In fact, these findings confirm that **10** contributes the C_2 -unit of the pyrazine ring. Moreover, feeding experiments revealed that **10** is decarboxylated before or during the biosynthesis of **1**.

Feeding experiments with L- $[\text{C}_3,^{15}\text{N}]$ -serine

To examine whether **10** serves also as N-source to **1**, further incubation experiments were conducted out using $[\text{C}_3,^{15}\text{N}]$ -10 and $[\text{H}_{10}]$ -6. Due to ^{15}N -labeling, a preceding biosynthetic deamination of $[\text{C}_3,^{15}\text{N}]$ -10 should be detectable, as it would result in a shift of the molecular ion from m/z 175 to m/z 177. Moreover, a base peak shift from m/z 127 to m/z 129 due to a *McLafferty* rearrangement and elimination of isotope labeled propene ($^{13}\text{C}_3\text{D}_6$). The fragment ion peak at m/z 97 would result in m/z 99, whereas the fragment ion peak at m/z 157 would result in m/z 159. In contrast, an incorporation of the ^{15}N -label would give rise to m/z 160 and m/z 130.

As displayed in Figure 3 C, intensities in m/z -ratios related to a preceding deamination (m/z 177, 159, 129, 99) as well as

those related to the incorporation of the ^{15}N -label (m/z 178, 160, 130, 100) increase. The abundances of relevant m/z -values in co-fed samples ($[\text{}^2\text{H}_{10}\text{-6} + [\text{}^{13}\text{C}_3, \text{}^{15}\text{N}]\text{-10}]$) were compared to those in control samples ($[\text{}^2\text{H}_{10}\text{-6}]$). Significant increases ($p < 0.01$) can be observed in m/z 130 by a factor of 16.6 (1% to 17%) and 9.8 in m/z 160 (2% to 17%) as well as by 6.9 in m/z 129 (2% to 11%) and 2.4 in m/z 159 (3% to 8%) (Figure 4). Results clearly demonstrate that the ^{15}N -label is mainly incorporated into **1**, as the highest increases were found in m/z 130 and m/z 160 corresponding to an incorporation of three stable isotopes.

Interestingly, significant intensity increases ($p < 0.01$) are detectable in m/z 131 (127+4) (0% to 3%) and m/z 161 (157+4) (0% to 3%). These can be explained by the supposed metabolic link between the biosynthesis of **1** and photorespiration. During the photorespiratory cycle NH_3 is re-assimilated. As shown in Scheme 10, there are two re-assimilations of NH_3 during photorespiration. One occurs in the peroxisome while **10** is deaminated to hydroxypyruvate, here released NH_3 is incorporated into glyoxylic acid (**8**) leading to glycine (**5**). Another re-assimilation of NH_3 initiates in the mitochondrion during the oxidative decarboxylation and deamination of **5** to $\text{CH}_2\text{-H}_4\text{Folate}$. In the chloroplast, released NH_3 is reincorporated into glutamine, which in turn aminates α -ketoglutarate to glutamate. Glutamate is then transported into the peroxisome and aminates **5** to **8**.^[24]

Intensity increases in m/z 131 and m/z 161 might therefore appear due to the incorporation of $[\text{}^{13}\text{C}_3, \text{}^{15}\text{N}]\text{-10}$ and $^{15}\text{NH}_3$ released during NH_3 re-assimilation. These results are consistent

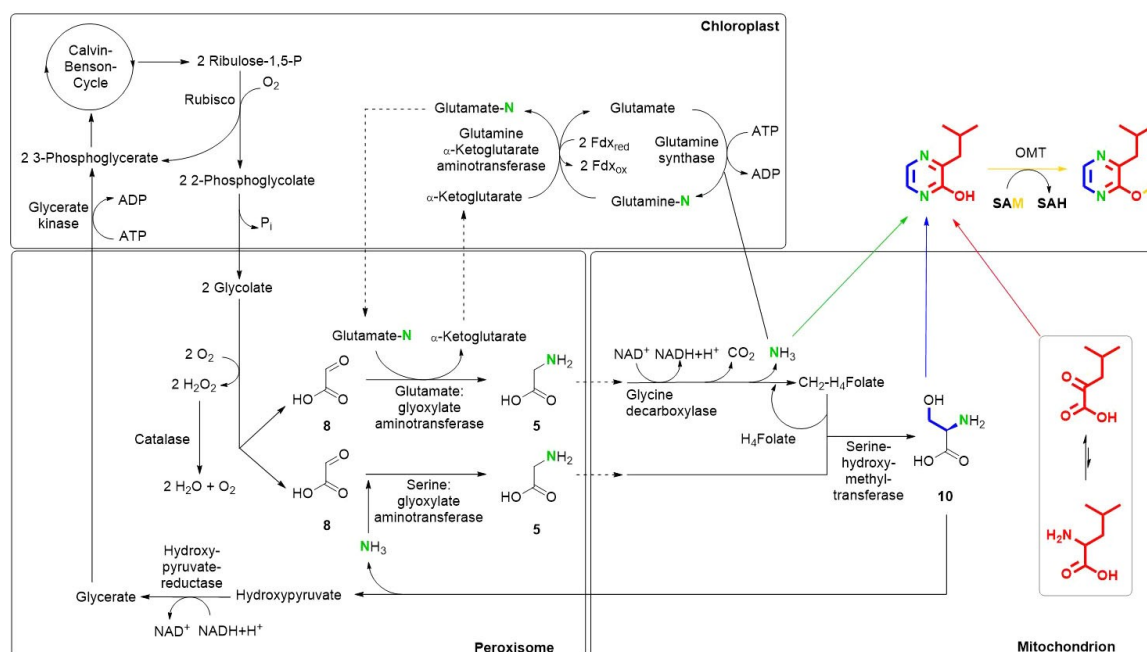
with prior feeding experiments proving the importance of L-glutamine (**9**) in the biosynthesis of **1**.^[23] As displayed in Scheme 10, ^{15}N -labeled **9** aminates α -ketoglutarate to glutamate. Glutamate in turn serves as a N-donor to **5**, which can be metabolized to **10**. Intensity increases in m/z 128 (127+1) (8% to 21%) and m/z 158 (157+1) (14% to 18%) abundances can be explained by both the incorporation of only one re-assimilated ^{15}N -atom into **1** and the interconversion of **10** and **5**.

In summary, the ^{15}N -labeling studies clearly show that **10** is mainly not deaminated during its incorporation into **1** and indirectly support that both N-atoms of **1** are **10**-derived. Moreover, feeding experiments gave evidence for an interface between the biosynthesis of MPs and the photorespiratory cycle via **10** and the assimilation of NH_3 .

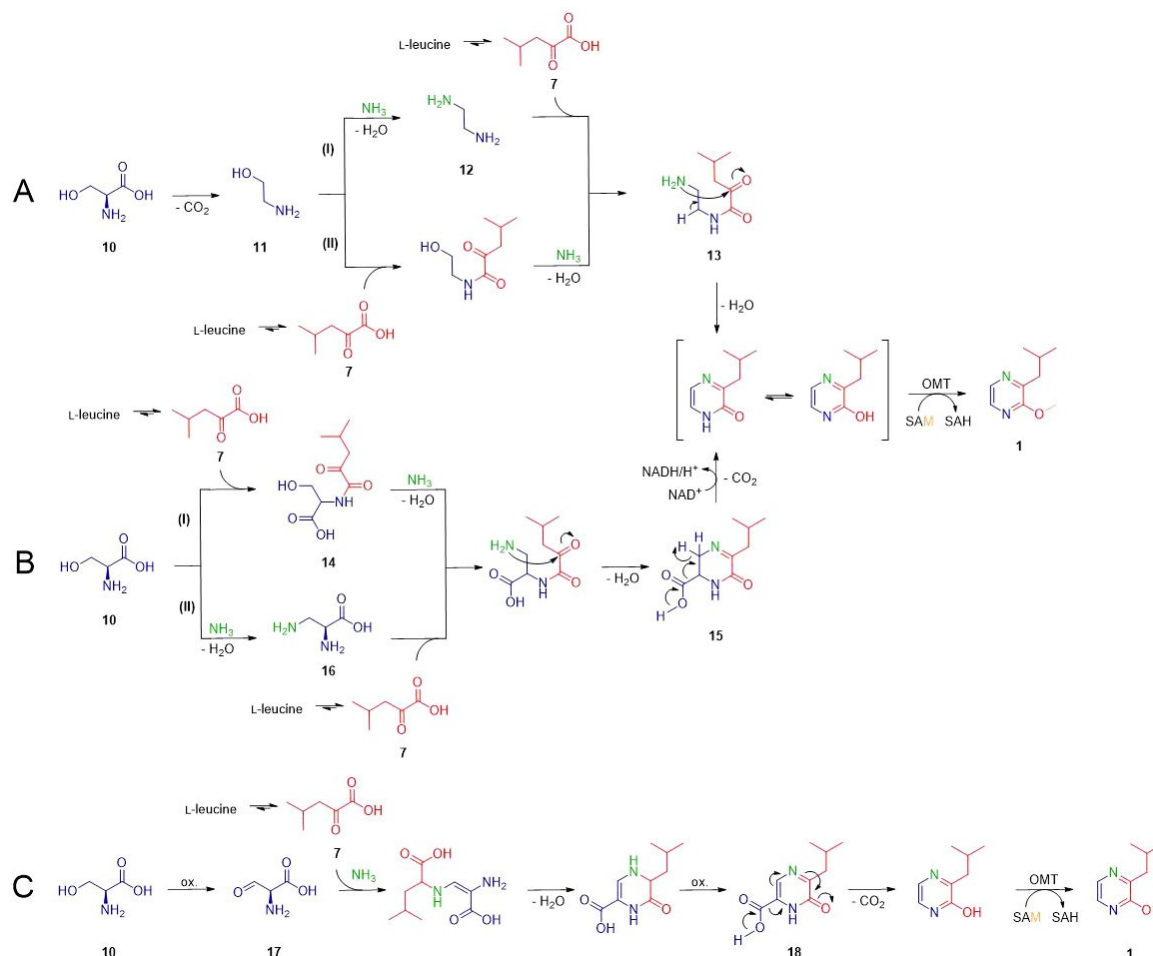
The biosynthetic pathway to **1**

^{13}C - and ^{15}N -labeling studies revealed that the direct precursors to **1** in plants differ from those of the bacterial biosynthesis.^[2,21,32] Prior feeding experiments revealed that during the biosynthesis of **1**, L-leucine (**6**) is mainly deaminated to its keto acid (**7**),^[23] whereas present studies show, that L-serine (**10**) plays a major role as a C_2 -building block and N-donor in the biosynthesis of **1**. Moreover, feeding ^{15}N -labeled **10** lead to a one- and twofold incorporation of the ^{15}N -label.

As outlined in Scheme 11, different biosynthetic pathways can be assumed based on the findings of the feeding experiments. On the one hand, it might be that free **10** is



Scheme 10. Putative interdependency of photorespiration and L-leucine catabolism with IBMP-biosynthesis. The localization of IBMP-storage and -biosynthesis within the cells is still unknown. Dashed lines represent intracellular transport. H_4Folate , tetrahydrofolate; OMT, O-methyltransferase; SAM, S-adenosylmethionine; SAH, S-adenosylhomocysteine.



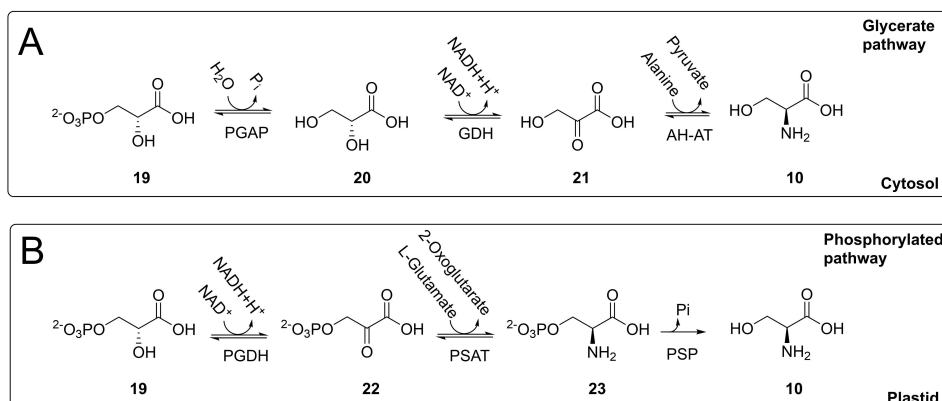
Scheme 11. Proposed mechanisms of IBMP formation in bell pepper plants starting with (A) a decarboxylation of L-serine, (B I) a condensation of L-serine and α -KIC, (B II) an amination of L-serine or (C) an oxidation of L-serine. α -KIC, α -ketoisocaproic acid; OMT, O-methyltransferase; SAM, S-adenosylmethionine; SAH, S-adenosylhomocysteine.

decarboxylated prior to its incorporation into **1** (Scheme 11A). In plants, a decarboxylation of **10** is known to be catalyzed by a type II pyridoxal 5'-phosphate (PLP)-dependent decarboxylase called serine decarboxylase (SDC).^[33] Decarboxylation of free **10** occurs in the cytosol and results in ethanolamine (**11**), a known intermediate for phosphatidylethanolamine and -choline as well as several volatiles.^[34] Ethanolamine is either first aminated to ethylenediamine (**12**), which forms an α -ketoamide with α -ketoisocaproic acid (**7**) before it is again aminated to compound **13** (I) or *vice versa* (II). An intramolecular cyclization affords the pyrazine ring in both cases. On the other hand, it is possible that first **14** is formed as a condensation product of **10** and **7** (Scheme 11B). After a transamination reaction and cyclization to **15** a decarboxylation may follow, similar to the oxidative decarboxylation of arogenate into tyrosine.^[35] As displayed in Scheme 11BII a prior conversion of **10** into 2,3-diaminopropionic acid (DAP, **16**) seems to be possible as well. DAP is a non-proteinogenic amino acid known as a short-lived inter-

mediate for the neurotoxin β -N-oxalyl- α,β -diamino propionic acid (ODAP).^[36] A condensation of **7** and **16** followed by a ring closure and a decarboxylation of **15** would also result in **1**. As displayed in Scheme 11C another possible pathway to **1** initiates with the oxidation of **10** to α -formyl-glycine (**17**), according to the chemical synthesis of cyclic endiamino peptides by Pappo et al.^[37] A condensation of **17** and **7** followed by an oxidation would result in the corresponding 2-(1H)-pyrazinone (**18**). Subsequent decarboxylation and O-methylation lead to **1**.

Metabolic link between photorespiration and the biosynthesis of **1**

In addition, feeding experiments indicated that photorespiration and the biosynthesis of **1** are biosynthetically linked. So far, it is unknown whether **1** is biosynthesized from photorespir-



Scheme 12. Non-photorespiratory pathways of serine biosynthesis. PGDH, 3-phosphoglycerate dehydrogenase; PSAT, phosphoserine aminotransferase; PSP, 3-phosphoserine phosphatase; PGAP, 3-phosphoglycerate phosphatase; GDH, glycerate dehydrogenase; AH-AT, alanine-hydroxypyruvate aminotransferase.

atory **10** exclusively. However, prior studies showing that no de novo biosynthesis of **1** can be observed in ripe bell pepper fruits^[23] and that the photorespiratory enzymes are inactivated due to the degradation of the chloroplast during ripening^[38] indicate that the biosynthesis of **1** and photorespiration are biosynthetically connected.

Photorespiration is the major biosynthetic pathway for **10** in photosynthetic cells. The photorespiratory cycle is a competitive reaction to photosynthesis. It starts with ribulose-1,5-bisphosphate carboxylase/oxygenase (Rubisco), a key enzyme in photosynthesis. Rubisco has also an oxygenase activity as it fixes oxygen from the atmosphere. The oxygenic side-product of Rubisco, 2-phosphoglycolate (2-PG) is a toxic intermediate that inhibits several chloroplastic enzymes in plants. 2-PG is detoxified during the photorespiratory pathway, as it is metabolized back to the photosynthetic intermediate 3-phosphoglyceric acid (3-PGA).^[24,26–28]

It is noteworthy that in plants two non-photorespiratory pathways of serine biosynthesis, called the glycerate and the phosphorylated pathway, coexist. The glycerate pathway (Scheme 12A) starts in the cytosol with a dephosphorylation of 3-phosphoglycerate (**19**), which is produced during the cytosolic glycolysis. Resulting glycerate (**20**) is then oxidized to hydroxypyruvate (**21**), which in turn leads to the formation of **10** catalyzed by an aminotransferase. In contrast, the phosphorylated pathway proceeds in plastids. First, **19** formed during the Calvin cycle is oxidized by a phosphoglycerate dehydrogenase (PGDH) enzyme yielding 3-phosphohydroxypyruvate (**22**), which is then, catalyzed by an aminotransferase, converted to 3-phosphoserine (**23**), which in turn is dephosphorylated to **10** (Scheme 12B).^[39] However, prior investigations clearly demonstrated that glycine (**5**) and glyoxylic acid (**8**) are incorporated into 3-isobutyl-2-methoxypyrazine (IBMP, **1**) giving evidence that the photorespiratory pathway is the dominant source of serine in the biosynthesis of methoxypyrazines.^[23]

Conclusion

In conclusion, feeding experiments with ¹³C- and ¹⁵N-labeled precursors confirm that IBMP (**1**) is biosynthesized from the amino acids L-serine (**10**) and L-leucine (**6**).

Based on the feeding experiments possible biosynthetic pathways to **1** were outlined. Results clearly demonstrated that **10** serves as a C₂-unit building block. Moreover, it is established that **10** is degraded by a decarboxylation during its incorporation into **1**. However, it is unsolved if this happens before or after ring closure. Further insight into the biosynthesis of **1** was possible by feeding experiments with ¹⁵N-labeled **10**, as findings confirmed that both nitrogen atoms originate from **10**. According to the observed labeling pattern of **1**, it has been assumed that ¹⁵N-labeled **10** is partially degraded and released ¹⁵NH₃ is incorporated into **1**. These findings strengthened the hypothesis of a metabolic link between the photorespiratory cycle and the biosynthesis of **1**. To elucidate the mechanism of the pyrazine ring formation in detail, further intermediates (see Scheme 11) and enzymes involved in the biosynthetic pathway of **1** need to be identified.

Acknowledgements

We thank the Institute of Crop Science and Resource Conservation (INRES) of the University of Bonn, Germany for providing bell pepper samples. We thank M. Engeser (Kekulé Institute of Organic Chemistry and Biochemistry, University of Bonn) for HR-MS measurements. Open Access funding enabled and organized by Projekt DEAL.

Conflict of Interest

The authors declare no conflict of interest.

Data Availability Statement

The data that support the findings of this study are available from the corresponding author upon reasonable request.

Keywords: 3-Alkyl-2-methoxypyrazines · headspace solid phase microextraction · isotopic labeling · gas chromatography · time-of-flight mass spectrometry

- [1] B. P. Moore, W. V. Brown, M. Rothschild, *Chemoecology* **1990**, *1*, 43.
- [2] J. S. Dickschat, S. Wickel, C. J. Bolten, T. Nawrath, S. Schulz, C. Wittmann, *Eur. J. Org. Chem.* **2010**, 2687.
- [3] K. E. Murray, F. B. Whitfield, *J. Sci. Food Agric.* **1975**, *26*, 973.
- [4] K. T. Ong, Z.-Q. Liu, M. G. Tay, *BJRST* **2017**, *7*, 60.
- [5] P. B. Miniyar, P. R. Murumkar, P. S. Patil, M. A. Barmade, K. G. Bothara, *Mini-Rev. Med. Chem.* **2013**, *13*, 1607.
- [6] F. B. Mortzfeld, C. Hashem, K. Vranková, M. Winkler, F. Rudroff, *Biotechnol. J.* **2020**, 15.
- [7] R. G. Jones, *J. Am. Chem. Soc.* **1949**, *71*, 78.
- [8] P. Legrand, Y. L. Janin, *Beilstein J. Org. Chem.* **2022**, *18*, 935.
- [9] H. Gutknecht, *Ber. Dtsch. Chem. Ges.* **1879**, *12*, 2290.
- [10] H. Masuda, S. Mihara, *J. Agric. Food Chem.* **1988**, *36*, 584.
- [11] a) I. Besson, C. Creuly, J. B. Gros, C. Larroche, *Appl. Microbiol. Biotechnol.* **1997**, *47*, 489; b) S. M. Fors, B. K. Olofsson, *Chem. Senses* **1986**, *11*, 65.
- [12] R. M. Seifert, R. G. Buttery, D. G. Guadagni, D. R. Black, J. G. Harris, *J. Agric. Food Chem.* **1970**, *18*, 246.
- [13] D. A. Gerritsma, I. D. Brindle, T. R. Jones, A. Capretta, *J. Labelled Cpd. Radiopharm.* **2003**, *46*, 243.
- [14] H.-G. Schmarr, W. Sang, S. Ganß, S. Koschinski, R. Meusinger, *J. Labelled Cpd. Radiopharm.* **2011**, *54*, 438.
- [15] D. Mutarutwa, L. Navarini, V. Lonzarich, D. Compagnone, P. Pittia, *J. Mass Spectrom.* **2018**, *53*, 871.
- [16] C. Legrum, P. Slabizki, H.-G. Schmarr, *Anal. Bioanal. Chem.* **2015**, *407*, 253.
- [17] A. Botezatu, G. J. Pickering, Y. Kotseridis, *Food Chem.* **2014**, *160*, 141.
- [18] D. Roujou de Boubée, C. van Leeuwen, D. Dubourdieu, *J. Agric. Food Chem.* **2000**, *48*, 4830.
- [19] a) R. M. Seifert, R. G. Buttery, D. G. Guadagni, D. R. Black, J. G. Harris, *J. Agric. Food Chem.* **1972**, *20*, 135; b) R. G. Buttery, R. M. Seifert, D. G. Guadagni, L. C. Ling, *J. Agric. Food Chem.* **1969**, *17*, 1322.
- [20] a) K. E. Murray, J. Sipton, F. B. Whitfield, *Chemistry & Industry* **1970**, 27, 897; b) H. E. Nursten, M. R. Sheen, *J. Sci. Food Agric.* **1974**, *25*, 643.
- [21] T. B. Cheng, G. A. Reineccius, J. A. Bjorklund, E. Leete, *J. Agric. Food Chem.* **1991**, *39*, 1009.
- [22] a) K. Hashizume, K. Tozawa, M. Endo, I. Aramaki, *Biosci. Biotechnol. Biochem.* **2001**, *65*, 795; b) J. D. Dunlevy, K. L. Soole, M. V. Perkins, E. G. Dennis, R. A. Keyzers, C. M. Kalua, P. K. Boss, *Plant Mol. Biol.* **2010**, *74*, 77.
- [23] F. Zamolo, M. Wüst, *J. Agric. Food Chem.* **2022**, *70*, 6719.
- [24] B. B. Buchanan, W. Gruissem, R. L. Jones, in *Biochemistry & molecular biology of plants*, American Society of Plant Biologists; Wiley Blackwell, Chichester, **2015**.
- [25] R. Douce, J. Bourguignon, M. Neuburger, F. Rébeillé, *Trends Plant Sci.* **2001**, *6*, 167.
- [26] R. M. Benstein, K. Ludewig, S. Wulfert, S. Wittek, T. Gigolashvili, H. Frerigmann, M. Gierth, U.-I. Flügge, S. Krueger, *The Plant Cell* **2013**, *25*, 5011.
- [27] C. Peterhansel, I. Horst, M. Niessen, C. Blume, R. Kebeish, S. Kürkcüoğlu, F. Kreuzaler, *TAB* **2010**, *8*, e0130.
- [28] S. Timm, A. Nunes-Nesi, A. Florian, M. Eisenhut, K. Morgenthal, M. Wirtz, R. Hell, W. Weckwerth, M. Hagemann, A. R. Fernie, *Metabolites* **2021**, *11*, 391.
- [29] M. Matucha, W. Jockisch, P. Verner, G. Anders, *J. Chromatogr. A* **1991**, *588*, 251.
- [30] J. H. Gross, *Mass spectrometry. A textbook*, Springer International Publishing, Cham, **2017**.
- [31] J. M. Mouillon, S. Aubert, J. Bourguignon, E. Gout, R. Douce, F. Rébeillé, *Plant J.* **1999**, *20*, 197.
- [32] T. Nawrath, J. S. Dickschat, B. Kunze, S. Schulz, *Chem. Biodiversity* **2010**, *7*, 2129.
- [33] a) D. Rontein, I. Nishida, G. Tashiro, K. Yoshioka, W. I. Wu, D. R. Voelker, G. Basset, A. D. Hanson, *J. Biol. Chem.* **2001**, *276*, 35523; b) S. H. Mudd, A. H. Datko, *Plant Physiol.* **1989**, *91*, 587.
- [34] a) E. Miedema, K. E. Richardson, *Plant Physiol.* **1966**, *41*, 1026; b) Y.-C. Liu, F. Gunawan, I. S. Yunus, Y. Nakamura, *Front. Plant Sci.* **2018**, *9*.
- [35] E. Jung, L. O. Zamir, R. A. Jensen, *Proc. Natl. Acad. Sci. USA* **1986**, *83*, 7231.
- [36] Y.-H. Kuo, F. Lambein, *Phytochemistry* **1991**, *30*, 3241.
- [37] D. Pappo, M. Vartanian, S. Lang, Y. Kashman, *J. Am. Chem. Soc.* **2005**, *127*, 7682.
- [38] R. M. Mateos, A. M. León, L. M. Sandalio, M. Gómez, L. A. Del Río, J. M. Palma, *J. Plant Physiol.* **2003**, *160*, 1507.
- [39] a) R. Ros, J. Muñoz-Bertomeu, S. Krueger, *Trends Plant Sci.* **2014**, *19*, 564; b) A. U. Igamberdiev, L. A. Kleczkowski, *Front. Plant Sci.* **2018**, *9*.

Manuscript received: November 25, 2022
Accepted manuscript online: December 22, 2022
Version of record online: February 15, 2023

Chemistry–A European Journal

Supporting Information

**L-Serine is the Direct Precursor for the Pyrazine Ring
Construction in the Biosynthesis of 3-Isobutyl-2-
Methoxypyrazine in Bell Pepper Fruits (*Capsicum
annuum* L.)**

Francesca Zamolo and Matthias Wüst*

Table of Contents

1. Experimental Procedures

1.1. Plant material

1.2. Chemicals

1.3. Sample preparation

1.4. GCxGC-TOF-MS analysis

2. Results and Discussion

- 2.1. Table S1** Nominal masses, exact masses, and chemical formula of characteristic fragment ions of 3-isobutyl-2-methoxypyrazine (IBMP) (reference compound) detected by high-resolution EI mass spectra (HR-EI-MS).

1. Experimental Procedures

1.1. Plant material:

The experiments were performed with bell pepper (*Capsicum annuum* L. cv 'Allrounder') (Rijk Zwaan, De Lier, Netherlands) obtained from the Institute of Crop Science and Resource Conservation (INRES), Chair of Horticultural Sciences of the University of Bonn, Germany. Fruits were harvested and incubated the same day.

1.2. Chemicals:

3-Isobutyl-2-methoxypyrazine (IBMP) (97%), L-[2,3-¹³C₂]-serine (99 atom% ¹³C, 97.8%) and L-[2-¹³C]-serine (95.6 atom% ¹³C, 99.50%) were purchased from *Sigma Aldrich* (St Louis, Missouri). L-[¹³C₃, ¹⁵N]-serine (99 atom% ¹³C, 98%) was obtained from *Biotrend* (Cologne, Germany). L-[²H₁₀]-leucine (99%) was purchased from *C/D/N isotopes* (Pointe-Claire, Quebec, Canada). 3-Isobutyl-[²H₉]-2-methoxypyrazine ([²H₉]-IBMP) (≥95%) was obtained from *AromaLab* (Martinsried, Germany). Sodium chloride was purchased from *Merck GmbH* (Darmstadt, Germany). Methanol (>99.99%) was obtained from *Honeywell* (Muskegon, Michigan). Water (HPLC, LC-MS grade) was obtained from *VWR International* (Fontenay-sous-Bois, Ile-de-France, France).

1.3. Sample preparation:

For feeding experiments pericarp tissue of freshly harvested, unripe bell pepper fruits (*Capsicum annuum* L. cv. 'Allrounder') was cut into pieces (~2 cm²). Samples were soaked in a sodium-hypochlorite-solution (NaOCl), to avoid microbial contamination and rinsed with water before they were separately placed on a sterile petri dish. Then 100 µL of an aqueous solution containing L-[²H₁₀]-leucine (0.1%) and 100 µL of the respective stable-isotope labeled L-serine (0.1%) were added. After an incubation time of 48 hours at room temperature, the samples were frozen using liquid nitrogen and crushed with a mortar. The homogenized sample (1 g) was weighed into a 10 mL headspace-vial and 2 mL of an 20% (w/v) aqueous NaCl-solution were added. Control samples were incubated with 100 µL L-[²H₁₀]-leucine (0.1%). Each experiment was repeated at least three times. HS-SPME sampling was performed using a divinylbenzene/polydimethylsiloxane-coated (DVB/CAR/PDMS, 50/30 µm, 2 cm) solid phase microextraction (SPME) fiber (*Supelco*, Bellefonte, Pennsylvania). Samples were incubated at 50°C for 10 min with agitation (500 rpm; 30 s on time; 10 s off time) followed by sample extraction at 50°C for 30 min. After incubation and extraction, the analytes were desorbed into the injector at 250°C for 10 min.

1.4. GCxGC-TOF-MS analysis:

Chromatographic separations were performed by using an Agilent 7890B gas chromatograph (*Agilent Technologies*, Palo Alto, California) equipped with a OPTIMA 5 MS (30 m, 0.25 mm i.d. x 0.1 µm df) primary column, a MEGA WAX FAST (2 m, 0.1 mm i.d. x 0.1 µm df) secondary column and a liquid nitrogen cryogenic modulator (Consumable-Free ZX2 thermal modulator). Helium was used as the carrier gas at a constant flow of 1 mL/min. The modulation period (PM) was set to 4 s with hot jet duration of 350 ms and with a shift of + 20°C regarding to the temperature program of the GC oven. The separation was performed using the following temperature program: 35°C (5 min), 3°C/min to 160°C, 20°C/min to 220°C (5 min). Detection was performed on a time-of-flight mass spectrometer (ToF-MS) (*Markes International Ltd*, Llantrisant, RCT, UK). Analytes were ionized by operating in electron impact ionization mode (EI) at - 70 eV. The transfer line and ion source temperatures were set to 250°C. Data analysis was performed using the software ChromSpace (*Markes International Ltd*, Llantrisant, RCT, UK). The software was used to remove unwanted background noise and for spectrum deconvolution. Analytes were identified by comparing the retention times and mass spectra with standard substances and using the NIST Mass Spectral Library (*National Institute of Standards and Technology*, Gaithersburg, Maryland). **1** and [²H₉]-**1** were identified by comparing GC retention times and mass spectra to standard substances.

2. Tables

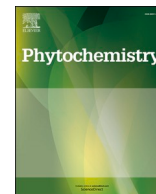
Table S1. Nominal masses, exact masses, and chemical formula of characteristic fragment ions of 3-isobutyl-2-methoxypyrazine (IBMP) (reference compound) detected by high-resolution EI mass spectra (HR-EI-MS).

Nominal mass [m/z]	Calculated mass [m/z]	Measured mass [m/z]	Chemical formula
166	166.11006	166.1090	C ₉ H ₁₄ N ₂ O ⁺
124	124.06311	124.0627	C ₆ H ₈ N ₂ O ⁺
94	94.05255	94.0519	C ₅ H ₆ N ₂ ⁺
81	81.04472	81.0440	C ₄ H ₅ N ₂ ⁺
66	66.03383	66.0347	C ₄ H ₄ N ⁺
54	54.03383	54.0339	C ₃ H ₄ N ⁺
53	53.02600	53.0272	C ₃ H ₃ N ⁺



Contents lists available at ScienceDirect

Phytochemistry

journal homepage: www.elsevier.com/locate/phytochem

Sites of biosynthesis, distribution and phloem transport of 3-isobutyl-2-Methoxypyrazine in *Capsicum annuum* (bell pepper) plants

Francesca Zamolo, Jan Phillip Heinrichs, Matthias Wüst*

University of Bonn, Institute of Nutritional and Food Sciences, Chair of Food Chemistry, Friedrich Hirzebruch Allee 7, D-53115, Bonn, Germany

ARTICLE INFO

Keywords:

Capsicum annuum
Solanaceae
3-Alkyl-2-methoxypyrazines
Biosynthesis
Tissue distribution
Deuterium labelling studies
Headspace solid-phase microextraction
Gas chromatography
Time-of-flight mass spectrometry

ABSTRACT

The distribution and translocation as well as the biosynthetic sites of 3-isobutyl-2-methoxypyrazine (IBMP) in bell pepper plants (*Capsicum annuum*) were examined. For IBMP-quantification, a stable-isotope dilution assay (SIDA) was developed, using headspace solid-phase microextraction (HS-SPME) combined with gas chromatography and time-of-flight mass spectrometry (ToF-MS). While IBMP was the most abundant MP in all aerial plant parts, IPMP was dominating in root tissues. The highest IBMP-levels were found in unripe bell pepper fruits. Moreover, feeding experiments with [²H₁₀]-l-leucine revealed that IBMP is biosynthesized in all plant parts, while in roots and ripe bell pepper fruit tissues no incorporation of the labelled precursor was detectable. A potential phloem translocation of IBMP could not be detected.

1. Introduction

3-Alkyl-2-methoxypyrazines (MPs) are aroma-active compounds occurring in many raw vegetables (Legrum et al., 2015; Murray and Whitfield, 1975; Mutarutwa et al., 2018). The most common MPs are 3-isobutyl-2-methoxypyrazine (IBMP), 3-sec-butyl-2-methoxypyrazine (sBMP) and 3-isopropyl-2-methoxypyrazine (IPMP). IBMP was identified in 1969 in green bell pepper (*Capsicum annuum* var. grossum, Sendt) (Buttery et al., 1969) followed by the identification of sBMP in galbanum oil (*Ferula galbaniflua*) (Bramwell et al., 1969) and IPMP in green peas (*Pisum sativum*) (Murray et al., 1970).

Furthermore, MPs are found in grapes (*Vitis vinifera*) and therefore contribute to the aroma of several wine varieties. While their aroma is desirable at low levels, higher levels are undesired and associated with immaturity (Roujou de Boubée et al., 2000). To lower MP-levels in wines, it is recommended to reduce the use of material other than grapes (MOG) such as leaves, petioles and rachises (Pickering et al., 2021). That is because MPs are distributed within the whole grapevine. While IPMP is accumulated in the roots, IBMP is the most abundant MP in all aerial parts of grapevines (Dunlevy et al., 2010; Roujou de Boubée, 2003). Moreover, it is well established that IBMP is detectable in all grape tissues. The highest IBMP-levels were detected in the grapes, especially in the exocarp, decreasing after fruit ripening (Dunlevy et al., 2010; Hashizume and Samuta, 1997; Lei et al., 2019; Roujou de Boubée,

2003). However, the distribution of IBMP in the leaves is ambiguous. While neither IBMP nor IPMP were detected in the leaves of Cabernet Sauvignon grapevines (Dunlevy et al., 2010), other studies showed that IBMP is detectable in the leaves of Cabernet Sauvignon and Chardonnay vines (Hashizume and Samuta, 1997; Roujou de Boubée, 2003).

Although the distribution of MPs in grapevine has been widely studied, their biosynthesis in different organs and tissues and their translocation are still unknown. On the one hand, stable-isotope feeding experiments showed a translocation of IBMP from the leaves to other plant parts (Roujou de Boubée, 2003). On the other hand, grafting studies indicated that IBMP is only biosynthesized in the fruit, as no transport through the shoot into the fruit has been detected (Koch et al., 2010). A translocation via the phloem has been hypothesized, but not yet been demonstrated.

Moreover, the biosynthetic pathway of MPs has not yet been fully revealed. In 1970 Murray et al. suggested that MPs are biosynthesized by a condensation of an α -amino amide of leucine, isoleucine or valine with glyoxal. As both α -amino amides and free glyoxal have never been detected in plants, either glyoxylic acid or a nitrogen-derivative of glyoxylate have been considered instead (Murray and Whitfield, 1975; Nursten and Sheen, 1974). However, feeding experiments with stable-isotope labelled precursors and bell pepper fruits demonstrated an incorporation of l-leucine and α -ketoisocaproate (α -KIC) into IBMP and that glycine and glyoxylic acid serve as “C₁ building blocks”

* Corresponding author.

E-mail address: matthias.wuest@uni-bonn.de (M. Wüst).

<https://doi.org/10.1016/j.phytochem.2022.113488>

Received 8 August 2022; Received in revised form 6 October 2022; Accepted 21 October 2022

Available online 30 October 2022

0031-9422/© 2022 Elsevier Ltd. All rights reserved.

(Zamolo and Wüst, 2022). In addition *Vitis vinifera* O-methyltransferases (VvOMTs), catalyzing the O-methylation of 3-alkyl-2-hydroxypyrazines (HPs) to MPs, had been identified (Dunlevy et al., 2010, 2013a; Guillaume et al., 2013).

In bell pepper fruits higher IBMP-levels are detectable than in grapes

(Ryona et al., 2010). However, little is known about the distribution of MP in bell pepper plants. To examine the presence of IBMP within the bell pepper plant, a method was developed including a stable-isotope dilution assay (SIDA), headspace solid phase microextraction (HS-SPME) and gas chromatography coupled to time-of-flight mass

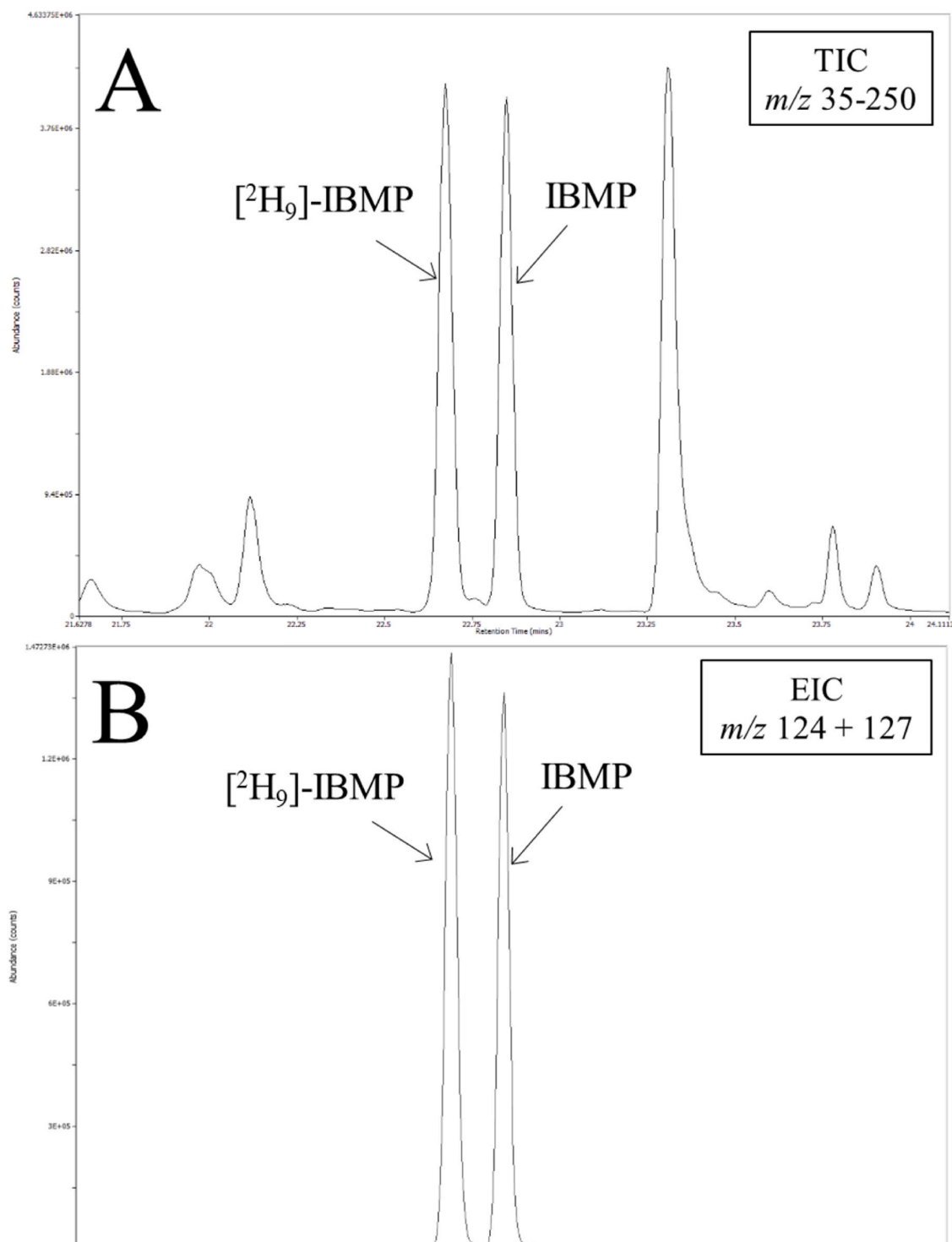


Fig. 1. Total ion chromatogram (TIC) (A) and extracted ion chromatogram (EIC) (B) of ripe bell pepper pericarp (*Capsicum annuum* cv. Allrounder) analyzed by HS-SPME-GC-ToF-MS.

spectrometry (GC-ToF-MS). Moreover, IBMP-translocation as well as its biosynthetically sites were examined by feeding experiments with stable-isotope labelled L-leucine and EDTA-facilitated phloem exudate collection.

2. Results and discussion

2.1. Distribution

For IBMP-quantification, a method including HS-SPME-GC-ToF-MS combined with a SIDA was developed. $[^2\text{H}_9]$ -IBMP was used as an internal standard, to overcome variations in analyte recovery, due to matrix effects and sample preparation. As shown in Fig. 1, $[^2\text{H}_9]$ -IBMP elutes earlier than IBMP, due to the inverse isotope effect, resulting in a complete separation of the two isotopologues. IBMP and $[^2\text{H}_9]$ -IBMP in feedings experiments with deuterium-labelled L-leucine were identified by comparing the retention times and mass spectra with standard substances. Mass spectra of the standards of IBMP and $[^2\text{H}_9]$ -IBMP are displayed in Fig. 2.

Prior to sample analysis the analytical performance of the method was validated by following parameters: linearity, accuracy, precision, limit of detection (LOD) and limit of quantification (LOQ). The method showed a good linearity ($r^2 = 0.997$) for the examined concentration range (0.1–150 ng/g). Satisfactory recoveries of spiked IBMP (10–96 ng/g) averaged between 97% and 102%. The intra-day and inter-day precision, expressed as relative standard deviation (RSD), were 2.57% and 3.98%, respectively. The LOD and LOQ were 0.16 ng/g and 0.28 ng/g, respectively. Showing a good sensitivity, accuracy, precision, and linearity, the developed method was applied to the quantification of IBMP in bell pepper plant (*Capsicum annuum* cv. Allrounder).

For quantification, calibration curves were determined using tomato pericarp as an IBMP-free matrix-matched sample. The matrix-matched samples were spiked with varying amounts of IBMP and a constant amount of $[^2\text{H}_9]$ -IBMP. Chromatograms were acquired in full-scan mode and then analyzed by extracting the most abundant mass traces (m/z 124, 127). Linear regression was performed plotting the

concentration ratios (IBMP/ $[^2\text{H}_9]$ -IBMP) versus the area ratios (IBMP/ $[^2\text{H}_9]$ -IBMP). Obtained calibration curves were also used for semi-quantifying IPMP.

MPs could be detected in all organs and tissues of bell pepper plants. Within the shoot system, including fruits, flowers, stem, and leaves, IBMP is the most abundant MP. In contrast, IPMP turns out to be the dominating MP in roots. As shown in Table 1, the vegetative parts such as roots (7.27 ± 1.18 ng/g FW), leaves (21.29 ± 1.23 ng/g FW) and stems (4.28 ± 0.56 ng/g FW) contain low IBMP-levels, while the reproductive parts implying flowers (31.92 ± 3.16 ng/g FW), ripe bell pepper fruits (45.97 ± 2.24 ng/g FW) and unripe bell pepper fruits (92.70 ± 4.00 ng/g FW) possess higher IBMP-contents.

In conclusion, fruits contain the highest IBMP-content in all stages of ripeness, whereas roots contain the highest IPMP-levels (79.33 ± 18.18 ng/g FW). The reasons for higher IBMP-accumulation in the reproductive plant parts are so far unclear. On the one hand, it has been hypothesized that IBMP serves as a natural plant defence (Dunlevy et al., 2010). However, microbiological tests demonstrated that IBMP shows no antimicrobial activity on yeast and bacteria at the concentration

Table 1

IBMP-contents in different organs and tissues of bell pepper plants (*Capsicum annuum* cv. Allrounder). Data are means \pm standard deviations ($n = 5$ –11) expressed as ng/g FW (fresh weight).

	Fruit (ripe)	Fruit (unripe)	Stem	Root	Leaf	Flower
Whole	45.97 \pm 2.24	92.70 \pm 4.00	4.28 \pm 0.56	7.27 \pm 1.18	21.29 \pm 1.23	31.92 \pm 3.16
Pedicel	19.07 \pm 1.92	21.00 \pm 3.72				
Pericarp	65.70 \pm 3.44	78.51 \pm 6.65				
Placenta	18.87 \pm 2.29	20.61 \pm 1.14				
Seed	7.23 \pm 0.14	36.80 \pm 3.16				

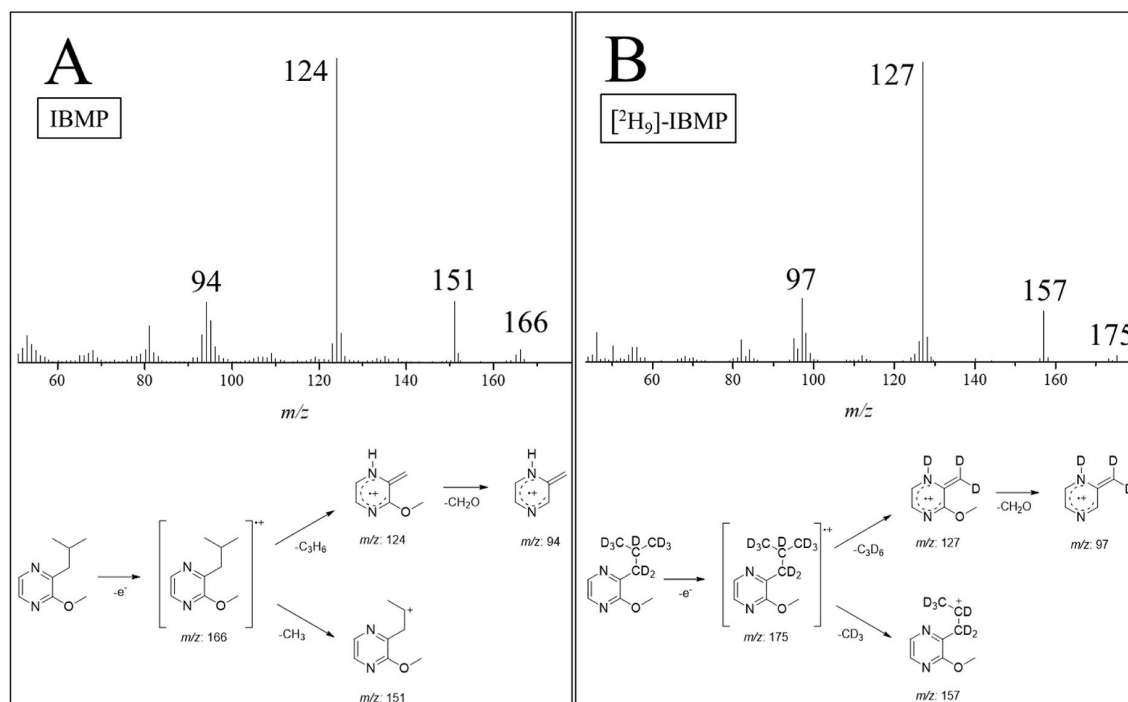


Fig. 2. EI-MS spectra and fragmentation pattern of IBMP (A) and EI-MS spectra and fragmentation pattern of $[^2\text{H}_9]$ -IBMP (B).

range of 0.01–1 ppm (Kögel et al., 2012). On the other hand, IBMP might act as a mediator in plant communication. As known, plants can release volatile organic compounds, which allows them to interact with other organisms (Negre-Zakharov et al., 2009). Previous studies have shown, that MPs function as a semiochemical in several aposematic insect species (Moore et al., 1990; Rothschild et al., 1984; Schmidtberg et al., 2019) as well as for nematodes (Kihika et al., 2017).

Subsequently, different fruit tissues of unripe and ripe fruits were analyzed concerning the distribution of IBMP within the fruit. For this purpose, the fruits were divided into pericarp, placenta, seeds, and pedicel. As shown in Fig. 3A and B, all analyzed fruit tissues contain IBMP. A decrease in IBMP-content is detectable in pericarp tissues after ripening (see Fig. 3C for the definition of the ripening stages). In both ripe and unripe fruits highest IBMP-values are found in the pericarp. While unripe bell pepper pericarp contains 78.51 ± 6.65 ng/g (FW) IBMP, significantly less (two-sample Student's *t*-test, $p < 0.05$) is detectable in pericarp tissues of ripe bell pepper fruits (65.70 ± 3.44 ng/g FW). Decreases in IBMP-levels after ripening are not significant in both placenta (20.61 ± 1.14 ng/g to 18.87 ± 2.29 ng/g FW) and pedicel (21.00 ± 3.72 ng/g to 19.07 ± 1.92 ng/g FW). Noticeable are the

significant IBMP-decreases in the seeds (36.80 ± 3.16 ng/g to 7.23 ± 0.14 ng/g FW). These differences may occur due to biological variation within the bell pepper fruits, as well as a change in the relative contribution of tissues during maturation. Studies showed that the proportions of fruit tissues change during ripening. For example, it has been shown that the placental tissue and the seeds increase in weight (Thanopoulos et al., 2013) and that the pericarp increases in thickness (Tadesse et al., 2002). Based on our data, we cannot evaluate whether dilution due to fruit ripening and changes in tissue proportions is responsible for the decreasing IBMP-levels.

In grapes, the highest IBMP contents could be detected in the flesh and skin, whereas less was found in the seeds (Dunlevy et al., 2013b). IBMP-levels decreased after ripening in all grape tissues (Dunlevy et al., 2010, 2013b; Roujou de Boubée et al., 2002). To examine whether a dilution due to berry enlargement is responsible for this, the IBMP content was determined on a per berry basis (Gregan and Jordan, 2016). However less IBMP has been detected in ripe fruits even on a per berry basis (Gregan and Jordan, 2016; Harris et al., 2012; Ryona et al., 2008). A decrease was also detected in *Vitis vinifera* *O*-methyltransferase (VvOMT) expression (Dunlevy et al., 2010, 2013b). It has been shown

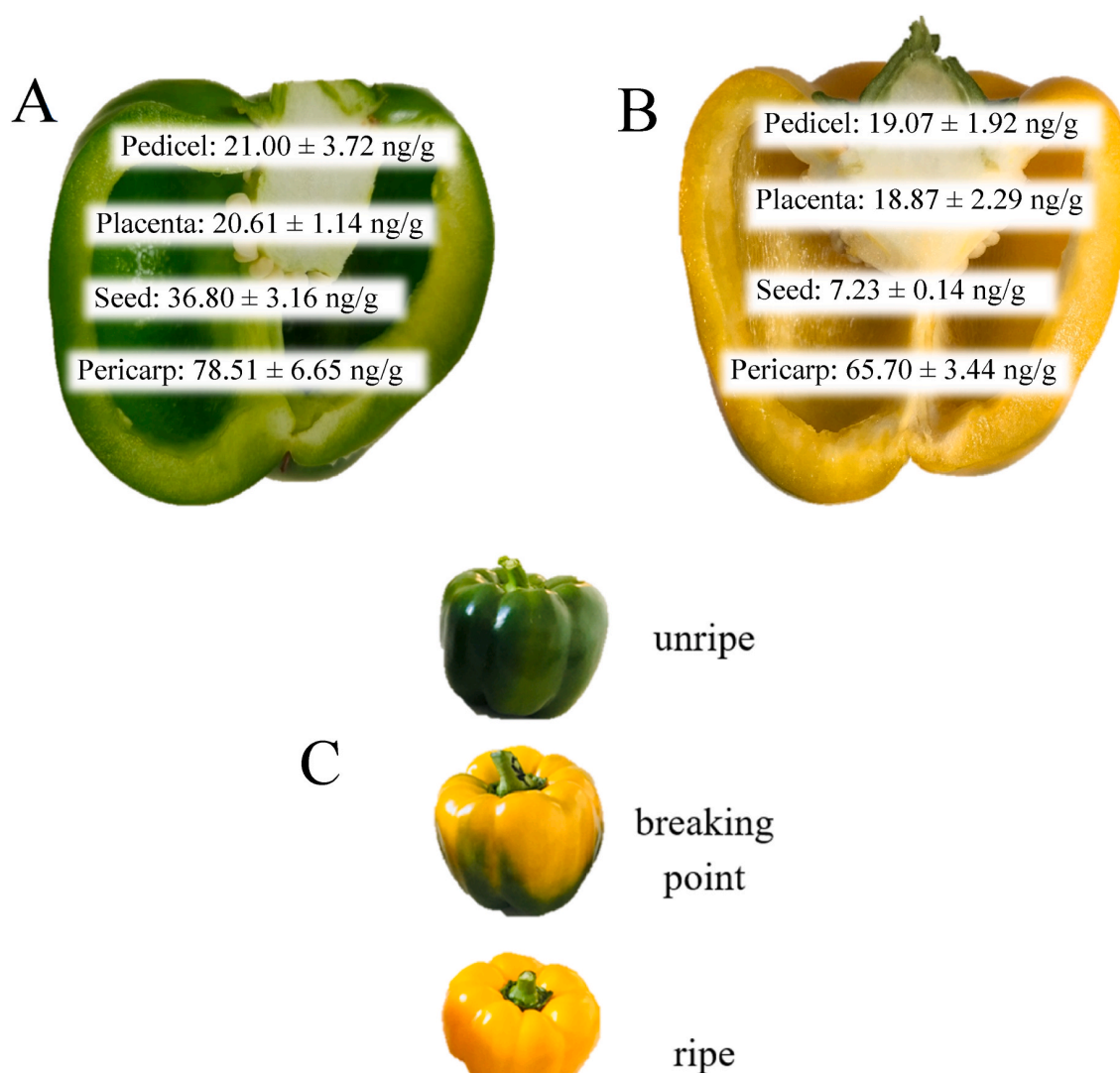


Fig. 3. IBMP-content (means \pm standard deviations ($n = 5-8$) expressed as ng/g FW (fresh weight)) in the various parts of unripe (A) and ripe (B) bell pepper fruits (*Capsicum annuum* cv. Allrounder). Ripening stages of bell pepper fruits: unripe (fully green), breaking point (green and yellow) and ripe (fully yellow) (C). (For interpretation of the references to colour in this figure legend, the reader is referred to the Web version of this article.)

that MP-levels are related with the expression of VvOMT, which are catalyzing the *O*-methylation of 3-alkyl-2-hydroxypyrazines (HPs) (Hashizume et al., 2001). First, a correlation between increasing levels of 3-isobutyl-2-hydroxypyrazine (IBHP) and decreasing IBMP-levels had been observed leading to the hypothesis that IBMP is demethylated to IBHP during bell pepper ripening (Ryona et al., 2010). However, further investigations showed that IBHP-levels are not stable, but decrease during grape ripening (Harris et al., 2012). It has been suggested, that the decrease in VvOMT expression leads to an accumulation of IBHP, which is no longer methylated to IBMP, but further metabolized (Harris et al., 2012).

In summary, it has been shown that IBMP can be detected in all parts of the bell pepper plant. IBMP-distribution in bell pepper plants slightly differs from that found in grapevines. Similar to grapevine, root tissues contain the highest MP-content within the whole plant. However, in grapevine the highest IBMP-content are detectable in the roots (Dunlevy et al., 2010), while IPMP is the most abundant MP in roots of bell pepper plants. The highest IBMP-levels are found in bell pepper fruits, which in turn possess the highest IBMP-content in the pericarp. In contrast, in grapevines IBMP accumulates in the stem of grape bunches and in the berry exocarp (Dunlevy et al., 2010; Roujou de Boubée, 2003; Roujou de Boubée et al., 2002).

2.2. Sites of biosynthesis

As it has been shown, IBMP accumulates in all parts of bell pepper plant. This might be due to either an IBMP-translocation through the plant or *de novo* IBMP-biosynthesis occurring in various plant organs and

tissues.

So far, feeding experiments revealed that IBMP is *de novo* biosynthesized in pericarp tissue of unripe bell pepper fruits. An incorporation of *L*-leucine into IBMP, leading to [²H₉]-IBMP has been demonstrated (Zamolo and Wüst, 2022). To examine the biosynthetic activity of different fruit tissues, *in vivo* feeding experiments were conducted using deuterium-labelled *L*-leucine ([²H₁₀]-*L*-leucine; see Fig. 4A). Fruits were dissected into pericarp, placenta, pedicel, and seeds. Samples are analyzed by HS-SPME-GCxGC-ToF-MS, as it enables a chromatographic separation of unlabelled and deuterium-labelled compounds and the detection of isotopic enrichments (mass shifts) due to deuterium-labelling. A mass spectrum of [²H₉]-IBMP that was biosynthesized from labelled [²H₁₀]-*L*-leucine is displayed in Fig. 4B.

As shown in Fig. 5, all examined tissues of unripe pepper fruits incorporate [²H₁₀]-*L*-leucine into IBMP, whereas fruits tissues of ripe fruits showed no incorporation of [²H₁₀]-*L*-leucine into IBMP neither in the placenta nor in the pedicel nor in the seeds. As it is known (see above), the IBMP-content in ripe fruits is lower than in unripe fruits. A possible degradation by demethylation of IBMP to IBHP has been hypothesized. However, a correlation between decreasing IBMP and increasing IBHP was only detectable in grapes, not in bell peppers. That is why a coexistence of further degradation pathways and products has been supposed (Ryona et al., 2010). Since IBMP-biosynthesis in the fruit tissue of the ripe fruit seems to have ceased, it might be possible that a down-regulation of enzyme activity leads to a decline in the IBMP-content as well.

Because IBMP is distributed throughout the whole bell pepper plant, it is conceivable that IBMP-biosynthesis also occurs in other plant

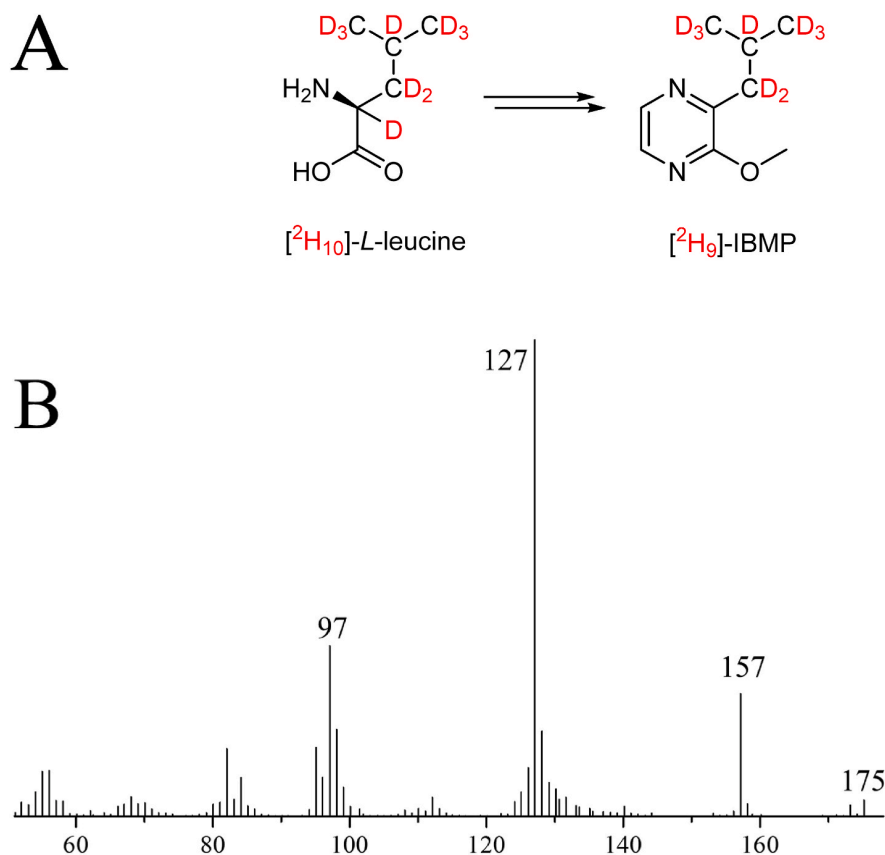


Fig. 4. Structure (A) and electron ionization (EI) mass spectra (B) of the biosynthetic product ([²H₉]-IBMP) after incorporation of stable-isotope labelled [²H₁₀]-*L*-leucine.

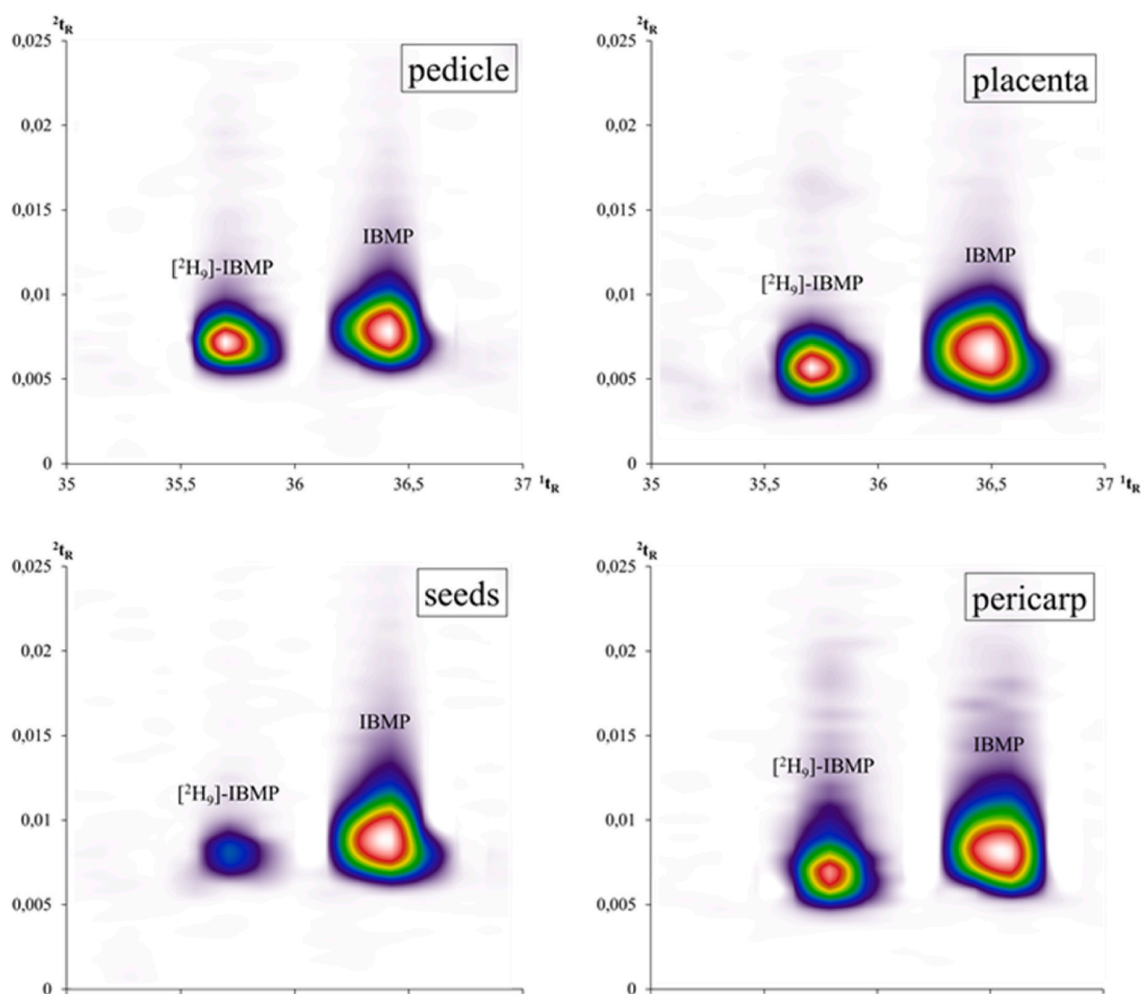


Fig. 5. Extracted-ion chromatograms (EIC; m/z 124, 127) obtained by HS-SPME-GC \times GC-ToF-MS-analysis after feeding [$^2\text{H}_{10}$]-L-leucine to several fruit tissues of unripe bell peppers (*Capsicum annuum* cv. Allrounder).

tissues. Therefore, *in vivo* feeding experiments were carried out using flower, leaf, stem, and root tissues of bell pepper plants. Abscised plant parts were incubated with deuterium-labelled L-leucine. First, the biosynthetic activity of the aerial plant parts was examined. Detached flowers, leaves, and stems were dipped into the incubation solution, to take up [$^2\text{H}_{10}$]-L-leucine via the transpiration stream. Samples were incubated at room temperature for 48 h. As the feeding solution was completely absorbed within 24 h, vials were refilled with water for the next 24 h of incubation. As shown in Fig. 6, an incorporation of [$^2\text{H}_{10}$]-L-leucine into IBMP could be confirmed for flowers, leaves, and stems. Thus, all aerial parts of bell pepper plants apart from ripe fruit tissues are capable of biosynthesizing IBMP. Interestingly, applying [$^2\text{H}_{10}$]-L-leucine to detached root tissues did not result in a detectable IBMP-biosynthesis. An incorporation of L-leucine into IBMP occurred neither in the tissue of the primary root nor in the root hairs. As mentioned before, roots contain more IPMP than IBMP. Low enzyme expression of relevant enzymes in the root may explain why no *de novo* biosynthesis of IBMP had been observed in the roots. In grapevine, roots showed the highest IBMP-contents, but only a low expression of VvOMT1, which mainly catalyses the *O*-methylation of IBHP to IBMP. In contrast, a higher expression of VvOMT2, which shows a higher activity to 3-isopropyl-2-hydroxypyrazine (IPHP), had been observed (Dunlevy et al., 2010; Vallarino et al., 2011). That is why further feeding experiments were conducted using [$^2\text{H}_8$]-L-valine, as a potential precursor to IPMP.

However, no incorporation of [$^2\text{H}_8$]-L-valine could be proven, neither in primary roots nor in root hairs.

In summary, IBMP-biosynthesis occurs predominantly in the aerial, green parts of the plant. While leaves, flowers, stem, and unripe fruits showed an incorporation of L-leucine into IBMP, no *de novo* IBMP-biosynthesis was detectable in ripe fruit and root tissues. This might be due to down-regulated enzymes or low enzyme expressions. In addition, *de novo* biosynthesis of IBMP in the flowers of bell pepper plants indicate that IBMP-biosynthesis appears already during flowering, continues during fruit development as well as fruit enlargement, and stops when fruit ripening starts.

2.3. Phloem transport

Since roots contain high IPMP-levels, but do not show the ability to biosynthesize it, it seems possible that IPMP-translocation is responsible for its distribution through the plant. In fact, a translocation of MP has already been discussed in the literature. First it has been hypothesized that IBMP-levels in the grapes would be a combination of IBMP biosynthesized in the fruit itself and IBMP transported from the leaves, as labelling experiments indicated that IBMP is first accumulated in the leaves and then supplied to the grapes during ripening (Roujou de Boubée, 2003). However, experiments were carried out with a physiologically inappropriate IBMP concentration, which makes the results

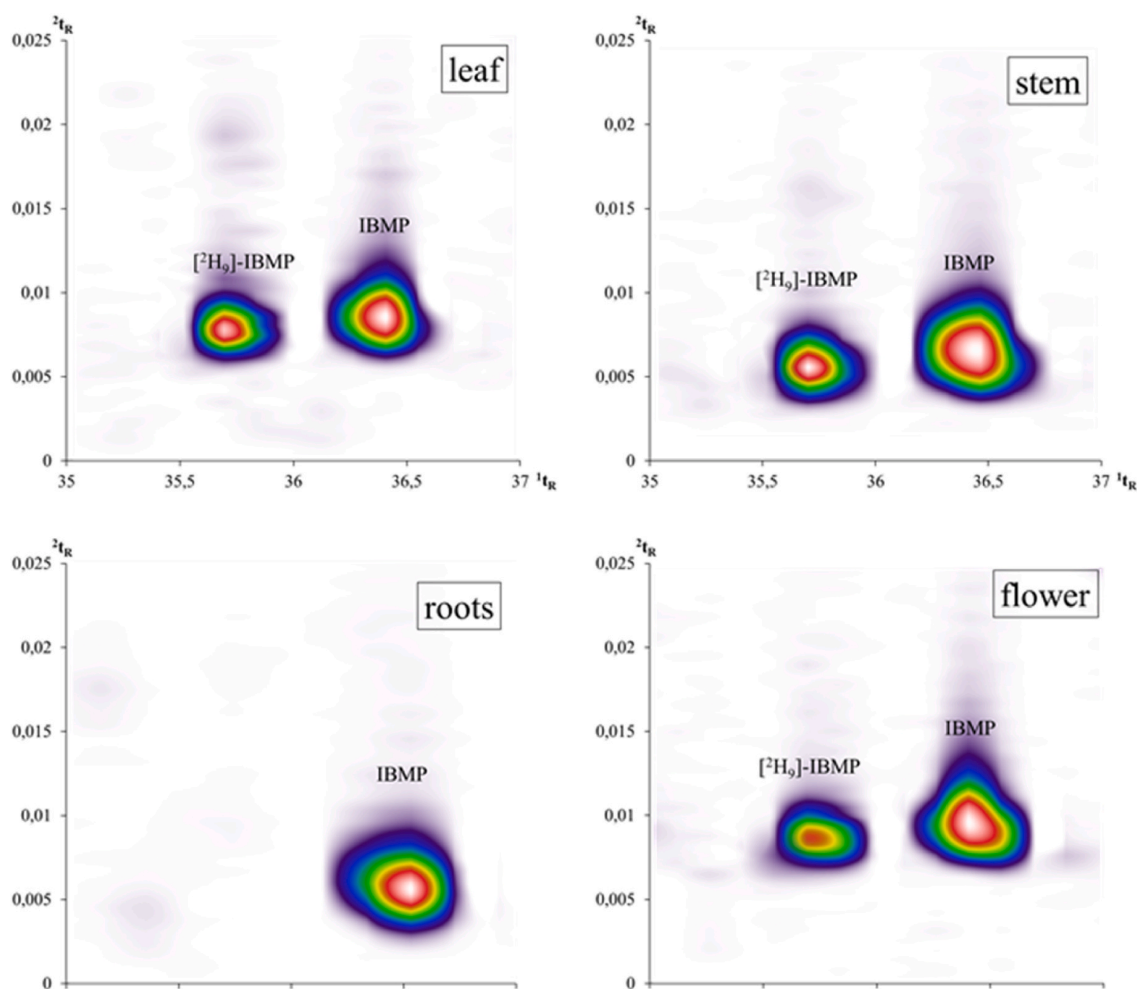


Fig. 6. Extracted-ion chromatograms (EIC; m/z 124, 127) obtained by HS-SPME-GC-MS analysis after feeding $[^2\text{H}_{10}]$ -L-leucine to several organs of bell pepper plants (*Capsicum annuum* cv. Allroundner).

obtained rather difficult to interpret. Moreover, grafting studies suggested that IBMP is not transported through the shoot (Koch et al., 2010).

In plants, leaves, fruits, stem, and roots are interconnected by a long-distance transport through their vascular system of xylem and phloem. The transport via the phloem is bidirectional, from source to sink. Leaves are the major source tissues and responsible for the transport of photosynthetic metabolites to sink tissues like fruits, stem, or roots. Besides primary metabolites, specialised metabolites like hormones, terpene and alkaloids are transported via the phloem (Buchanan, 2015; Nogia and Pati, 2021; Turgeon and Wolf, 2009; White, 2012).

As the presence of MP in the phloem has not yet been demonstrated, phloem sap of excised leaves of bell pepper plants (*Capsicum annuum*) was collected and analyzed by HS-SPME-GC-ToF-MS. While IPMP was not detectable, low levels of IBMP were detectable in petiole phloem exudates. However, IBMP-levels were not significantly higher than in water-treated control samples ($p > 0.05$). This might be due to cellular contamination of the phloem sap as cell damages occur during cutting the petiole (Buchanan, 2015).

As in the phloem exudate IBMP-levels were low and IPMP was not detectable (LOD ~ 0.16 ppb), a translocation of MP via the phloem seems unlikely. On the one hand, it might be that MPs are not transported via the phloem. On the other hand, it is possible that MPs first need to be chemically modified e.g. by conjugation. It has been

hypothesized that IBHP (as a degradation product of IBMP) is also present as a glycoconjugate (Ryona et al., 2010). Glycosylated MP would likely be soluble in the phloem.

3. Conclusions

An accurate, reproducible, and sensitive method combining HS-SPME and GC-ToF-MS was developed, to examine the distribution of IBMP in different bell pepper plant tissues. While analyzing different plant parts it has been shown that MP are present in the whole bell pepper plant, including roots, stem, leaves, flowers, and fruits. IPMP is mainly accumulated in the root tissue, whereas IBMP turned out to be the most abundant MP in all aerial parts of bell pepper plants. IBMP-concentrations in fruits and flowers exceed those of the vegetative organs such as roots, stems, and leaves. Thus, IBMP accumulates predominantly in the reproductive parts of bell pepper plants. Pericarp tissue of unripe bell pepper fruits turned out to be the major site of IBMP accumulation. In addition, the sites of IBMP-biosynthesis was examined by *in vivo* feeding studies. Feeding experiments with deuterium labelled L-leucine revealed that all aerial plant parts were able to biosynthesize IBMP, except tissues of ripe bell pepper fruits. Moreover, neither an incorporation of $[^2\text{H}_{10}]$ -L-leucine into IBMP nor an incorporation of $[^2\text{H}_8]$ -L-valine into IPMP was detectable in the root tissues. That is why a translocation of IBMP through the plant via the phloem was considered.

However, HS-SPME-GC-ToF-MS-analysis of phloem exudates confirmed that a translocation of IBMP is not observed.

4. Experimental

4.1. Plant material

The experiments were performed with bell pepper (Solanaceae, *Capsicum annuum* L. cv 'Allrounder') (Rijk Zwaan, De Lier, Netherlands) obtained from the Institute of Crop Science and Resource Conservation (INRES), Chair of Horticultural Sciences of the University of Bonn, Germany. For MP-quantification fruits, leaves, stems and roots were cut from intact plants. Fruits were further dissected into pericarp, placenta, pedicel, and seeds. Samples were pooled by tissue, before they were homogenized and analyzed. For feeding experiments fruits were harvested and incubated the same day.

4.2. Chemicals

3-Isobutyl-2-methoxypyrazine (IBMP) (97%) were purchased from Sigma Aldrich (St Louis, Missouri). 3-Isobutyl- $^{2}\text{H}_9$ -2-methoxypyrazine ($^{2}\text{H}_9$ -IBMP) ($\geq 95\%$) was obtained from AromaLab (Martinsried, Germany). L-Leucine-2,3,3,4,5,5,5',5',5'- d_{10} ($^{2}\text{H}_{10}$ -L-leucine) (99%) was purchased from C/D/N Isotopes (Pointe-Claire, Quebec, Canada). L-Valine-2,3,4,4,4,5,5,5- d_8 ($^{2}\text{H}_8$ -L-valine) was from Biotrend (Cologne, Germany). Sodium chloride was purchased from Merck GmbH (Darmstadt, Germany). Methanol ($>99.99\%$) was obtained from Honeywell (Muskegon, Michigan). Phosphate buffer solution (pH 7) and water (HPLC, LC-MS grade) were purchased from VWR International (Darmstadt, Germany).

4.3. Concentration of $^{2}\text{H}_9$ -IBMP

The concentration of $^{2}\text{H}_9$ -IBMP in stock solutions was determined by GC-FID analysis. The FID response factors were calculated using sBMP as the internal standard. Therefore, defined amounts of IBMP and sBMP were analyzed by GC-FID yielding an FID response factor. Then mixtures containing a defined volume of $^{2}\text{H}_9$ -IBMP and a defined amount of sBMP were analyzed by GC-FID. By means of the response factors of IBMP, the concentration of $^{2}\text{H}_9$ -IBMP was determined (Greger and Schieberle, 2007).

4.4. Validation

Linearity was verified by spiking IBMP-free tomato pericarp homogenate as a matrix-matched sample with IBMP (0.1–150 ng/g) and $^{2}\text{H}_9$ -IBMP (60 ng/g). Then the concentration-ratios of IBMP to $^{2}\text{H}_9$ -IBMP were plotted against their respective area-ratios and the correlation coefficient (r^2) was calculated. Recovery experiments were conducted to determine the method accuracy. Therefore, homogenized tomato pericarp was spiked with IBMP (10–96 ng/g) and 82.5 ng/g $^{2}\text{H}_9$ -IBMP. Method recovery was calculated by comparing the IBMP-contents calculated from the calibration curve to those added to the matrix. Intra-day precision was verified by analyzing six replicates of 80 ng/g IBMP within one day. To determine the inter-day precision, only one replicate of 80 ng/g IBMP was tested daily within six days. Both intra-day and inter-day precision were determined as the relative standard deviation (RSD). The limit of detection (LOD) and limit of quantitation (LOQ) were estimated by calibration curves in the range of the expected LOD and LOQ. Therefore, tomato pericarp was spiked with ten levels of IBMP (0.1–1 ng/g). Unspiked tomato pericarp were analyzed as control samples. Samples were analyzed in triplicate under repeatability conditions.

4.5. Quantification

IBMP was quantified using SIDA. Therefore, a five-point calibration was constructed by spiking 1 g tomato pericarp (matrix-matched sample) with defined amounts of IBMP and $^{2}\text{H}_9$ -IBMP. While the IBMP-concentration varied, $^{2}\text{H}_9$ -IBMP-concentration of was set constant for each calibration level (82.5 ng/g). After an equilibration time of 1 h, 2 mL of a 20% (w/v) NaCl-solution were added and sealed vials were transposed into the HS-system. Each sample was repeated triple. After data acquisition, the chromatograms were extracted with m/z 124 (IBMP) and m/z 127 ($^{2}\text{H}_9$ -IBMP). To determine calibration curves, the peak area ratio (IBMP/ $^{2}\text{H}_9$ -IBMP) was plotted against the ratio of their respective concentrations (IBMP/ $^{2}\text{H}_9$ -IBMP). Calibration curves were used for IBMP-quantification and semi-quantifying IPMP.

For quantification 1 g of homogenized plant material was weighed into a 10 mL-HS-vial to which 82.5 ng/g of $^{2}\text{H}_9$ -IBMP were added. To allow an equilibration, vials were stored for 1 h at room temperature. Prior to HS-SPME-GC-ToF-MS-analysis an aqueous solution containing 20% (w/v) NaCl was added.

Headspace solid phase microextraction (HS-SPME) was carried out using a divinylbenzene/carboxen/polydimethylsiloxane (DVB/CAR/PDMS, 50/30 μm , 2 cm) fiber (Supelco, Bellefonte, Pennsylvania). Samples were incubated at 70 °C for 5 min with agitation (450 rpm; 30 s on time; 10 s off time) followed by sample extraction at 70 °C for 10 min. After incubation and extraction, the analytes were desorbed into the injector at 250 °C for 10 min.

GC-MS analysis was carried out using a Agilent 7890B gas chromatograph (Agilent Technologies, Palo Alto, California) equipped with a OPTIMA 5 MS (30 m, 0.25 mm i.d. x 0.1 μm d_f) capillary column, coupled to a time-of-flight mass spectrometer (Markes International Ltd, Llantrisant, RCT, UK) operating in the electron impact ionization mode (EI) with an ionizing voltage set at -70 eV. The transfer line was set to 250 °C. The ion source temperature was 250 °C. A constant flow of 1.0 mL/min helium was used as carrier gas. The temperature program initially set to 50 °C for 3 min, was increased to 80 °C at a rate of 10 °C/min, followed by a rate of 3 °C/min up to 125 °C, then raised to 260 °C for 5 min at a rate of 20 °C/min. The injector temperature was kept at 250 °C. Mass spectra were collected in full scan (m/z 35–250). IBMP and $^{2}\text{H}_9$ -IBMP were identified based on comparison of their retention time and mass spectra to standard substances. Since the signal of the molecular ion (M^+) of IBMP and $^{2}\text{H}_9$ -IBMP were low, signals of the most intense mass traces were used for quantification. The most abundant mass traces of IBMP (m/z 124) and $^{2}\text{H}_9$ -IBMP (m/z 127) were extracted. All samples were analyzed in triplicate.

4.6. Phloem exudate

Phloem exudate from cut petioles was obtained using the EDTA-facilitated exudation method (King and Zeevaart, 1974). For this purpose, leaves of bell pepper plants (*Capsicum annuum* cv 'Allrounder') (~1.5 g) were collected. The petioles of excised leaves were recut under water, before they were transferred to 10 mL HS-vials containing a 20 mM EDTA in 5 mM phosphate buffer (pH 7) solution. EDTA was used as a chelating agent to avoid phloem sealing (King and Zeevaart, 1974). First, samples were kept in a closed and humidified chamber at room temperature in complete darkness for 2 h. Then they were rinsed with water to remove remaining EDTA (Guellette et al., 2012) before they were placed in 2 mL water for exudate collection in complete darkness for 6 h at room temperature. The required humidity to prevent the loss of exudate due to transpiration was achieved by wet paper towels, which were placed into the chamber (Tetyuk et al., 2013). Samples were immediately analyzed by HS-SPME-GC-ToF-MS. The use of EDTA can lead to false-positive results due to cell damages (Tetyuk et al., 2013). That is why control experiments were carried out by incubating samples in water only.

4.7. Feeding experiments

Feeding experiments were carried out using bell pepper (*Capsicum annuum* L. cv. 'Allrounder'). Samples were treated directly after harvesting (Zamolo and Wüst, 2022).

- I. Fruit tissues: Pericarp, calyx and placenta were cut into pieces (~ 4 g each). Then 200 µL of a solution of [²H₁₀]-L-leucine (1 mg/mL) was added.
- II. Flowers: Pedicel were cut off and flowers were put onto a sterile petri dish containing 200 µL of a solution of [²H₁₀]-L-leucine (1 mg/mL).
- III. Leaves and stems: Fresh cut petioles and stems were put into the GC vial containing 500 µL water and 200 µL of a solution of [²H₁₀]-L-leucine (1 mg/mL). GC-vials were wrapped with Parafilm. Since the feeding solution was absorbed within 24 h via the transpiration stream, the same volume of water was added until the end of the experiment.
- IV. Roots: The primary root of a fully developed plant was cut into slices and incubated with 200 µL of a solution of [²H₁₀]-L-leucine (1 mg/mL). In addition, root hairs were collected and incubated with 200 µL of a solution of [²H₁₀]-L-leucine (1 mg/mL).

After incubation at room temperature for 48 h, the samples were frozen using liquid nitrogen and crushed with a mortar. The homogenized sample (1 g) was weighed into a 10 mL headspace-vial and 2 mL of an 20% (w/v) aqueous NaCl-solution were added. Control samples were incubated with water. Each experiment was repeated at least three times.

Solid phase microextraction (SPME) was carried out using a DVB/CAR/PDMS-fiber (divinylbenzene/carboxen/polydimethylsiloxane, 50/30 µm, 2 cm) (Supelco, Bellefonte, Pennsylvania). Samples were incubated at 50 °C for 10 min with agitation (500 rpm; 30 s on time; 10 s off time) followed by sample extraction at 50 °C for 30 min. After incubation and extraction, the analytes were desorbed into the injector at 250 °C for 10 min.

Chromatographic separation was carried out on an Agilent 7890B gas chromatograph (Agilent Technologies, Palo Alto, California) equipped with a OPTIMA 5 MS (30 m, 0.25 mm i.d. x 0.1 µm df) primary column, a MEGA WAX FAST (2 m, 0.1 mm i.d. x 0.1 µm df) secondary column and a liquid nitrogen cryogenic modulator (Consumable-Free ZX2 thermal modulator). Helium was used as the carrier gas at a constant flow of 1 mL/min. The temperature program started at 35 °C for 5 min, was increased at 3 °C/min to 160 °C, then ramped at 20 °C/min to 220 °C and maintained at 220 °C for 5 min. The modulation period (PM) was set to 4 s with hot jet duration of 350 ms and with a shift of +20 °C regarding to the temperature program of the GC oven. Detection was performed on a time-of-flight mass spectrometer (ToF-MS) (Markes International Ltd, Llantrisant, RCT, UK) operating in the electron impact ionization (EI) mode with an ionizing voltage set at -70 eV. The transfer line was set to 250 °C. The ion source temperature was 250 °C. Data analysis was performed using the software ChromSpace (Markes International Ltd, Llantrisant, RCT, UK). The software was used to remove unwanted background noise and for spectrum deconvolution. Analytes were identified by comparing the retention times and mass spectra with standard substances and using the NIST Mass Spectral Library (National Institute of Standards and Technology, Gaithersburg, Maryland). IBMP and [²H₉]-IBMP were identified using standard substances. For this purpose, both GC retention times and mass spectra were compared.

Declaration of competing interest

The authors declare that they have no known competing financial interests or personal relationships that could have appeared to influence the work reported in this paper.

Data availability

Data will be made available on request.

Acknowledgement

We thank the Institute of Crop Science and Resource Conservation (INRES), Chair of Horticultural Sciences of the University of Bonn, Germany for providing bell pepper plants.

References

- Bramwell, A.F., Burrell, J., Riezebos, G., 1969. Characterisation of pyrazines in galbanum oil. *Tetrahedron Lett.* 10, 3215–3216. [https://doi.org/10.1016/S0040-4039\(01\)88391-X](https://doi.org/10.1016/S0040-4039(01)88391-X).
- Buchanan, B.B. (Ed.), 2015. *Biochemistry & Molecular Biology of Plants*, second ed. Wiley Blackwell, Chichester u.a.
- Buttery, R.G., Seifert, R.M., Guadagni, D.G., Ling, L.C., 1969. Characterization of some volatile constituents of bell peppers. *J. Agric. Food Chem.* 17, 1322–1327. <https://doi.org/10.1021/jf60166a061>.
- Dunlevy, J.D., Dennis, E.G., Soole, K.L., Perkins, M.V., Davies, C., Boss, P.K., 2013a. A methyltransferase essential for the methoxypyrazine-derived flavour of wine. *Plant J. : Cell Mol. Biol.* 75, 606–617. <https://doi.org/10.1111/tpj.12224>.
- Dunlevy, J.D., Soole, K.L., Perkins, M.V., Dennis, E.G., Keyzers, R.A., Kalua, C.M., Boss, P.K., 2010. Two O-methyltransferases involved in the biosynthesis of methoxypyrazines: grape-derived aroma compounds important to wine flavour. *Plant Mol. Biol.* 77–89. <https://doi.org/10.1007/s11103-010-9655-y>.
- Dunlevy, J.D., Soole, K.L., Perkins, M.V., Nicholson, E.L., Maffei, S.M., Boss, P.K., 2013b. Determining the methoxypyrazine biosynthesis variables affected by light exposure and Crop level in Cabernet Sauvignon. *Am. J. Enol. Vitic.* 64, 450–458. <https://doi.org/10.5344/ajev.2013.13070>.
- Gregan, S.M., Jordan, B., 2016. Methoxypyrazine accumulation and O-methyltransferase gene expression in Sauvignon blanc grapes: the role of leaf removal, light exposure, and berry development. *J. Agric. Food Chem.* 64, 2200–2208. <https://doi.org/10.1021/acs.jafc.5b05806>.
- Greger, V., Schieberle, P., 2007. Characterization of the key aroma compounds in apricots (*Prunus armeniaca*) by application of the molecular sensory science concept. *J. Agric. Food Chem.* 55, 5221–5228. <https://doi.org/10.1021/jf0705015>.
- Guelette, B.S., Benning, U.F., Hoffmann-Benning, S., 2012. Identification of lipids and lipid-binding proteins in phloem exudates from *Arabidopsis thaliana*. *J. Exp. Bot.* 63, 3603–3616. <https://doi.org/10.1093/jxb/ers028>.
- Guillaumie, S., Ilg, A., Réty, S., Brette, M., Trossat-Magnin, C., Decroocq, S., Léon, C., Keime, C., Ye, T., Baltenweck-Guyot, R., Claudel, P., Bordenave, L., Vanbrabant, S., Duchêne, E., Delrot, S., Darriet, P., Huguene, P., Gomès, E., 2013. Genetic analysis of the biosynthesis of 2-methoxy-3-isobutylpyrazine, a major grape-derived aroma compound impacting wine quality. *Plant Physiol.* 162, 604–615. <https://doi.org/10.1104/pp.113.218313>.
- Harris, S.A., Ryoua, I., Sacks, G.L., 2012. Behavior of 3-isobutyl-2-hydroxypyrazine (IBHP), a key intermediate in 3-isobutyl-2-methoxypyrazine (IBMP) metabolism, in ripening wine grapes. *J. Agric. Food Chem.* 60, 11901–11908. <https://doi.org/10.1021/jf302990m>.
- Hashizume, K., Samuta, T., 1997. Green odorants of grape cluster stem and their ability to cause a wine stemmy flavor. *J. Agric. Food Chem.* 45, 1333–1337. <https://doi.org/10.1021/jf960635a>.
- Hashizume, K., Tozawa, K., Endo, M., Aramaki, I., 2001. S-Adenosyl-L-methionine-dependent O-methylation of 2-hydroxy-3-alkylpyrazine in wine grapes: a putative final step of methoxypyrazine biosynthesis. *Biosci. Biotechnol. Biochem.* 65, 795–801. <https://doi.org/10.1271/bbb.65.795>.
- Kihika, R., Murungi, L.K., Coyne, D., Ng'ang'a, M., Hassanali, A., Teal, P.E.A., Torto, B., 2017. Parasitic nematode *Meloidogyne incognita* interactions with different *Capsicum annuum* cultivars reveal the chemical constituents modulating root herbivory. *Sci. Rep.* 7, 2903. <https://doi.org/10.1038/s41598-017-02379-8>.
- King, R.W., Zeevaert, J.A., 1974. Enhancement of Phloem exudation from cut petioles by chelating agents. *Plant Physiol.* 53, 96–103. <https://doi.org/10.1104/pp.53.1.96>.
- Koch, A., Doyle, C.L., Matthews, M.A., Williams, L.E., Ebeler, S.E., 2010. 2-Methoxy-3-isobutylpyrazine in grape berries and its dependence on genotype. *Phytochemistry* 71, 2190–2198. <https://doi.org/10.1016/j.phytochem.2010.09.006>.
- Kögel, S., Eben, A., Hoffmann, C., Gross, J., 2012. Influence of diet on fecundity, immune defense and content of 2-isopropyl-3-methoxypyrazine in *Harmonia axyridis* Pallas. *J. Chem. Ecol.* 38, 854–864. <https://doi.org/10.1007/s10886-012-0139-1>.
- Legrum, C., Slabizki, P., Schmarr, H.-G., 2015. Enantiodifferentiation of 3-sec-butyl-2-methoxypyrazine in different species using multidimensional and comprehensive two-dimensional gas chromatographic approaches. *Anal. Bioanal. Chem.* 407, 253–263. <https://doi.org/10.1007/s00216-014-8061-8>.
- Lei, Y., Xie, S., Chen, H., Guan, X., Zhang, Z., 2019. Behavior of 3-isobutyl-2-methoxypyrazine biosynthesis related to proposed precursor and intermediate in wine grape. *Food Chem.* 277, 609–616. <https://doi.org/10.1016/j.foodchem.2018.10.121>.
- Moore, B.P., Brown, W.V., Rothschild, M., 1990. Methylalkylpyrazines in aposematic insects, their hostplants and mimics. *Chemoecology* 1, 43–51. <https://doi.org/10.1007/BF01325227>.
- Murray, K.E., Shtipon, J., Whitfield, F.B., 1970. 2-methoxypyrazines and the flavour of green peas (*Pisum sativum*). *Chem. Ind. (London)* 27, 897–898.

- Murray, K.E., Whitfield, F.B., 1975. The occurrence of 3-alkyl-2-methoxypyrazines in raw vegetables. *J. Sci. Food Agric.* 26, 973–986. <https://doi.org/10.1002/jsfa.2740260714>.
- Mutarutwa, D., Navarini, L., Lonzarich, V., Compagnone, D., Pittia, P., 2018. GC-MS aroma characterization of vegetable matrices: focus on 3-alkyl-2-methoxypyrazines. *J. Mass Spectrom.* 53, 871–881. <https://doi.org/10.1002/jms.4271>.
- Negre-Zakharov, F., Long, M.C., Dudareva, N., 2009. Floral scents and fruit aromas inspired by nature. In: Osbourn, A.E., Lanzotti, V. (Eds.), *Plant-derived Natural Products*. Springer US, New York, NY, pp. 405–431.
- Nogia, P., Pati, P.K., 2021. Plant secondary metabolite transporters: diversity, functionality, and their modulation. *Front. Plant Sci.* 12, 758202. <https://doi.org/10.3389/fpls.2021.758202>.
- Nursten, H.E., Sheen, M.R., 1974. Volatile flavour components of cooked potato. *J. Sci. Food Agric.* 25, 643–663. <https://doi.org/10.1002/jsfa.2740250607>.
- Pickering, G.J., Willwerth, J., Botezatu, A., Thibodeau, M., 2021. Prevalence and management of alkyl-methoxypyrazines in a changing climate: viticultural and oenological considerations. *Biomolecules* 11. <https://doi.org/10.3390/biom11101521>.
- Rothschild, M., Moore, B.P., Brown, W.V., 1984. Pyrazines as warning odour components in the Monarch butterfly, *Danaus plexippus*, and in moths of the genera *Zygaena* and *Amata* (Lepidoptera). *Biol. J. Linn. Soc.* 23, 375–380. <https://doi.org/10.1111/j.1095-8312.1984.tb00153.x>.
- Roujou de Boubée, D., 2003. Research on 2-methoxy-3-isobutylpyrazine in grapes and wines. Paris, France 1–21.
- Roujou de Boubée, D., Pons, A.M.C.M., Dubourdiou, D., 2002. Location of 2-Methoxy-3-isobutylpyrazine in Cabernet Sauvignon grape bunches and its extractability during vinification. *Am. J. Enol. Vitic.* 1–5.
- Roujou de Boubée, D., van Leeuwen, C., Dubourdiou, D., 2000. Organoleptic impact of 2-methoxy-3-isobutylpyrazine on red bordeaux and loire wines. Effect of environmental conditions on concentrations in grapes during ripening. *J. Agric. Food Chem.* 48, 4830–4834. <https://doi.org/10.1021/jf000181o>.
- Ryona, I., Leclerc, S., Sacks, G.L., 2010. Correlation of 3-isobutyl-2-methoxypyrazine to 3-isobutyl-2-hydroxypyrazine during maturation of bell pepper (*Capsicum annuum*) and wine grapes (*Vitis vinifera*). *J. Agric. Food Chem.* 58, 9723–9730. <https://doi.org/10.1021/jf102072w>.
- Ryona, I., Pan, B.S., Intrigliolo, D.S., Lakso, A.N., Sacks, G.L., 2008. Effects of cluster light exposure on 3-isobutyl-2-methoxypyrazine accumulation and degradation patterns in red wine grapes (*Vitis vinifera* L. Cv. Cabernet Franc). *J. Agric. Food Chem.* 56, 10838–10846. <https://doi.org/10.1021/jf801877y>.
- Schmidtberg, H., Shukla, S.P., Halitschke, R., Vogel, H., Vilcinskas, A., 2019. Symbiont-mediated chemical defense in the invasive ladybird *Harmonia axyridis*. *Ecol. Evol.* 9, 1715–1729. <https://doi.org/10.1002/ece3.4840>.
- Tadesse, T., Hewett, E.W., Nichols, M.A., Fisher, K.J., 2002. Changes in physicochemical attributes of sweet pepper cv. Domino during fruit growth and development. *Sci. Hortic.* 93, 91–103. [https://doi.org/10.1016/S0304-4238\(01\)00317-X](https://doi.org/10.1016/S0304-4238(01)00317-X).
- Tetyuk, O., Benning, U.F., Hoffmann-Benning, S., 2013. Collection and analysis of Arabidopsis phloem exudates using the EDTA-facilitated Method. *JoVE : JoVE*. <https://doi.org/10.3791/51111> e51111.
- Thanopoulos, C., Bouranis, D., Passam, H.C., 2013. Comparative development, maturation and ripening of seedless and seed-containing bell pepper fruits. *Sci. Hortic.* 164, 573–577. <https://doi.org/10.1016/j.scienta.2013.10.010>.
- Turgeon, R., Wolf, S., 2009. Phloem transport: cellular pathways and molecular trafficking. *Annu. Rev. Plant Biol.* 60, 207–221. <https://doi.org/10.1146/annurev-arplant.043008.092045>.
- Vallarino, J.G., Lopez-Cortes, X.A., Dunlevy, J.D., Boss, P.K., Gonzalez-Nilo, F.D., Moreno, Y.M., 2011. Biosynthesis of methoxypyrazines: elucidating the structural/functional relationship of two *Vitis vinifera*O-methyltransferases capable of catalyzing the putative final step of the biosynthesis of 3-alkyl-2-methoxypyrazine. *J. Agric. Food Chem.* 59, 7310–7316. <https://doi.org/10.1021/jf200542w>.
- White, P.J., 2012. Long-distance transport in the xylem and phloem. In: *Marschner's Mineral Nutrition of Higher Plants*. Elsevier, pp. 49–70.
- Zamolo, F., Wüst, M., 2022. Investigation of biosynthetic precursors of 3-isobutyl-2-methoxypyrazine using stable isotope labeling studies in bell pepper fruits (*Capsicum annuum* L.). *J. Agric. Food Chem.* 6719–6725. <https://doi.org/10.1021/acs.jafc.2c01747>.